

A COMPARATIVE STUDY OF LHERZOLITE NODULES
IN BASALTIC ROCKS FROM BRITISH COLUMBIA

by

ALASTAIR LEWIS LITTLEJOHN

B.Sc., University of Aberdeen, 1969

A THESIS SUBMITTED IN PARTIAL FULFILMENT OF
THE REQUIREMENTS FOR THE DEGREE OF
MASTER OF SCIENCE

In the Department
of
Geology

We accept this thesis as conforming to the
required standard

THE UNIVERSITY OF BRITISH COLUMBIA

April, 1972

In presenting this thesis in partial fulfilment of the requirements for an advanced degree at the University of British Columbia, I agree that the Library shall make it freely available for reference and study.

I further agree that permission for extensive copying of this thesis for scholarly purposes may be granted by the Head of my Department or by his representatives. It is understood that copying or publication of this thesis for financial gain shall not be allowed without my written permission.

ALASTAIR L. LITTLEJOHN

Department of GEOLOGY

The University of British Columbia
Vancouver 8, Canada

Date 29th. Februry 1972

ABSTRACT

Lherzolite nodules in basaltic rocks from three localities in British Columbia include rocks of mantle origin and crystal cumulates. Partial chemical analyses show that the compositional ranges of the minerals are narrow for both major and minor elements and fall within the ranges reported for lherzolite nodules elsewhere. Each suite is characterised by a definite range of concentrations of some elements. Olivine in nodules from Castle Rock and Jacques Lake show fabrics resulting from deformation in the solid state prior to their incorporation into their host rocks but those from Nicola Lake are undeformed.

The distribution of iron and magnesium between coexisting phases is examined using an ideal ionic solution model. Differences in the distribution coefficients between the suites are probably due to different temperature and pressure conditions at the source of the nodules. The distribution of iron and magnesium between coexisting spinel and olivine gives nominal temperatures of formation of 838°C for Nicola Lake nodules, 1085°C for Jacques Lake nodules and $>1600^{\circ}\text{C}$ for Castle Rock nodules. Differences among the suites in the distribution of Ni, Co, Mn and Zn between coexisting silicates are independent of variations in composition and are apparently due to different conditions of formation.

The Castle Rock and Jacques Lake lherzolites are residual fragments of the upper mantle left after extraction of an under-saturated basaltic liquid from parental mantle rock. The source of the Castle Rock nodules probably lies at greater depth than that of the Jacques Lake nodules. The Nicola Lake nodules are crystal cumulates and formed at an early stage of basalt genesis within the upper mantle or lower crust.

TABLE OF CONTENTS

		Page
CHAPTER 1	Introduction.	1
CHAPTER 2	The Localities of Nodules in British Columbia.	4
	(a) Nodule localities.	4
	(b) Petrography of the host rocks.	4
CHAPTER 3	Petrography of the Nodules.	9
	(a) General.	9
	(b) Petrographic descriptions.	9
	(c) Secondary textural features.	14
CHAPTER 4	Petrofabric Study.	20
	(a) General.	20
	(b) Description of the fabrics.	21
	(c) Discussion.	26
CHAPTER 5	Mineral Compositions.	36
	(a) General.	36
	(b) Olivine.	37
	(c) Orthopyroxene.	37
	(d) Clinopyroxene.	40
	(e) Spinel.	43
CHAPTER 6	The Distribution of Iron and Magnesium Between Coexisting Minerals.	48
	(a) Theory.	48
	(b) Results for coexisting silicates.	50
	(c) The effects of temperature and pressure.	52
	(d) The distribution between spinel and olivine.	56
	(e) Results for coexisting spinel and pyroxenes.	61
CHAPTER 7	The Distribution of Trace Elements Between Coexisting Silicates.	63
	(a) Theory.	63
	(b) The distribution of Ni, Mn, Co and Zn.	65
	(c) Other elements.	73
CHAPTER 8	The Origin of the Nodules.	76
	(a) Temperature and pressure.	76
	(b) The nature of the source.	83
CHAPTER 9	The Upper Mantle in British Columbia.	94
CHAPTER 10	Conclusions.	98
BIBLIOGRAPHY		100
APPENDIX 1	Analytical Techniques.	107
APPENDIX 2	Error Propagation in Temperature Calculations.	112

LIST OF TABLES

Table		Page
1	Modes of Nodules with Analysed Minerals.	36
2	Partial Chemical Analyses of Olivines.	38
3	Partial Chemical Analyses of Orthopyroxenes.	39
4	Partial Chemical Analyses of Clinopyroxenes.	41
5	Partial Chemical Analyses of Spinel.	45
6	Values of K_D for Coexisting Olivine and Pyroxenes with Analysis of Variance.	51
7	Values of K_D for Coexisting Spinel and Olivine with Analysis of Variance.	58
8	Temperatures of Formation of Coexisting Spinel and Olivine.	58
9	Values of K_D for Coexisting Spinel and Pyroxenes with Analysis of Variance.	62
10	(Tr/Cr) Ratios of Analysed Minerals.	67
11	Trace Element Distribution Coefficients.	70
12	Analysis of Trace Element Variance between Jacques Lake and Castle Rock Suites.	71
13	Values of k_{Ti} and k_{Cr} for Coexisting Pyroxenes with Analysis of Variance.	75

LIST OF FIGURES

Figure		Page
1	Localities of Ultramafic Nodules in British Columbia.	5
2	Basalt Coating around Lherzolite Nodule.	7
3	Modes of Ultramafic Nodules from British Columbia.	10
4	Aggregate of Spinel and Clinopyroxene.	12
5	Exsolved Clinopyroxene in Orthopyroxene.	12
6	Exsolved Spinel in Orthopyroxene.	13
7	Exsolved Spinel in Olivine.	13
8	Mineralogical Banding in Castle Rock Lherzolite.	15
9	Alignment of Sheared Spinel Grains.	15
10	Reaction of Orthopyroxene at Margin of Host.	17
11	Porous-looking Outer Rim of Clinopyroxene.	17
12	Fluid Inclusions in Olivine.	19
13	Olivine Fabric Diagram for JL-A.	23
14	Olivine Fabric Diagram for JL-50.	23
15	Olivine Fabric Diagram for JL-24.	24
16	Strained Olivine with Abundant Kink Bands in Jacques Lake Lherzolite.	25
17	Olivine Fabric Diagram for NL-8.	24
18	Mutually Interfering Grain Boundaries between Olivines and Orthopyroxene in Nicola Lake Lherzolite.	25
19	Olivine Fabric Diagram for S-2.	28
20	Olivine Fabric Diagram for S-4.	28
21	Olivine Fabric Diagram for CR-8.	29
22	Strain-free, Recrystallised Olivine in Castle Rock Lherzolite.	30

LIST OF FIGURES
(continued)

Figure		Page
23	Enstatite Fabric Diagram for CR-8.	29
24	Variation of Na_2O and TiO_2 with Al_2O_3 in Clinopyroxene.	42
25	Variation of Al_2O_3 , CaO and Na_2O with $\text{MgO}:\text{FeO}$ in Clinopyroxene.	44
26	Composition of Analysed Spinel.	47
27	Distribution of Iron and Magnesium between Coexisting Olivine and Orthopyroxene.	54
28	Relative Proportions of Zn, Co, Ni and Mn between Coexisting Olivine, Orthopyroxene and Clinopyroxene.	68
29	Relative Proportions of Pb and Cu between Coexisting Olivine, Orthopyroxene and Clinopyroxene.	74
30	Composition of Analysed Pyroxenes in terms of MgSiO_3 - CaSiO_3 - Al_2O_3 .	78
31	Variation of Al_2O_3 between Spinel and Pyroxenes.	80
32	Relative Stabilities of Various Ultramafic Mineral Assemblages.	81
33	Various Lherzolite Solidi.	90
34	Part of the Liquidus Diagram of the System Fo - Di - SiO_2 at 20Kb. Pressure.	93
35	Major Structural Features Related to Recent Volcanism in British Columbia.	97

ACKNOWLEDGEMENTS

I would like to express my thanks and appreciation to Dr. H.J. Greenwood for suggesting this topic and supervising the work. Thanks are also due to Dr. J. Souther who provided the Castle Rock specimens, to Dr. K. Fletcher who gave his advice freely on atomic absorption techniques and to Mr. J. Harakal who did most of the probe work. The advice and help of Dr. R. Delavault, Miss S. Barr and Mr. A. Dhillon during the analytical portion of the study, and that of Mr. C. Fletcher on the use of computers is greatly appreciated. The loan of a typewriter from Mr. G. Cargill was invaluable. The receipt of an N.R.C. Post-graduate Scholarship during the period of this study is greatly appreciated.

CHAPTER 1

Introduction

Ultramafic nodules occur in basaltic rocks throughout the world (Forbes and Kuno 1965, 1967). The most common type of nodule is spinel peridotite, consisting of various proportions of olivine, diopside, enstatite and spinel. Garnet, hornblende, phlogopite, anorthite and more rarely melilite and leucite also occur as primary phases in ultramafic nodules (Green 1968). Gabbroic and granulitic rocks derived from the subvolcanic basement often occur in association with the ultramafic types. Gabbro appears to be the commonest type of nodule found in basalts of all types, but ultramafic nodules usually occur in basaltic rocks of alkalic affinities (White 1966; Forbes and Kuno 1967). Only rarely are they found in tholeiitic basalts.

Despite their relative scarcity, ultramafic nodules are important since they may yield information on the nature of the upper mantle and on the genesis of basalts. Ross et. al. (1954) first drew attention to the relationship between ultramafic nodules, dunites and the upper mantle. They found that ultramafic nodules around the world have a uniform mineralogy and chemistry and suggested that the nodules were derived from a uniform mantle peridotite. However, White (1966), Jackson (1968) and Kuno (1969) studied suites of nodules from Hawaii and found that they could be grouped according to mineralogy, chemistry and the character of the host rock. These authors have divided Hawaiian nodules into four groups. These are (a) a lherzolite series which forms part of the

upper mantle; (b) a dunite-wehrlite-pyroxenite series which forms crystal cumulates in the lower parts of the Hawaiian magma reservoirs; (c) an eclogite series which forms pockets in the dominantly lherzolitic mantle; (d) a gabbro series which forms part of the crust. Studies by Yamaguchi (1964), Kuno (1967), Aoki (1968) and Ishibashi (1970) have shown that there is also a wide variety of nodule types in Japan.

No single hypothesis seems adequate to explain the origin of all ultramafic nodules. Several hypotheses have been advanced to explain the origin of these rocks, including (a) they are fragments of the mantle; (b) they are crystalline residues of partially melted mantle; (c) they are products of crystal settling, formed during ascent of their basaltic hosts; (d) they are products of crystal settling, formed at some early stage of basalt formation, not necessarily the present host rock; (e) they are fragments of some earlier formed ultramafic body in the crust.

That any one of the above hypotheses holds for all nodules is not generally accepted. However there is still controversy over the origin of any particular type of nodule. Lherzolite, the commonest ultramafic variety, is of particular interest as it is analogous to "pyrolite", a hypothetical mantle rock (Ringwood 1966, 1969). White (1966) considers lherzolite nodules to be residue from fusion of the primitive mantle. Jackson (1968) considers lherzolite to be part of a heterogeneous mantle and dunite to be the refractory residue. Carter (1970) suggests that most lherzolite nodules are refractory residue from the upper mantle but that those relatively rich in iron

are cumulates. Kuno and Aoki (1970) have found a wide variety of lherzolite compositions throughout the world and suggest that this is a result of different degrees of partial melting in the mantle which is itself composed of lherzolite with a relatively low Mg:Fe ratio. O'Hara (1963, 1967, 1968) and Brothers (1960) support the hypothesis that lherzolite and other nodules are cognate. An accidental origin is considered, in general, to be unlikely, although instances are known where ultramafic nodules, including lherzolites, are thought to be xenoliths of sub-volcanic stratiform complexes (Fuster et. al. 1969).

In order to examine some of the problems outlined, particularly with regard to lherzolite, suites of nodules from British Columbia have been collected and studied by the writer. The objectives were twofold: (a) to describe the occurrence and types of nodules which have been found in British Columbia; and (b) to determine the differences and similarities between suites and relate these if possible to the source of the nodules.

The nodules and host rocks were studied by standard petrographic techniques. Petrofabric studies on the olivine and enstatite of the nodules were carried out using a 4-axes universal stage. The minerals of the nodules were separated and analysed by means of atomic-absorption spectrophotometry, electron microprobe and by wet-chemical means.

CHAPTER 2

The Localities of Nodules in British Columbia.

(a) Nodule localities.

The localities of ultramafic nodules which have been documented in the literature in British Columbia are shown on Fig. 1. Of these, suites from Castle Rock, Jacques Lake and Nicola Lake were studied. The host rocks were not studied in detail.

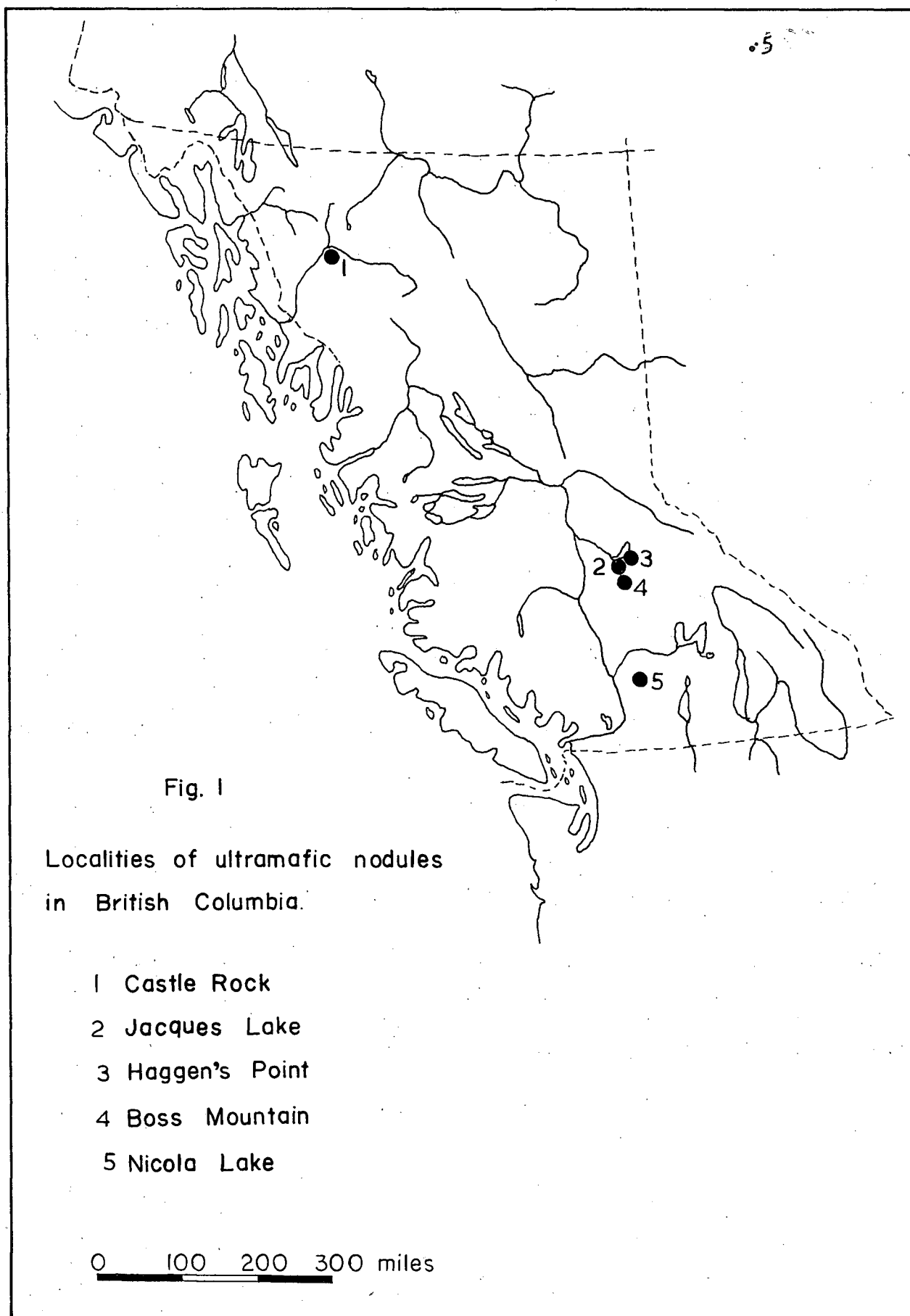
(b) Petrography of the host rocks.

(i) Castle Rock.

Castle Rock is a small peak on the northern flank of the Klastline Plateau, 40 miles east of Telegraph Creek in Northern British Columbia. It is one of several Quaternary volcanic centers which occur in the region (Souther 1970). Rounded nodules from 2 to 6 inches in diameter are found in a volcanic breccia, made up of sub-rounded fragments of a black fine-grained alkali basalt in a matrix of palagonite. The contact of the nodules and breccia is sharp; in some specimens there is a thin film of basalt coating the nodule. This film, petrographically identical to the basalt fragments, consists of small laths of plagioclase (An_{60}) set in a matrix of glass, olivine, magnetite and minor clinopyroxene. The film appears to have prevented the disintegration of the nodules during the explosive extrusion of the breccia. The breccia also contains small xenoliths of diorite; presumably these are fragments of an underlying intrusive body.

(ii) Jacques Lake.

The nodules at the Jacques Lake locality are found in a



small dissected cone 4 miles south of Quesnel Lake in Central British Columbia. The host rock is a coarse tuff exhibiting crude layering in places. The tuff is made up of rock fragments of various types and sizes, cemented by a brownish-green matrix consisting of small rock fragments and partly devitrified glass. The rock fragments consist of sedimentary, plutonic, metamorphic and volcanic xenoliths which are presumably representative of the crust beneath Jacques Lake. No single type is predominant and the size and frequency of each kind are highly variable. Ultramafic nodules, mainly lherzolite, are found infrequently throughout the cone.

Many of the nodules are coated with a thin film of basalt consisting of small laths of altered plagioclase in a fine-grained matrix of glass, magnetite and olivine (Fig. 2). This coating appears to be the original basalt within which the nodules were suspended before the extrusion of the tuff and has served a similar purpose to the coating around the Castle Rock nodules. The nodules are generally rounded or sub-rounded and range from 1 to 15 inches in diameter. Most are less than 6 inches in diameter.

The cone is Quaternary in age and appears to be similar to several other cones and flows of alkali basalt which occur in the area (Cambell 1961).

(iii) Nicola Lake.

Ultramafic nodules are found in scattered boulders 3 miles south of Nicola Lake in Central British Columbia. The host rock is a dark grey, fine-grained, vesicular basalt. It consists



Fig. 2

Basalt coating around lherzolite nodule in Jacques
Lake tuff.

of small laths of unzoned plagioclase (An_{60}), rounded olivine grains, interstitial glass and minor magnetite. Often partly corroded xenocrysts of olivine and pyroxene are found. The basalt is alkaline in character.

The age of the basalt is unknown but is possibly Tertiary. The boulders appear to have been brought to their present position by glacial action from the north where there is a large volume of Tertiary basalt. (K. C. McTaggart pers. comm.).

CHAPTER 3

Petrography of the nodules.

(a) General.

All the nodules studied consist of various proportions of olivine, clinopyroxene, orthopyroxene and spinel. Olivine is the dominant phase; orthopyroxene generally exceeds clinopyroxene; spinel is a minor phase.

The modes of 29 nodules from the three localities are shown on a ternary diagram (Fig. 3). For this purpose spinel is omitted but all nodules contain from 0.5 to 2% (by volume) spinel. Modes were calculated by point-counting from 30 to 300 grains in thin section, depending on the size of the nodule. Some of the results for the smaller nodules may not be accurate (particularly those from Nicola Lake), but are included for comparison. Modes of other nodules from British Columbia are shown for comparison. The data are taken from Soregaroli (1967) and Tredger (1969) for Boss Mountain and Haggan's Point respectively.

All the nodules studied are lherzolites. The nomenclature is in accordance with the classification of Jackson (1968). According to White (1966) and Kuno and Aoki (1970) lherzolite is the predominant ultramafic rock found as nodules at other localities around the world.

(b) Petrography of the nodules.

All the nodules from each suite have allotriomorphic granular textures, although there are some differences between the suites. The Castle Rock and Nicola Lake nodules are medium-

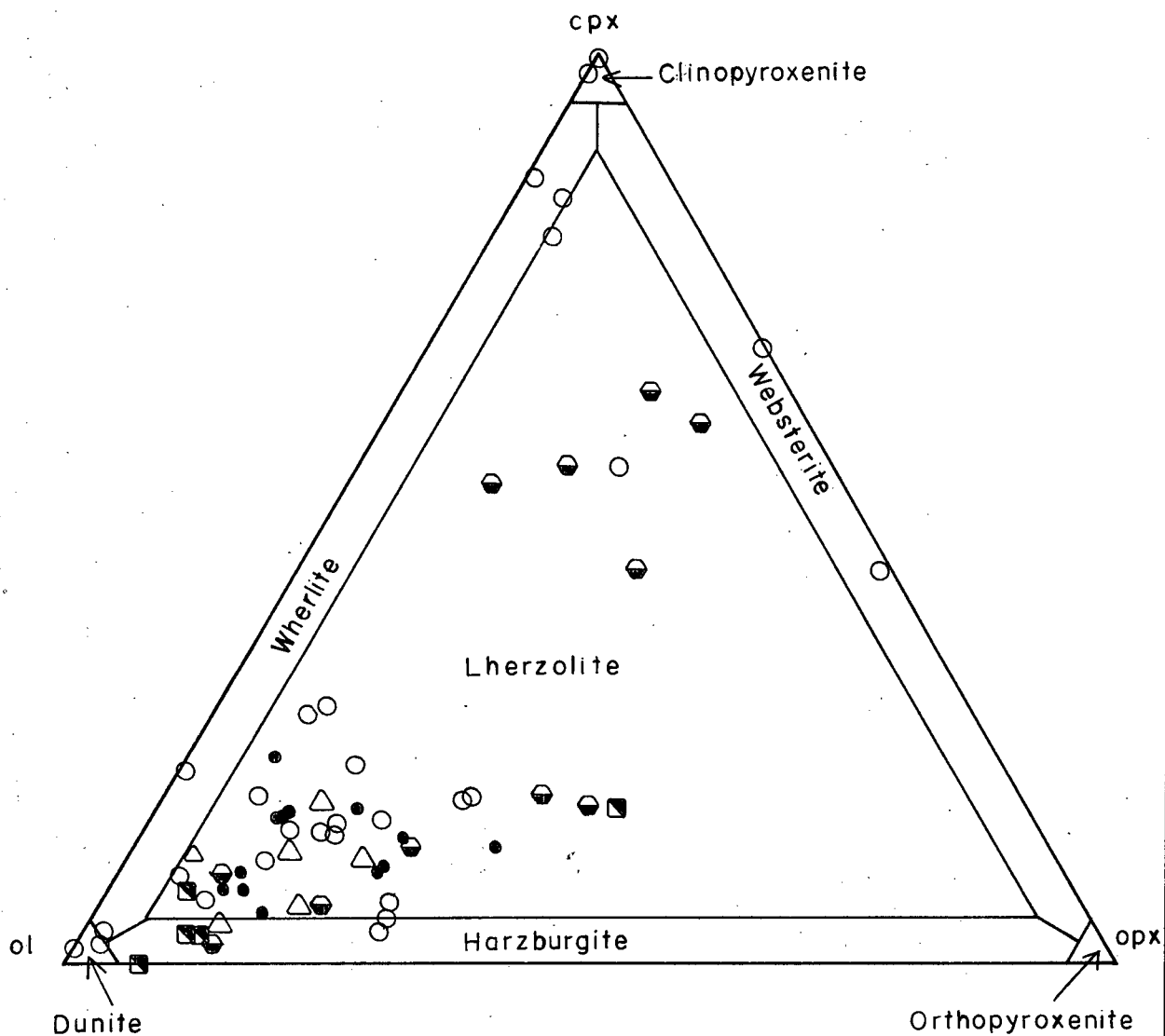


Fig. 3 : Modal composition of ultramafic nodules from British Columbia.

- | | |
|----------------|------------------|
| ● Jacques Lake | ○ Boss Mountain |
| △ Castle Rock | ◐ Haggen's Point |
| ■ Nicola Lake | |

grained, whereas the Jacques Lake ones are coarse-grained and are very friable.

Olivine forms an interlocking mosaic of rounded grains ranging in size from 0.5 to 2.00 mm. in diameter. In many of the Nicola Lake specimens some grains have mutually interfering boundaries. In some of the Jacques Lake specimens olivine may be up to 5.00 mm. in diameter. In all suites it is pale green. Orthopyroxene forms subhedral grains some of which are larger than the olivine and partly enclose it and others that are small, anhedral and are interstitial to the olivine. It is dark brown in hand specimen and colourless in thin section. Clinopyroxene forms small anhedral grains, generally not more than 0.5 mm. in diameter, interstitial to both olivine and orthopyroxene. It tends to occur as aggregates of three or four grains. It is a bright emerald green in hand specimen and colourless or pale green in thin section. Spinel occurs as irregularly shaped grains interstitial to and partly enclosing the silicates, particularly the pyroxenes (Fig. 4). It is black in hand specimen and reddish-brown in thin section.

Exsolution lamellae are found in some of the silicates. Lamellae of clinopyroxene in orthopyroxene (parallel to $\{100\}$ of the host) are found only in the largest orthopyroxenes. They are thin and pinch out towards the boundary of the host (Fig. 5). Both pyroxenes and very rarely olivine contain thin lamellae of a brown isotropic mineral which is presumed to be spinel (Figs. 6, 7). In the pyroxenes the lamellae are sub-parallel

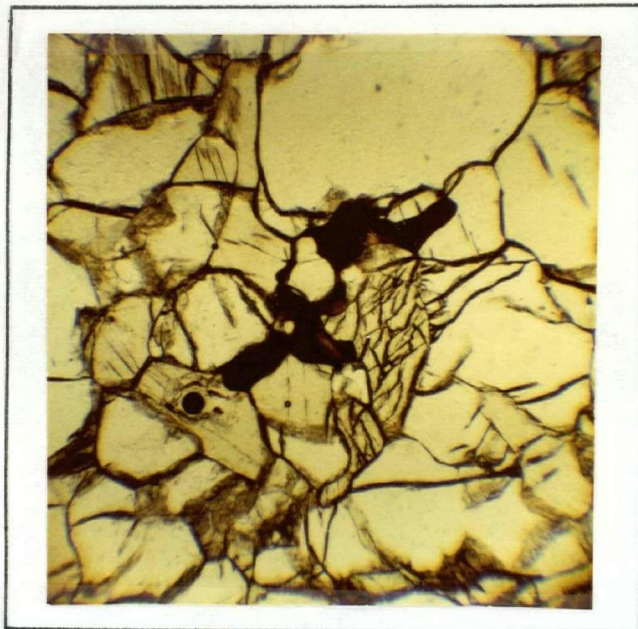


Fig. 4

Aggregate of spinel (brown) and clinopyroxene (grains with cleavage); grains with no cleavage showing are olivine; specimen S-2. X-30; plane polarised light.

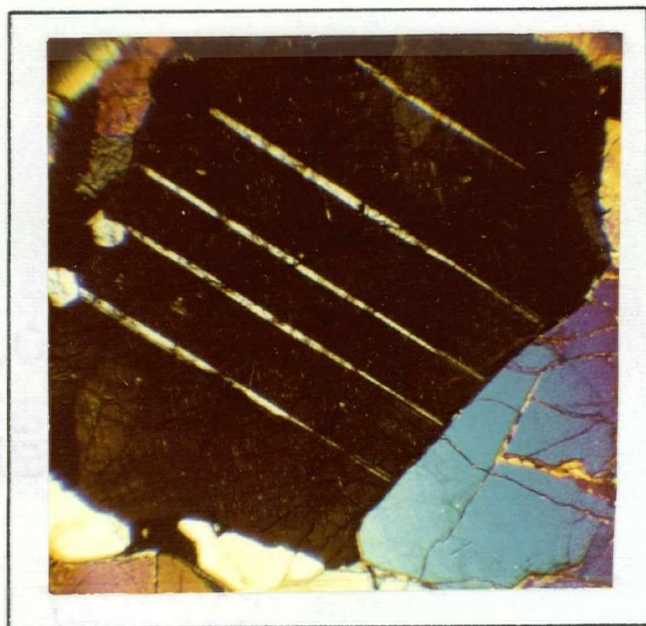


Fig.5

Exsolution of clinopyroxene in orthopyroxene (dark); specimen JL-50. X-30; crossed nicols.

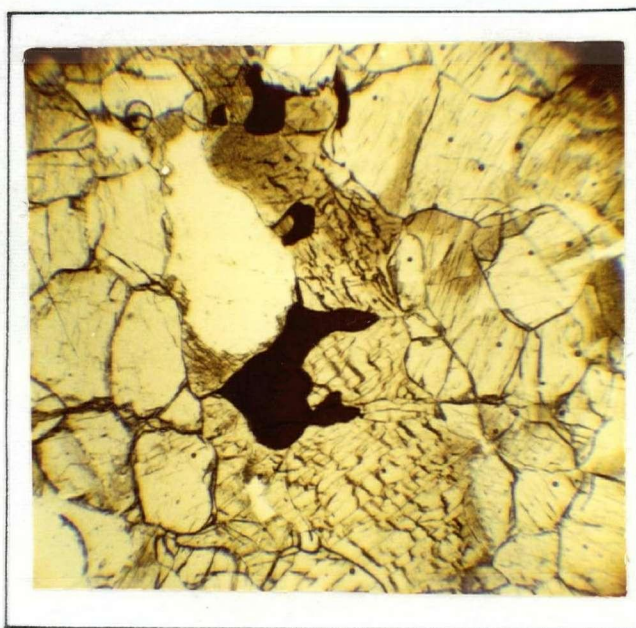


Fig. 6

Exsolved spinel (brown) in orthopyroxene (grains with cleavage); specimen S-3. X-30; plane polarised light.



Fig. 7

Spinel (brown lamellae) exsolved in olivine (yellow); specimen JL-50. X-30; crossed nicols.

to {001} and in the olivine they are parallel to the (010) cleavage.

Many of the nodules show signs of deformation such as kink bands in the olivines. A discussion of deformation follows in Chapter 4.

Some specimens from Castle Rock are layered. Specimen S-4 has two well-defined bands, each about 5 mm. thick, of clinopyroxene which are separated by a thicker band of olivine (Fig. 8). In other nodules there is an ill-defined layering marked by thin disseminated stringers of spinel (Fig. 9) or orthopyroxene. Other nodules are massive. Specimens from Jacques Lake do not in general show layering. Rarely, banding similar to that observed in S-4 above was seen in the field. Unfortunately these specimens could not be broken out of the host tuff. None of the Nicola Lake nodules show layering but their small size might make this difficult to see.

(c) Secondary textural features.

Most of the nodules from all three suites show evidence of disequilibrium between the enclosing rock and the primary minerals. Usually reaction has taken place at the margin of the nodule, although in some specimens (particularly from Jacques Lake) basalt has been able to permeate the whole rock so that the minerals of the interior have been affected.

Olivine shows the least effects of reaction with the host. Where in contact with basalt, the margin of the olivine grains commonly shows a fine-grained rim of secondary olivine and magnetite.



Fig. 8

Mineralogical banding in specimen S-4 from Castle Rock. The bright green bands are diopside; lighter green is olivine.

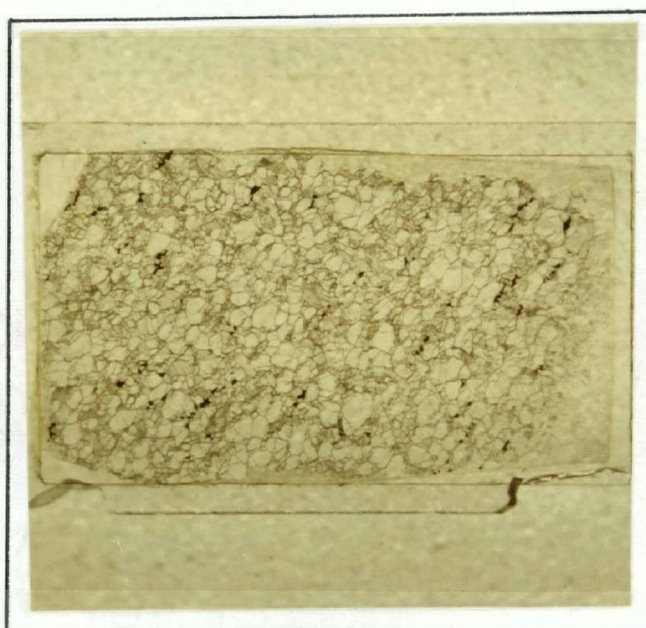


Fig. 9

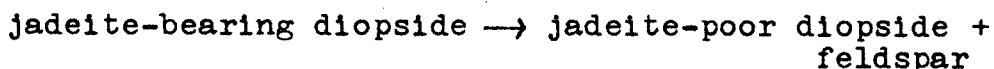
Sheared spinel (brown) cutting through silicates; specimen S-2 from Castle Rock.

Spinel grains in contact with the host have a dark margin, presumed to magnetite.

Orthopyroxene, where in contact with the host rock, has a rim of rim of finely divided material of high birefringence set in a dark cryptocrystalline matrix (Fig.10). This appears to be a result of incongruent melting of orthopyroxene which has produced olivine and glass.

The clinopyroxene of some nodules in contact with the host rock has a thin rim of secondary clinopyroxene. In the Jacques Lake nodules and rarely in those from Castle Rock, the clinopyroxenes have a porous-looking outer zone which may be up to a third of the diameter of the grain in width (Fig. 11). The entire grain extinguishes uniformly and has uniform birefringence. The spongy zone is riddled with an extremely fine-grained dark material which appears to be partially devitrified glass. This rim is entirely different from the rims observed at the margins of the nodules which are of secondary pyroxene with different extinction from the parent.

According to White (1966) similar features are a result of a depletion in the jadeite component of the pyroxene thus:



The reaction rims occur throughout the rock and for reasons given in Chapter 8, they are considered here to be a result of partial melting.

All the reaction phenomena described here have been reported elsewhere (Wilshire and Binns 1961; Talbot et. al. 1963;

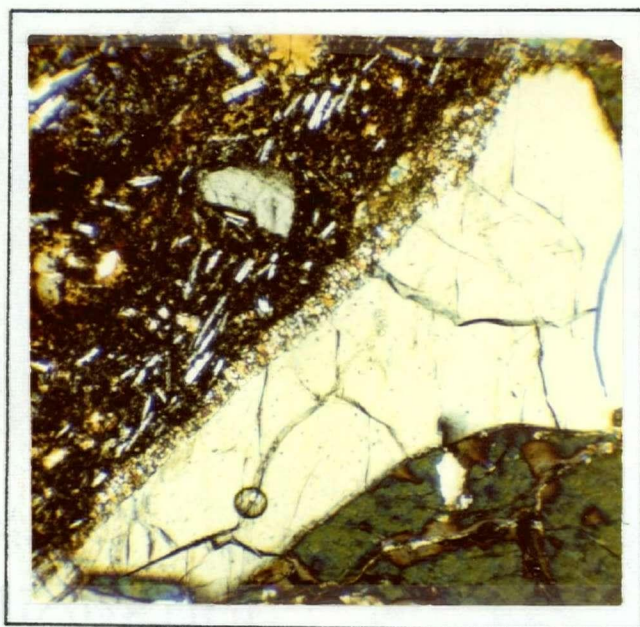


Fig. 10

Reaction of orthopyroxene at margin of host. The highly birefringent material is secondary olivine; specimen S-4. X-100; crossed nicols.

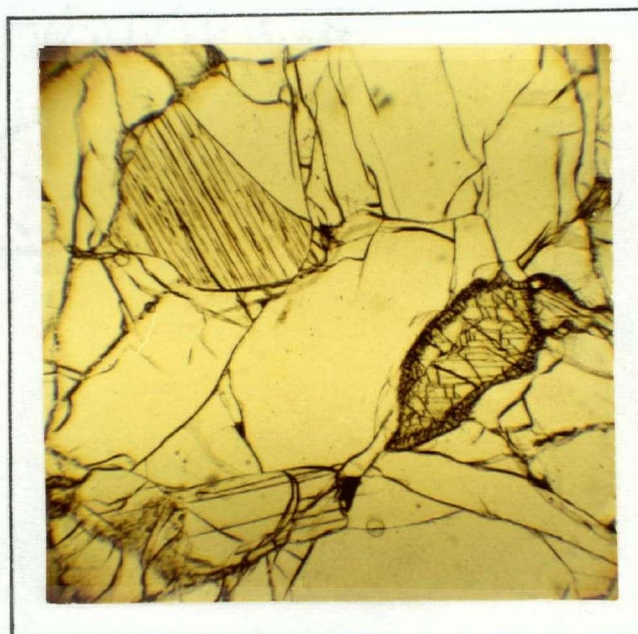


Fig.11

Porous-looking outer rim of clinopyroxene (on right). The orthopyroxene (on left) is unaffected. The mineral with no cleavage showing is olivine; specimen JL-24. X-30; plane polarised light.

Yamaguchi 1964; White 1966; Kutolin and Frolova 1970). The reaction textures indicate disequilibrium between nodules and magma at a high crustal level but do not preclude equilibrium at greater depth.

Fluid inclusions were found in olivines in most nodules from all the suites. In some cases they were also observed in pyroxenes. Many of these are two phase (gas + liquid) inclusions. Roedder (1965) has found two phase fluid inclusions in olivines from many localities. Most of these are CO_2 ; H_2O is found in some nodules. The composition of the inclusions in the B.C. nodules is unknown.

Most of the inclusions are found along fractures (Fig. 12) and along the cleavage of the olivine. In some cases planes of inclusions cut across fractures (Fig. 12). They are most abundant where the basalt has penetrated the nodule. They thus appear to be secondary and may have formed after the nodules were captured by their hosts. Some inclusions may be primary, but distinguishing these from secondary ones is uncertain.

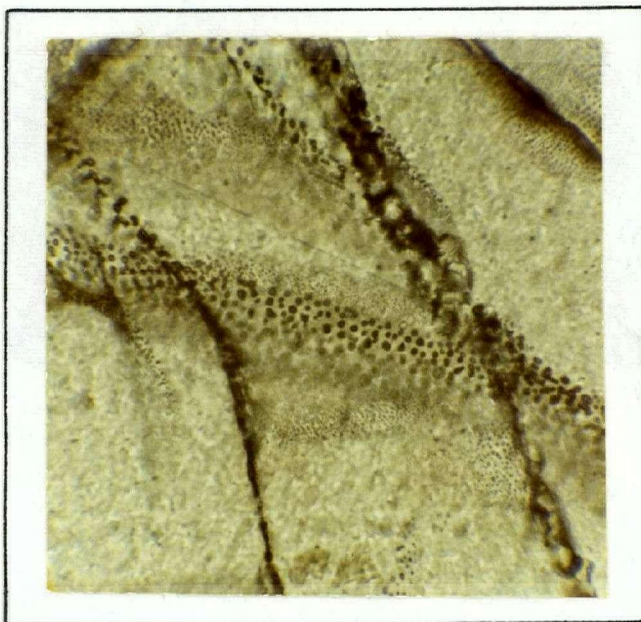


Fig. 12

Fluid inclusions aligned along fractures in
olivine; specimen JL-50. X-400.

CHAPTER 4

Petrofabric Study.

(a) General.

Previous work on ultramafic nodules has revealed that the olivine in many nodules has a preferred orientation (Turner 1942; Brothers 1959, 1960; Talbot et. al. 1963; Collee 1963; Black and Brothers 1965; Brothers and Rodgers 1969). These authors have shown that there is a variety of olivine fabrics in nodules and have attempted to draw analogies between the olivine orientation patterns found in nodules and those found in olivine-bearing rocks from other environments. Thus Brothers (1960) compared olivine fabrics in nodules to those in flow-banded troctolites and basic dykes and suggested the nodules formed by crystal settling in a moving magma. Other workers consider that the fabrics of olivine from nodules are similar to those of rocks which have been deformed.

In order to determine whether olivines from nodules in British Columbia have a preferred orientation, and if so, whether such an orientation could be related to the source of the nodules, fabric diagrams for olivine of three nodules from Castle Rock, three from Jacques Lake and one from Nicola Lake were prepared. An enstatite fabric diagram of one of the Castle Rock nodules was also prepared.

The orientation of the olivine and enstatite principal optic directions was measured on a 4-axes universal stage. Two of these were determined in this way, the third being found by construction. The diagrams were constructed on the lower

hemisphere of a Schmidt net. Measurements were made on every grain intersected on suitably spaced lines of traverse in order to minimise sampling errors.

(b) Description of the fabrics.

Figs. 13, 14 and 15 are the fabric diagrams for the Jacques Lake nodules. All three nodules have similar olivine fabrics, although there are some differences between each one. The main element of the fabrics is the three mutually perpendicular maxima. In specimen JL-24 (Fig. 15) and JL-A (Fig. 13) this is modified. In these fabrics β forms a weak partial girdle. In addition JL-24 (Fig. 15) has a fabric in which α forms a well-developed girdle while still retaining the strong γ maximum.

Kink bands in the olivines are common, particularly in the larger grains (Fig. 16). The grain boundaries tend to be straight and to have triple grain boundary angles of 120° .

The olivine from the Nicola Lake nodule has a very weak preferred orientation in which the three principal optic directions are mutually perpendicular. Each maximum is ill-defined and the fabric is essentially random (Fig. 17).

Kink bands in these olivines are also fairly common but polygonisation is not a textural feature of the olivines of this nodule. The texture of this nodule, and also others of this suite, is typical of cumulate rocks in which the grain boundaries are mutually interfering (Fig. 18).

Figs. 19, 20 and 21 are the fabric diagrams for the olivines of the Castle Rock nodules. The main feature of these is that γ forms a strong maximum perpendicular to a β - α girdle. α and β form less prominent maxima within the girdle. Specimen

Explanation of Figs. 13, 14, 15 and 17.

Fig. 13

Olivine fabric diagram of specimen JL-A from Jacques Lake.
50 grains.

Contours at 2, 4, 6, 8% of 1% area.

Maximum concentrations are 8, 8, 10% for α , β , γ respectively.

Mode: ol. 77, opx. 11, cpx. 11, spin. 1.

Fig. 14

Olivine fabric diagram of specimen JL-50 from Jacques Lake.
50 grains.

Contours at 2, 4, 6, 8% of 1% area.

Maximum concentrations are 6, 10, 10% for α , β , γ respectively.

Mode: ol. 63, opx. 19, cpx. 17, spin. 1.

Fig. 15

Olivine fabric diagram of specimen JL-24 from Jacques Lake.
50 grains.

Contours at 2, 4, 6, 8, 10% of 1% area.

Maximum concentrations are 14, 8, 10% for α , β , γ respectively.

Mode: ol. 90, opx. 2, cpx. 7, spin. 1.

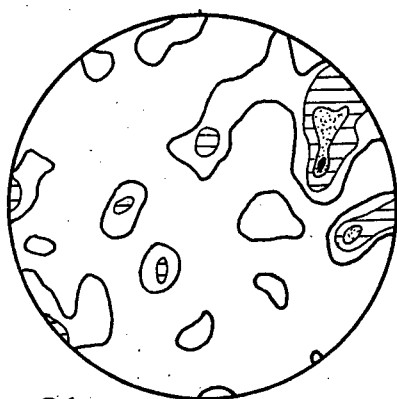
Fig. 17

Olivine fabric diagram of specimen NL-8 from Nicola Lake.
50 grains.

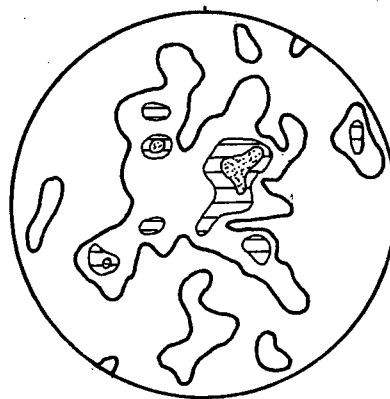
Contours at 2, 4, 6, 8% of 1% area.

Maximum concentrations are 8, 8, 10% for α , β , γ respectively.

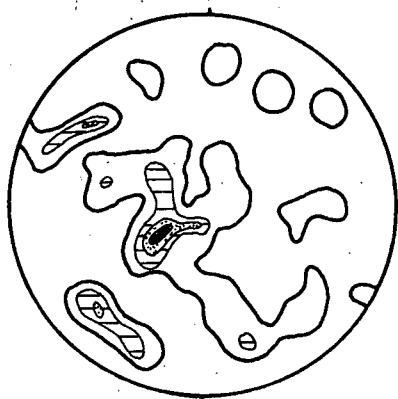
Mode: ol. 83, opx. 7, cpx. 9, spin. 1.



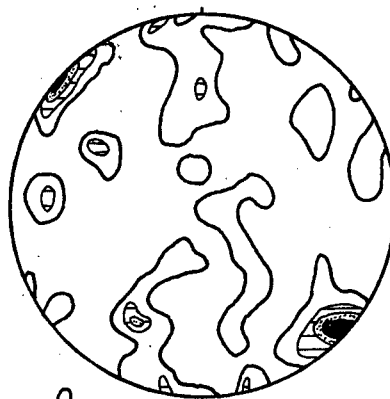
α



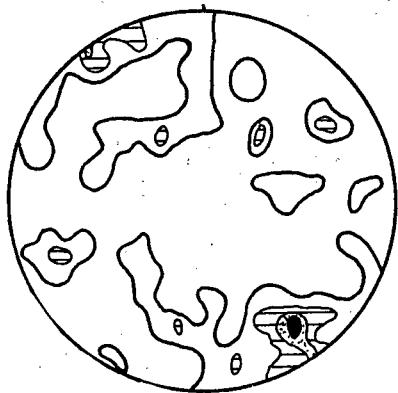
α



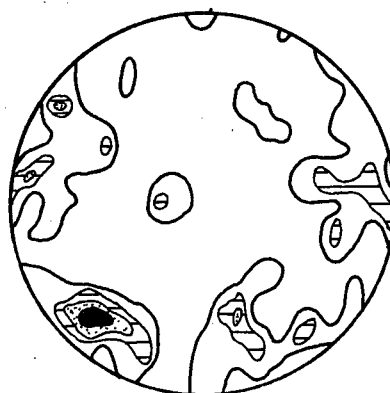
β



β



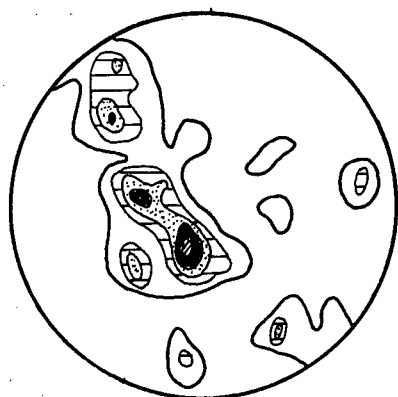
γ



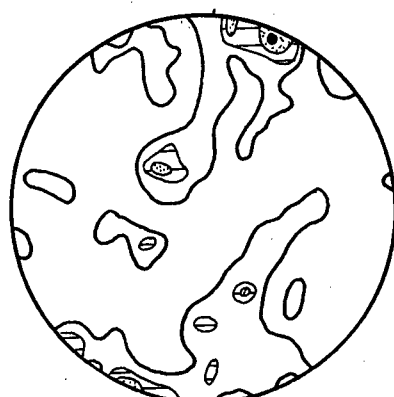
γ

Fig. 13

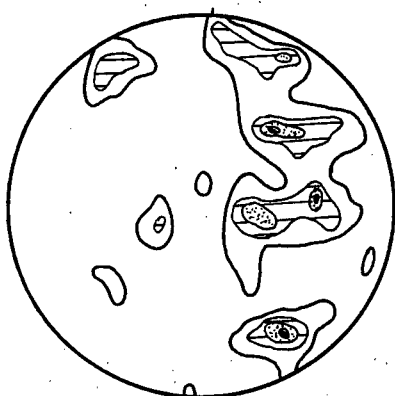
Fig. 14



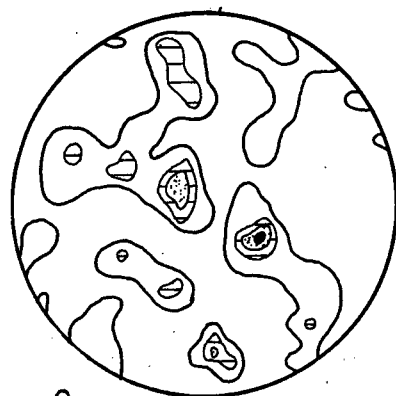
α



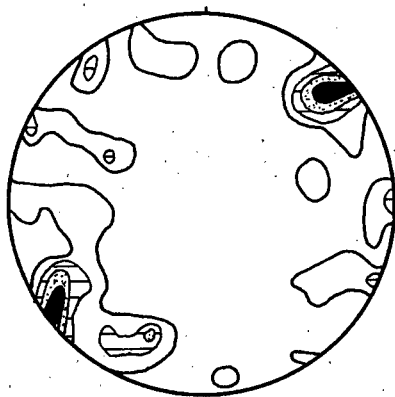
α



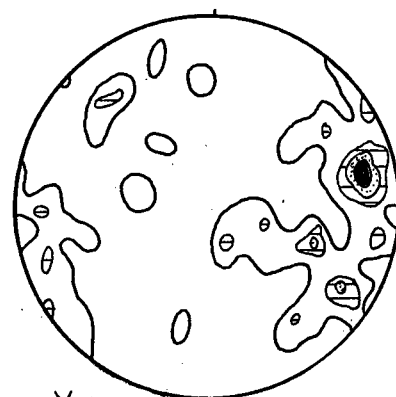
β



β



γ



γ

Fig. 15

Fig. 17

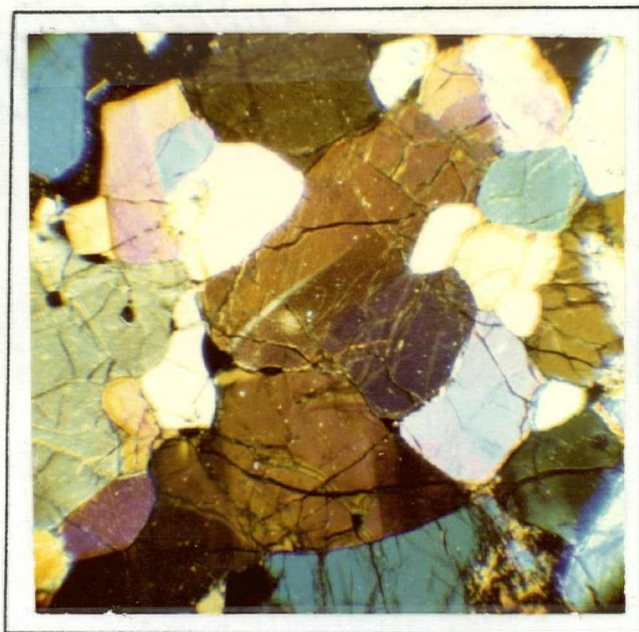


Fig. 16

Strained olivine with abundant kink bands;
specimen JL-50 from Jacques Lake.
X-30; crossed nicols.

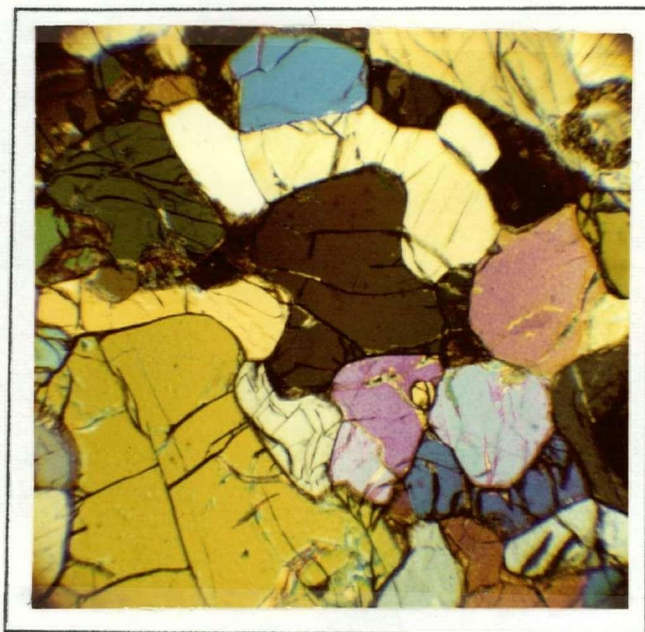


Fig. 18

Mutually interfering grain boundaries between
olivine and orthopyroxene (grey and yellow);
specimen NL-8 from Nicola Lake.
X-30; crossed nicols.

S-4 is layered and has been described previously. The orientation of the layering is shown in Fig. 20. The plane of the layering and the $\beta - \alpha$ girdle coincide and γ is perpendicular to the layering.

Many of the olivines of the Castle Rock nodules have kink bands. These are found only in the larger grains. The smaller ones are strain-free and form a mosaic with straight grain boundaries meeting at 120° , (Fig. 22).

In addition to the olivine, an enstatite fabric diagram for sample CR-8 was constructed (Fig. 23). The enstatite in this nodule has a poor preferred orientation. There is a suggestion that γ is perpendicular to an ill-defined $\beta - \alpha$ girdle, but more data are required to confirm this. Comparison with the olivine fabric from the same rock (Fig. 21) shows that there is apparently no correspondence between the olivine and the enstatite fabrics. This is in contrast to the findings of Collee (1963) and Rodgers and Brothers (1969).

(c) Discussion.

According to Rodgers and Brothers (1969) there are five orientation rules for olivine in ultramafic nodules. These are :

- (1) α maximum perpendicular to a $\beta - \gamma$ girdle.
- (2) γ maximum perpendicular to a $\beta - \alpha$ girdle.
- (3) γ and β maxima perpendicular to a α girdle.
- (4) γ , β , α mutually perpendicular.
- (5) No obvious orientation.

Transitional fabrics also occur. The fabrics which are found in lherzolite nodules are (1) and (4). This study has shown that

Explanation of Figs. 19, 20, 21 and 23.

Fig. 19

Olivine fabric diagram of specimen S-2 from Castle Rock.
 100 grains.
 Contours at 1, 2, 4, 6, 8, 10% of 1% area.
 Maximum concentrations are 6, 7, 12% for α , β , γ respectively.
 Mode: ol. 77, opx. 16, cpx. 6, spin. 1.

Fig. 20

Olivine fabric diagram for specimen S-4 from Castle Rock.
 50 grains.
 Contours at 2, 4, 6, 8, 12% of 1% area.
 Maximum concentrations are 6, 12, 18% for α , β , γ respectively.
 Mode: ol. 72, opx. 15, cpx. 12, spin. 1.

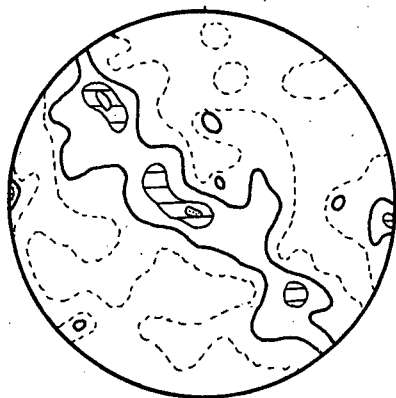
The great circle is the plane of the layering.

Fig. 21

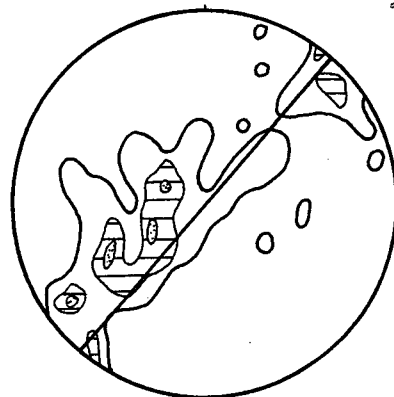
Olivine fabric diagram for specimen CR-8 from Castle Rock.
 50 grains.
 Contours at 2, 4, 6, 8% of 1% area.
 Maximum concentration are 8, 8, 10% for α , β , γ respectively.
 Mode: ol. 63, opx. 23, cpx. 12, spin. 2.

Fig. 23

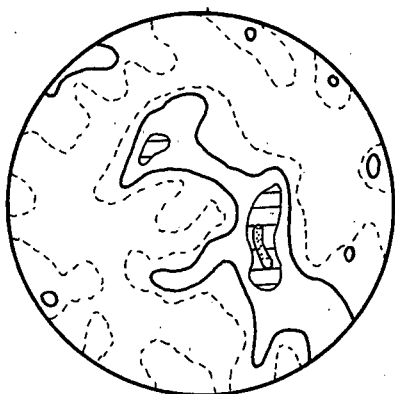
Enstatite fabric diagram for specimen CR-8 from Castle Rock.
 50 grains.
 Contours at 2, 4, 6, 8% of 1% area.
 Maximum concentrations are 6, 6, 8% for α , β , γ respectively.
 Mode: ol. 63, opx. 23, cpx. 12, spin. 2.



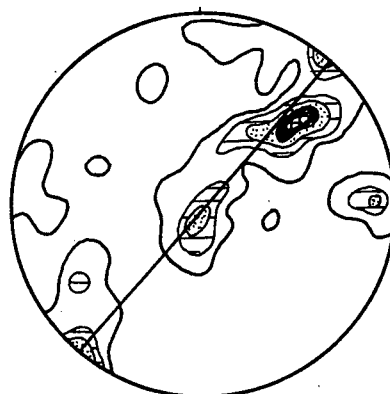
α



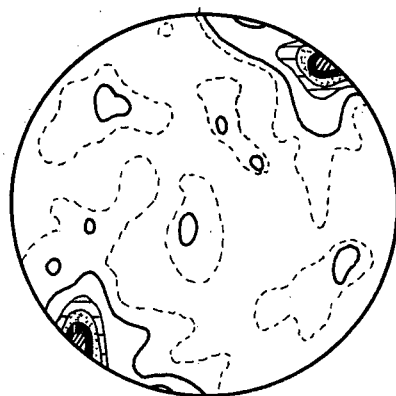
α



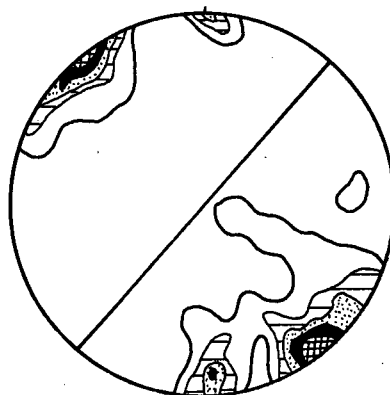
β



β



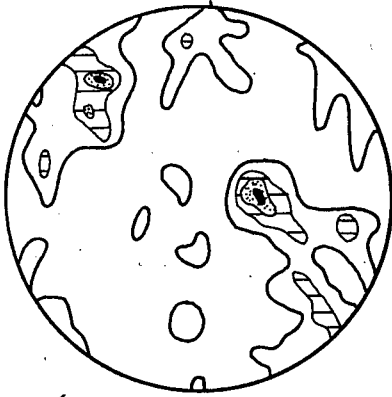
γ



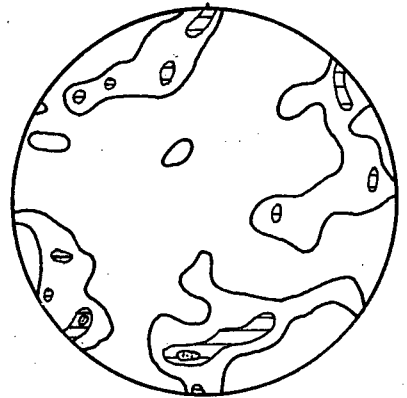
γ

Fig. 19

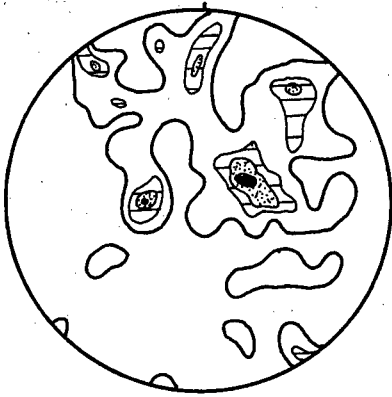
Fig. 20



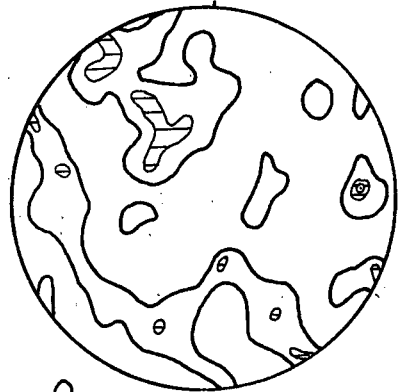
α



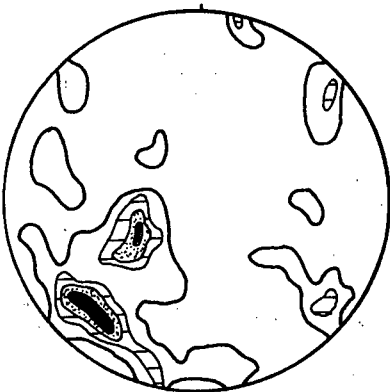
α



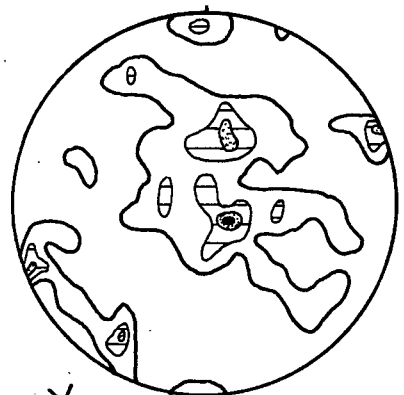
β



β



γ



γ

Fig. 21

Fig. 23

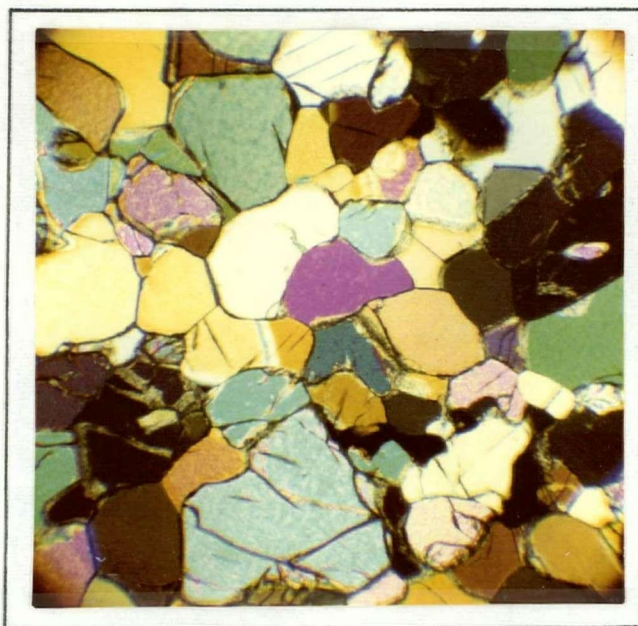


Fig. 22

Strain free, recrystallised olivine with
triple grain boundaries of 120° ; specimen
CR-8 from Castle Rock.
X-30; crossed nicols.

olivine in lherzolite nodules may also follow rule (2). This type of fabric has only been found previously (apart from peridotites) in dunite and harzburgite nodules (Rodgers and Brothers 1969) and in an isolated "olivine nodule" (Talbot et. al. 1963). The mode of this nodule was not reported.

Raleigh (1968) and Carter and Ave'Lallement (1970) have found that deformation of olivine at high temperature results in gliding on $\{0kl\}$. The axis of external rotation is $[100]$. The orientation of the glide plane is dependant on temperature and strain rate. At high temperature and low strain rate the glide plane is (010). This is the plane on which slip occurs in most naturally deformed olivines, resulting in the formation of kink bands. Polygonisation and recrystallisation result in the disappearance of the kink bands. Kink bands in olivine are not in themselves evidence of deformation in the solid state, Brothers (1962) has found that these bands are present in olivines in some basalts and gabbros which are undeformed. They may result from flow in the magma from which the olivine crystallised.

Both kink banding and polygonisation are common in the olivines of the Jacques Lake and Castle Rock nodules (Figs. 16 and 22). This suggests that these nodules have been deformed and have recrystallised (Raleigh 1968; Ragan 1969; Carter and Ave'Lallement 1970). The Nicola Lake nodules, on the other hand, are apparently undeformed since evidence of recrystallisation is absent.

Evidence from the olivine fabrics supports the above suggestions. The typical fabrics developed by olivine formed from a magma are types (4) and (5) and less commonly type (1) of the above

classification (Brothers 1959, 1962, 1964). The Nicola Lake olivine fabric is transitional between types (4) and (5) and could therefore have resulted from the olivine having crystallised from a magma.

There is a range of fabrics shown by the Jacques Lake nodules. The fabric for JL-50 (Fig. 15) corresponds to type (4). JL-A (Fig. 13) is a modified type (4) fabric in which β forms a weak girdle.

Slip on the system $\{okl\}$, $[100]$ may explain the variations in the fabrics of this suite. If the initial fabric of the source rock was a simple pattern (possibly produced by crystal settling or perhaps by deformation) represented by JL-50 (Fig. 14), then deformation would result in the maxima for $\alpha \equiv [010]$ and $\beta \equiv [001]$ being rotated about $\gamma \equiv [100]$ which is the zone axis for glide. This would result in the formation of girdles in α and β ; γ would remain as a maximum. Specimen JL-24 (Fig. 15) shows this to some extent where α forms a girdle perpendicular to γ and β forms a weaker girdle. Perhaps translation as well as rotation was involved in the formation of this fabric as β is not in the same plane as α . An exact geometrical analysis of these fabrics is not possible since a sample of 50 grains is insufficient to determine precise angular relationships. Further complications are introduced by the fact that the orientation of recrystallised olivine grains is, in part, controlled by the initial fabric (Ave'Lallement and Carter 1970).

Despite the speculative nature of the above discussion, the range of fabrics (which are unlike those produced solely by crystal accumulation), coupled with evidence of recrystallisation given above suggests that the Jacques Lake nodules have been

deformed. Recrystallisation is not complete as some of the larger olivines are still strained (Fig. 16). This could explain why there is a range of fabrics of the olivines of this suite.

A single fabric type has been found in the Castle Rock nodules. This is type (2) of the above classification ($\gamma \perp \beta - \alpha$ girdle). Fabrics developed by olivine formed from a magma have been reported above. As far as could be determined from the literature the fabrics of these olivines have no analogues among olivines from igneous environments. This type of fabric has been found in deformed Alpine peridotites and other types of ultramafic nodules (Ave'Lallement and Carter 1970; Talbot et. al. 1963; Rodgers and Brothers 1969). More commonly the typical olivine fabric of a strongly deformed peridotite is one where $\alpha \perp \beta - \gamma$ girdle (type (1) of the above classification).

The nodules from Castle Rock are layered. This has been described in Chapter 3. Mineralogical layering in a rock can arise in at least two ways. These are: (a) by accumulation of minerals in a magma, and (b) by metamorphism and deformation or metasomatism. Both these processes may result in a preferred orientation of some mineral (in this case, olivine).

To produce a fabric by crystal accumulation requires a dimensional orientation of olivine. No such orientation was found in the Castle Rock olivines. This can be explained by suggesting that intercumulus growth took place which masked the original shape of the grains (Jackson 1961). However this would still produce a fabric which is typical of cumulate rocks. This is not the case for the Castle Rock nodules.

Metamorphic banding in peridotites is a common feature (Thayer 1969; Loney et.al. 1970). The banding takes the form of monomineralic veins and dykes and discontinuous stringers of minerals. Both types are found in the Castle Rock nodules (Figs. 8 and 9). The form of the spinel in specimen S-2 in which it appears to be flattened and to cut through the silicates (Fig. 9) suggests that there may have been an element of shear in the formation of the layering. Loney et. al. (1970) have found that mineralogical layering is sub-parallel or parallel to an axial plane foliation in a deformed peridotite. The axial plane is perpendicular to an α maximum and parallel to a β - δ girdle. It is possible that the fabric of these nodules is related to a similar deformational feature although in this case the layering contains a β - α girdle and δ forms a maximum at right angles to it. This type of fabric is characteristic of some deformed peridotites (Ave'Lallement and Carter 1970).

It is thus suggested that the Castle Rock and Jacques Lake nodules have been deformed. The basis of this is a comparison with the fabrics of deformed peridotites and magmatic olivines and by the textures of the olivines in these nodules. Deformation must have occurred prior to the nodules having been captured by the magmas which brought them to the surface.

The different fabric types of the two suites suggests that the source rocks of the suites underwent different deformational histories. Factors which influence the type of fabric which is developed by the olivine of a peridotite are the orientation of the principal stresses with respect to the original fabric,

temperature, strain rate and the presence or absence of water (Ave'Lallement and Carter 1970). Pressure has apparently little influence on the fabric type although Ave'Lallement and Carter (1970) imply (p.2214) that very high pressure is required to produce a fabric similar to that found in the Castle Rock nodules. This fabric type has not been reproduced experimentally so that the conditions under which it formed are unknown. Experimental recrystallisation of olivine takes place at temperatures above 900°C (Ave'Lallement and Carter 1970) so that the deformation of these nodules probably occurred at high temperature.

CHAPTER 5

Mineral Compositions.

(a) Introduction.

Partial mineral analyses presented in this study were carried out by means of atomic absorption spectrophotometry, electron microprobe and by wet chemical means. Details of the analytical methods and the precision of the results are given in Appendix 1. Only the four primary minerals (olivine, orthopyroxene, clinopyroxene, spinel) were analysed.

The results of this study reaffirm the findings of many workers that the minerals of ultramafic nodules (particularly lherzolite) have a restricted compositional range. The compositional range of these minerals is similar in both major and minor elements to the ranges of other published analyses. This study also shows that the compositional range of the minerals in any particular suite of nodules is characteristic of that suite.

The analysed minerals were chosen from nodules which had as wide a range of modal compositions as possible so as to include all possible variations.

TABLE 1 : Modes of nodules with analysed minerals.

Sample	Locality	Ol.	Cpx.	Opx.	Spin.
JL-A	Jacques Lake	77	11	11	1
JL-39	"	71	16	12	1
JL-10	"	62	12	24	2
JL-B	"	68	22	8	2
JL-55	"	80	8	10	2
95	Castle Rock	74	6	19	1
S-3	"	83	5	11	1
CR-8	"	63	12	23	2
ERC-11	"	66	17	15	2
NL-8	Nicola Lake	83	9	7	1

(b) Olivine.

Partial chemical analyses of olivines are given in Table 2. Of the four primary minerals, olivine has the most restricted range. It ranges from $Fo_{89.5}$ to $Fo_{91.0}$ in the Castle Rock and Jacques Lake nodules. The olivine of the Nicola Lake nodule has a composition of $Fo_{91.8}$. The range is similar to that found elsewhere (e.g. White 1966). There is no significant difference in the range of major elements in olivine among the suites.

The range of values for Ni, Mn, Co, Cu and Zn and also CaO and Na_2O is similar to the range found elsewhere (Ross et. al. 1954; Forbes and Banno 1966; Simkin and Smith 1970; Carter 1970). The Pb content of the olivines is variable and appears to be high for ultramafic rocks. Goles (1967) suggests 0.5ppm. as an average for ultramafic rocks as a whole. While no data are available on the Pb content of olivines from ultramafic rocks, this figure suggests that the olivines of these nodules are enriched in Pb (Table 2) relative to the olivines of other ultramafic rocks.

(b) Orthopyroxenes.

Partial analyses of orthopyroxenes are given in Table 3. The Jacques Lake orthopyroxenes range in composition from $En_{89.4}$ to $En_{90.1}$ and those from Castle Rock range from $En_{90.5}$ to $En_{91.9}$. The Nicola Lake orthopyroxene has a composition of $En_{89.5}$. The Castle Rock samples are slightly more magnesian than those of Jacques Lake or Nicola Lake. The Al_2O_3 content ranges from 3.50 to 5.90%. With one exception (ERC-11), the Castle Rock orthopyroxenes contain less Al_2O_3 than those of Jacques Lake (Table 3).

TABLE 2

Partial chemical analyses of olivines.

Sample	95	S-3	CR-8	ERC-11	NL-8	JL-A	JL-39	JL-10	JL-B	JL-55
Oxide(wt.%)										
FeO*	9.25	8.45	9.56	9.60	8.38	9.66	9.91	9.95	9.70	10.42
MgO	50.0	50.0	46.9	48.1	52.8	48.4	47.9	47.1	50.8	48.3
CaO	0.05	0.05	0.03	0.04	0.04	0.05	0.03	0.04	0.05	0.04
MnO	0.11	0.10	0.10	0.12	0.09	0.12	0.12	0.11	0.12	0.16
NiO	0.32	0.31	0.32	0.34	0.24	0.33	0.35	0.33	0.31	0.36
Na ₂ O	0.21	0.19	0.22	0.08	0.19	0.33	0.61	0.32	0.59	0.27
Fe/Fe+Mg	10.13	9.20	10.29	10.08	8.18	10.08	10.39	10.22	9.71	10.52
Minor elements in ppm.										
Ni	2472	2845	2511	2640	1895	2619	2737	2604	2465	2861
Mn	897	751	763	911	702	929	956	889	913	1027
Co	119	133	122	140	132	140	129	125	130	137
Zn	53	52	49	62	46	48	62	55	57	48
Pb	80	64	28	64	22	35	78	80	77	72
Cu	1.2	0.8	0.6	0.7	1.1	1.2	1.2	1.2	1.0	0.7

*Total iron as FeO

TABLE 3

Partial chemical analyses of orthopyroxenes.

Sample	95	S-3	CR-8	ERC-11	NL-8	JL-A	JL-39	JL-10	JL-B	JL-55
Oxide(wt.%)										
TiO ₂	0.06	0.06	0.08	0.14	0.10	0.22	0.26	0.14	0.16	0.12
Al ₂ O ₃	3.68	3.54	3.50	5.90	4.04	4.46	4.68	4.40	4.60	4.66
Cr ₂ O ₃	0.37	0.35	0.31	0.26	0.10	0.46	0.48	0.48	0.33	0.33
FeO*	5.80	5.27	5.74	5.91	6.17	6.43	6.42	6.17	6.20	6.56
MgO	32.2	33.6	32.5	31.6	29.5	31.9	31.3	30.7	31.6	31.1
CaO	0.76	0.73	0.67	1.33	1.03	0.94	0.82	0.85	0.79	1.38
MnO	0.11	0.11	0.11	0.11	0.12	0.11	0.10	0.11	0.11	0.11
NiO	0.11	0.11	0.12	0.12	0.12	0.11	0.10	0.11	0.10	0.12
Na ₂ O	0.21	0.13	0.27	0.45	0.24	1.00	0.32	0.31	0.24	0.50
K ₂ O	0.01	0.01	0.01	0.01	0.01	0.01	0.01	0.01	0.01	0.01
Fe/Fe+Mg	9.20	8.08	9.02	9.51	10.51	10.16	10.31	10.15	9.91	10.59
Fe/Fe+Mg+Ca	9.06	7.99	8.90	9.25	10.28	9.97	10.14	9.94	9.75	10.18
Mg/Fe+Mg+Ca	89.42	90.60	89.76	88.09	87.51	88.16	88.19	88.26	88.66	87.06
Ca/Fe+Mg+Ca	1.52	1.41	1.34	2.66	2.21	1.87	1.67	1.80	1.59	2.76
CaTs(mol.%)	3	3	2	5	0	2	2	3	3	5
MgTs(mol.%)	2	4	3	7	0	5	4	2	4	4
Minor elements in ppm.										
Ti	330	360	480	840	600	1320	1560	840	960	720
Cr	2500	2380	2130	1750	675	3130	3250	3250	2250	2250
Ni	838	856	889	906	934	851	820	815	761	931
Mn	839	743	812	823	849	854	882	862	866	903
Co	63	60	63	70	64	66	68	65	59	64
Zn	40	33	34	40	38	38	36	38	46	33
Pb	22	27	23	42	33	29	39	33	49	27
Cu	1.2	1.1	1.1	1.1	0.6	1.1	0.5	1.0	1.9	2.0

*Total iron as FeO

The above compositions are similar to the compositions of orthopyroxenes from other suites (e.g. White 1966).

The range of values for Ti, Cr, Ni, Mn, Co, Cu, Zn and also Na_2O , K_2O and CaO is similar to that found elsewhere (Ross et. al. 1954; White 1966; Carter 1970). There is a difference between suites in some of the trace element contents, independent of variations in major element concentrations. This is discussed in Chapter 7. As with the olivines, the orthopyroxenes have a high Pb content relative to the average for ultramafic rocks (Table 3).

(d) Clinopyroxenes.

Partial chemical analyses of clinopyroxenes are given in Table 4. In terms of three end-members the Jacques Lake clinopyroxenes range in composition from $\text{Di}_{45.6}\text{En}_{49.5}\text{Fs}_{4.9}$ to $\text{Di}_{48.4}\text{En}_{46.6}\text{Fs}_{5.0}$; those from Castle Rock range from $\text{Di}_{36.0}\text{En}_{58.6}\text{Fs}_{5.4}$ to $\text{Di}_{47.7}\text{En}_{48.8}\text{Fs}_{4.3}$. The Castle Rock clinopyroxenes are generally more magnesian and less calcic than those from Jacques Lake (Table 4). The Nicola Lake specimen is the least calcic with a composition of $\text{Di}_{43.3}\text{En}_{51.0}\text{Fs}_{5.4}$. The clinopyroxenes contain from 2.78 to 7.12% Al_2O_3 . With one exception (ERC-11), the Castle Rock clinopyroxenes contain less Al_2O_3 than those of Jacques Lake. The Nicola Lake specimen has an intermediate concentration of Al_2O_3 . The Al_2O_3 content increases with Na_2O and TiO_2 (Fig. 24) which suggests that these elements are substituting for Al in the pyroxene structure. The above compositions are similar to the compositions of clinopyroxenes of other lherzolite suites (e.g. White 1966).

TABLE 4

Partial chemical analyses of clinopyroxenes.

Sample	95	S-3	CR-8	ERC-11	NL-8	JL-A	JL-39	JL-10	JL-B	JL-55
Oxide(wt.%)										
TiO ₂	0.20	0.05	0.22	0.40	0.40	0.45	0.64	0.48	0.60	0.52
Al ₂ O ₃	4.92	2.78	5.00	6.70	5.90	5.60	6.84	5.60	7.12	7.10
Cr ₂ O ₃	0.88	0.93	0.85	0.83	0.85	0.90	0.85	0.83	0.80	0.90
FeO*	2.44	2.27	2.26	3.40	2.99	2.75	2.69	2.74	2.61	2.74
MgO	15.4	18.2	16.4	20.8	15.8	15.6	14.6	15.5	14.3	14.4
CaO	20.0	19.6	21.8	19.6	20.8	20.9	21.3	20.0	17.8	18.8
MnO	0.06	0.06	0.05	0.08	0.07	0.07	0.07	0.07	0.07	0.07
NiO	0.06	0.07	0.06	0.08	0.08	0.06	0.05	0.05	0.05	0.05
Na ₂ O	1.00	0.63	1.26	1.09	1.39	1.00	1.54	0.90	2.11	1.34
K ₂ O	0.01	0.01	0.01	0.01	0.01	0.01	0.01	0.01	0.01	0.01
Fe/Fe+Mg	8.19	6.54	7.18	8.55	9.60	9.02	9.37	9.02	9.31	9.66
Fe/Fe+Mg+Ca	4.32	3.66	3.96	5.37	5.41	4.81	5.00	4.69	4.91	4.97
Mg/Fe+Mg+Ca	48.40	52.26	51.20	58.55	50.97	48.16	48.19	48.26	48.66	47.06
Ca/Fe+Mg+Ca	47.28	44.08	45.12	35.26	43.26	46.91	46.63	47.93	47.24	48.52
CaTs(mol.%)	3	6	4	6	5	6	4	9	6	10
Minor elements in ppm.										
Ti	1200	300	1320	2400	2400	2700	3840	2880	3600	3120
Cr	5990	6330	5830	5650	5820	6160	5820	5650	5470	6160
Ni	482	547	497	615	608	440	398	413	361	357
Mn	488	475	413	638	529	540	563	558	542	562
Co	50	50	46	81	63	49	48	50	53	42
Zn	21	20	18	26	22	19	19	20	15	16
Pb	89	83	69	60	104	84	77	73	104	77

*Total iron as FeO

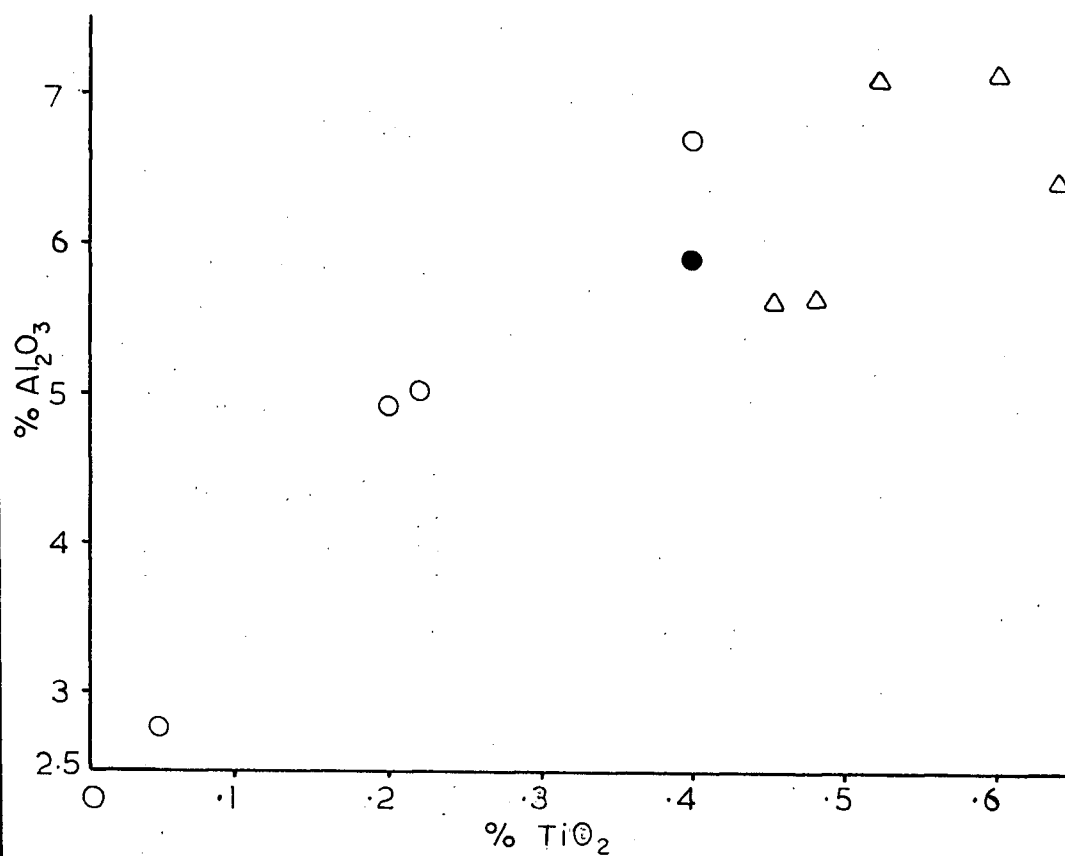
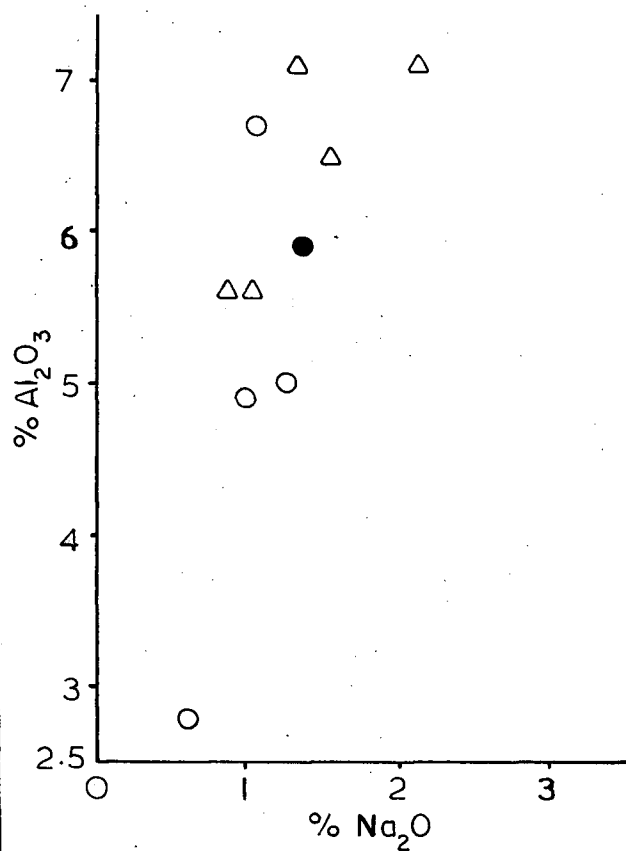
Fig. 24 :

Variation of Na_2O and TiO_2 with Al_2O_3 in clinopyroxenes.

Δ Jacques Lake.

\circ Castle Rock.

\bullet Nicola Lake.



The composition of the clinopyroxene is one means of distinguishing nodules of the lherzolite series from those of the dunite-wehrlite-gabbro series and the eclogite series (White 1966; Kuno 1969). Consequently the variation of Al_2O_3 , CaO and Na_2O with the ratio $\text{MgO}:\text{FeO}$ has been plotted in Fig. 25. As can be seen all the clinopyroxenes from this study fall in the field of the lherzolite series.

The range of values for Ti, Cr, Ni, Mn, Co, Cu, Zn and also Na_2O and K_2O are similar to the values reported elsewhere (Ross et. al. 1954; White 1966; Carter 1970). There are differences between suites in some of the trace element contents, independent of variations in major element concentration. This is discussed in Chapter 7. As with the olivines and orthopyroxenes, the clinopyroxenes have a high Pb content (Table 4) compared to the average given by Goles (1967) for ultramafic rocks.

(e) Spinel.

Partial chemical analyses of spinels are given in Table 5. The composition of natural chrome-bearing spinels adheres closely to the model formula $(\text{Mg}, \text{Fe}^{2+})(\text{Cr}, \text{Al}, \text{Fe}^{3+})_2\text{O}_4$; the sum of the oxides is generally more than 98% (Irvine 1965). Consequently only these constituents were analysed to determine the variations in composition.

The composition of chromian spinels may be graphically represented by means of a triangular prism, each of the six corners corresponds to one of the end-members (MgCr_2O_4 ; FeCr_2O_4 ; MgFe_2O_4 ; Fe_2O_3 ; MgAl_2O_4 ; FeAl_2O_4). Plotting is done by

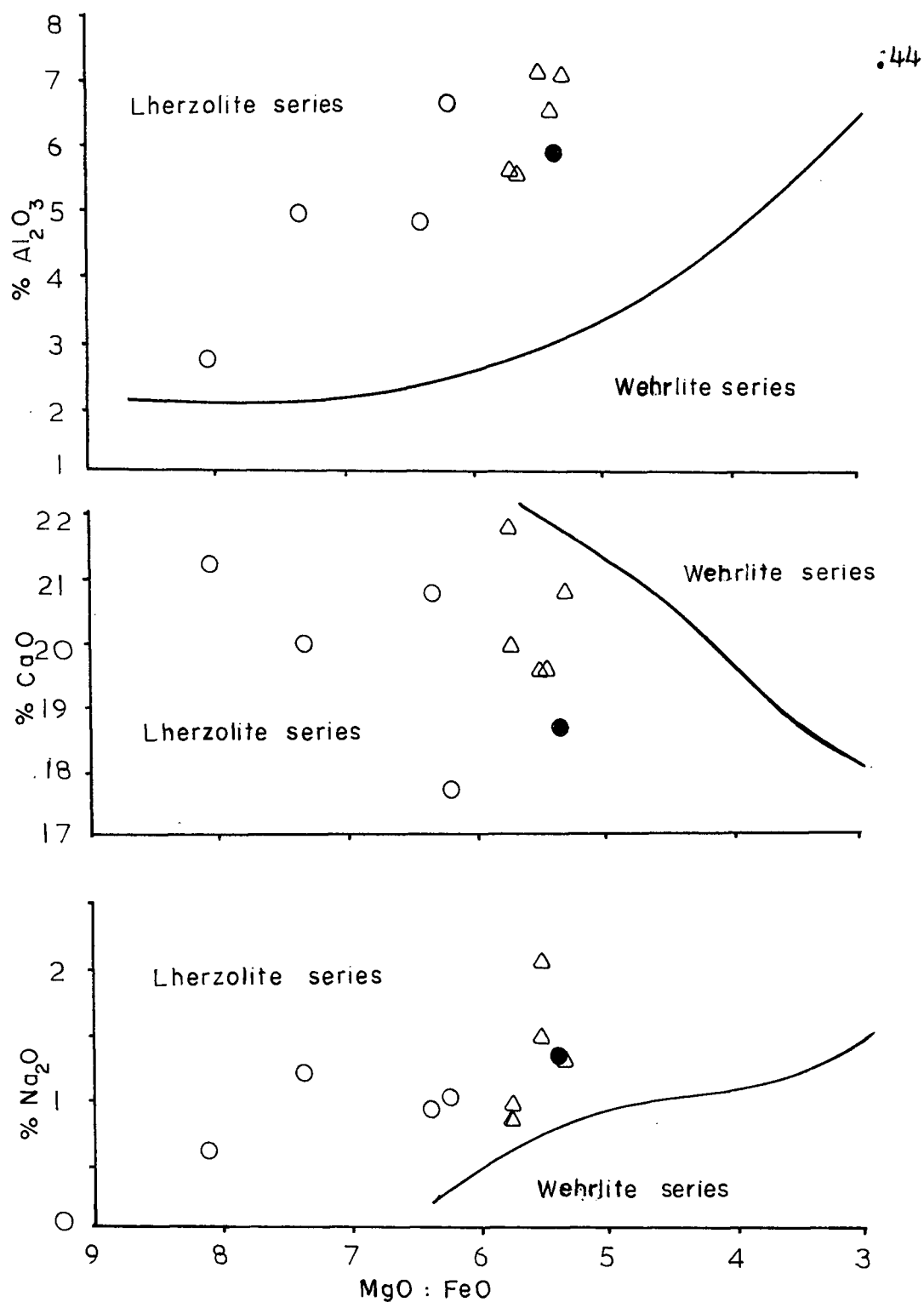


Fig. 25 : Variation of Al_2O_3 , CaO and Na_2O with $\text{MgO}:\text{FeO}$ in clinopyroxenes. The lines are the boundary lines between the compositional fields of lherzolite and wehrlite series clinopyroxenes, taken from Kuno (1969).

△ Jacques Lake: ○ Castle Rock: ● Nicola Lake.

TABLE 5

Partial chemical analyses of spinels.

Sample	95	S-3	CR-8	ERC-11	NL-8	JL-A	JL-39	JL-10	JL-B	JL-55
Oxide(wt.%)										
MgO	20.27	19.56	21.38	23.58	19.05	19.73	20.15	19.93	21.86	19.06
FeO	8.91	9.01	8.43	4.43	11.53	10.95	11.29	11.33	9.53	10.88
Fe ₂ O ₃ *	2.98	5.03	3.17	8.42	-	-	-	0.46	0.97	-
Al ₂ O ₃	50.49	35.19	53.35	54.19	58.71	57.39	63.57	57.35	63.72	64.59
Cr ₂ O ₃	15.38	31.82	14.19	8.43	10.06	12.93	9.24	11.76	7.42	7.30
Total	98.03	100.61	100.52	99.05	99.34	101.00	104.25	100.93	103.30	101.83
Fe ²⁺ /Fe ²⁺ +Mg	19.8	20.5	18.1	9.5	25.3	23.7	24.2	24.2	20.3	24.3
Fe ³⁺ /Fe ³⁺ +Al+Cr	3.0	5.2	3.1	8.2	-	-	-	0.4	0.9	-
Al/Fe ³⁺ +Al+Cr	79.0	56.5	80.8	82.2	88.6	85.5	90.2	86.3	91.9	92.2
Cr/Fe ³⁺ +Al+Cr	18.0	38.3	16.1	9.6	11.4	14.8	9.8	13.4	7.2	7.8

*Calculated by assuming model formula RR₂O₄

Ionic formula based on 32 (O)

Mg ²⁺	6.507	6.554	6.671	6.760	5.909	6.052	5.900	6.275	6.391	5.668
Fe ²⁺	1.605	1.694	1.476	0.789	2.007	1.886	1.885	2.002	1.563	1.815
Fe ³⁺	0.729	0.852	0.498	1.335	-	-	-	0.068	0.144	-
Al	12.822	9.328	13.167	13.353	14.401	13.940	14.728	13.777	14.736	15.194
Cr	2.620	5.656	2.237	1.415	1.655	2.102	1.463	1.965	1.151	1.151
R ²⁺	8.112	8.248	8.147	7.546	7.915	7.940	7.755	8.225	7.954	7.483
R ³⁺	15.926	15.836	15.902	16.103	16.056	16.042	16.164	15.801	16.031	16.345

projection as shown in Fig. 26. The compositions of the analysed spinels are shown on the two projections. As can be seen, the spinels fall close to the MgAl_2O_4 apex of the prism. This is similar to other analysed spinels from lherzolite nodules (Ross et. al. 1954; El Hamad 1963; Ishibashi 1969; Kutolin and Frolova 1970; Carter 1970). Spinel from other types of nodules do not necessarily plot in this part of the prism (Kutolin and Frolova 1970).

Each nodule suite is characterised by having the composition of the spinel phase lying in a particular volume of the spinel prism (Fig. 26). The Castle Rock spinels are richer in Fe_2O_3 and Cr_2O_3 than those from Jacques Lake and Nicola Lake; also the Cr_2O_3 content of the Castle Rock spinels is more variable. The range of MgO variation is small. The Nicola Lake nodule has the least magnesian spinel. There is no difference in the range of MgO content between the Jacques Lake and Castle Rock spinels.

The relatively high Fe_2O_3 content of the Castle Rock spinels (Table 5) suggests that these crystallised under higher f_{O_2} than the Nicola Lake and Jacques Lake spinels (Irvine 1965, 1967).

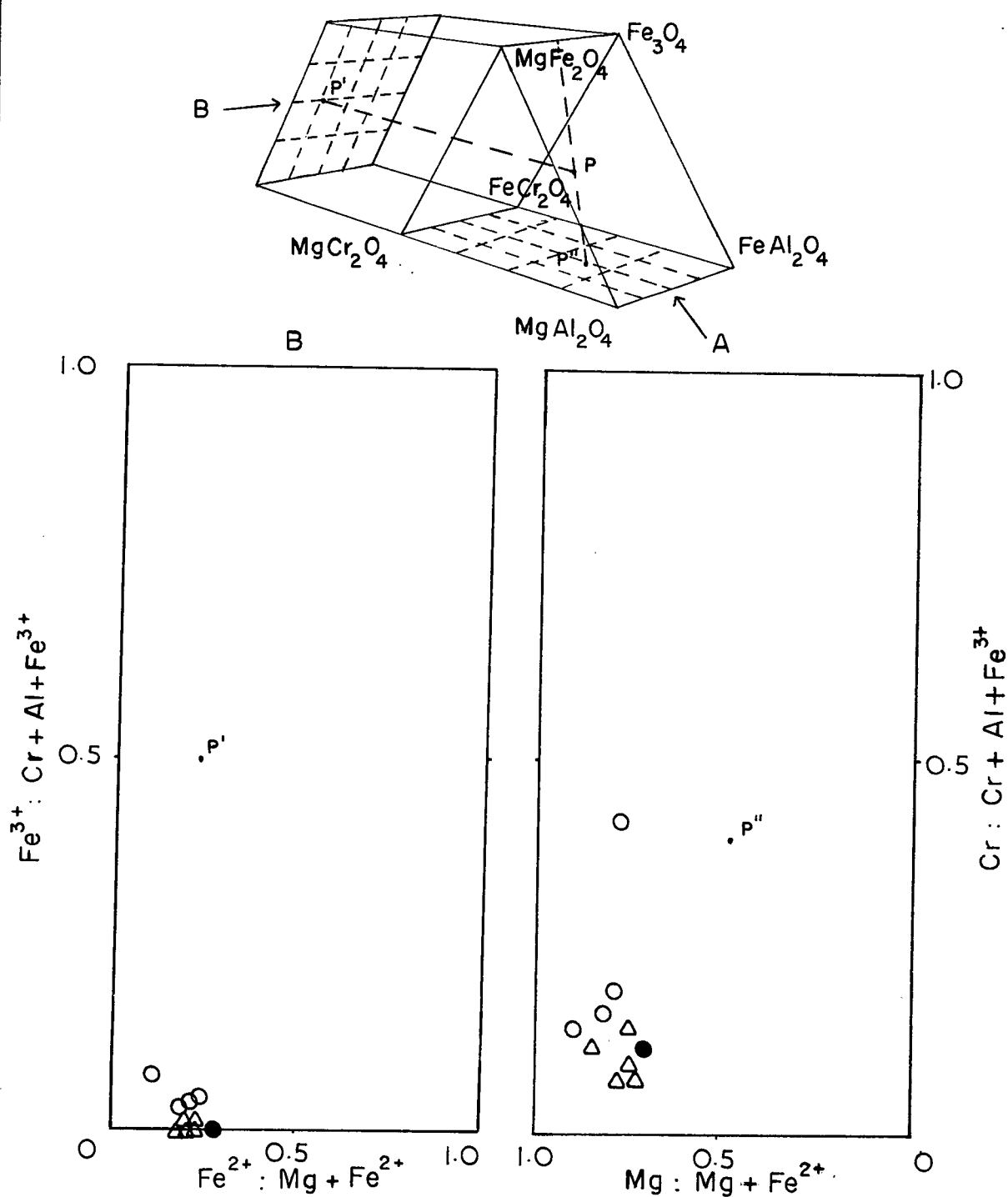


Fig. 26 : Composition of analysed spinels.

Δ Jacques Lake : \circ Castle Rock : \bullet Nicola Lake.

CHAPTER 6

The Distribution of Iron and Magnesium
Between Coexisting Minerals.

(a) Theory.

The distribution of cations between coexisting phases has been discussed in detail by Ramberg and DeVore (1951), Mueller (1961), Bartholome (1962), Kretz (1961, 1963) and more recently by Grover and Orville (1969). The following summary is based on the work of Kretz (1961, 1963).

An equilibrium exchange reaction for the distribution of A and B between coexisting phases (A,B)M and (A,B)N can be written:



The thermodynamic equilibrium constant for such a reaction is:

$$K_D = \frac{a_{BM} \cdot a_{AN}}{a_{AM} \cdot a_{BN}} \quad (2)$$

where a_{PQ} is the activity of the appropriate end-member compound. Equation (2) can be written:

$$K_D = \frac{x_B^{BM} \cdot \gamma_B^{BM} \cdot x_A^{AN} \cdot \gamma_A^{AN}}{x_A^{AM} \cdot \gamma_A^{AM} \cdot x_B^{BN} \cdot \gamma_B^{BN}} \quad (3)$$

where x_P^{PQ} is the mole fraction of P in PQ and γ_P^{PQ} is the activity coefficient of P in PQ. If (A,B)M and (A,B)N behave as ideal solutions, then the activity coefficients are unity and equation (3) becomes:

$$K_D = \frac{x_B^{BM} \cdot x_A^{AN}}{x_A^{AM} \cdot x_B^{BN}} \quad (4)$$

If the ideal solution model is correct then K_D is a function of temperature and pressure only. The temperature dependence of K_D is given by:

$$\left(\frac{\partial \ln K_D}{\partial T} \right)_P = \frac{\Delta H^\circ}{RT^2} \quad (5)$$

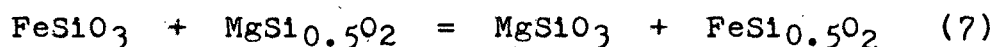
where ΔH° is the change in enthalpy of reaction (1), R is the gas constant, and T the temperature in $^\circ K$. The pressure dependence of K_D is given by:

$$\left(\frac{\partial \ln K_D}{\partial P} \right)_T = - \frac{\Delta V^\circ}{RT} \quad (6)$$

where ΔV° is the molar change in volume of reaction (1) and P is the pressure in bars.

As a first approximation, olivine, orthopyroxene and clinopyroxene can be treated as ideal solid solutions of the type (A,B)M and equation (4) can be used to determine the distribution coefficient with respect to the exchange of iron and magnesium between two coexisting phases. The distribution of iron and magnesium between spinel and any of the above minerals is considered later.

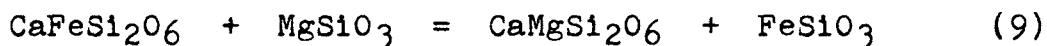
The appropriate reaction is:



for olivine and orthopyroxene, and

$$K_D(1) = \frac{x_{Mg}^{opx} \cdot x_{Fe}^{ol}}{x_{Fe}^{opx} \cdot x_{Mg}^{ol}} \quad (8)$$

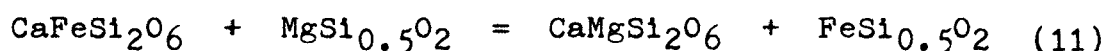
For coexisting pyroxenes the reaction is:



and

$$K_D(2) = \frac{X_{\text{Mg}}^{\text{opx}} \cdot X_{\text{Fe}}^{\text{cpx}}}{X_{\text{Fe}}^{\text{opx}} \cdot X_{\text{Mg}}^{\text{cpx}}} \quad (10)$$

For coexisting olivine and clinopyroxene the reaction is:



and

$$K_D(3) = \frac{X_{\text{Mg}}^{\text{cpx}} \cdot X_{\text{Fe}}^{\text{ol}}}{X_{\text{Fe}}^{\text{cpx}} \cdot X_{\text{Mg}}^{\text{ol}}} \quad (12)$$

(b) Results for coexisting silicates.

Values of $K_D(1)$, $K_D(2)$, and $K_D(3)$ are listed in Table 6. Also given is an analysis of the variance for the K_D values between the Jacques Lake and Castle Rock minerals. The Nicola Lake minerals are considered separately.

The K_D 's were calculated by assuming that all the iron in the minerals is in the ferrous state. While this is a good approximation for olivine and to some extent orthopyroxene, it is not so good for the clinopyroxenes since they may contain up to 2% ferric iron (Ross et. al. 1954). Nevertheless it is still useful to calculate the K_D 's so obtained and compare the results for each suite.

$K_D(1)$ and $K_D(3)$ for the Jacques Lake nodules are less than the values for the Castle Rock nodules. This is a significant difference as the F values exceed the 1% level of F (Snedecor and Cochran 1967). Also, $K_D(1)$ and $K_D(3)$ for the Nicola Lake

TABLE 6

Values of K_D for coexisting olivine and pyroxenes,
with analysis of variance.

Sample	Locality	$K_D(1)$	$K_D(2)$	$K_D(3)$
JL-A	Jacques Lake	0.99	0.88	1.13
JL-39	"	1.01	0.90	1.12
JL-10	"	1.01	0.88	1.15
JL-B	"	0.97	0.93	1.04
JL-55	"	0.98	0.91	1.11
95	Castle Rock	1.25	0.87	1.26
S-3	"	1.16	0.79	1.45
CR-8	"	1.17	0.78	1.48
ERC-11	"	1.08	0.89	1.20
Variance	Between suites	.006	.008	.127
	Within suites	.016	.002	.065
Degrees of freedom	Between suites	1	1	1
	Within suites	7	7	7
F		33.00	4.00	15.88
NL-8	Nicola Lake	0.89	0.90	0.84

sample are lower than any of the others. There is no difference in the values of $K_D(2)$ between any of the suites.

The distribution coefficients for each mineral pair are similar to the coefficients determined from other lherzolite nodules (Kretz 1963; O'Hara 1963; White 1966). Direct comparison with other suites is not possible since total iron was expressed as FeO.

In the ideal solution model, K_D is a function of pressure and temperature only. If the minerals depart from ideality, then K_D will also be a function of composition, since the activity coefficients will not be unity. Nafziger and Muan (1967) found that magnesian olivine is slightly non-ideal but ortho-

pyroxene is ideal. However, introducing activity coefficients in equation (3) to evaluate K_D will not change the relative values of K_D since there is a restricted range of compositions. It was found that each K_D is independent of any other component in the minerals. Therefore the conclusions with respect to the differences in K_D between the suites are still valid.

(c) The effects of temperature and pressure.

Medaris (1969) has determined experimentally the partitioning curve for iron and magnesium between olivine and orthopyroxene at 900°C. The appropriate expression is:

$$\log \left(\frac{X_{Fe}}{X_{Mg}} \right)_{ol} = 0.1630 + 1.1128 \log \left(\frac{X_{Fe}}{X_{Mg}} \right)_{opx} \quad (13)$$

where X_{Fe} and X_{Mg} are the mole fractions of iron and magnesium in the minerals. There is good agreement between this curve and the theoretical partitioning curve derived by Grover and Orville (1969), who considered the exchange of iron and magnesium between olivine and orthopyroxene to take place between a single site in olivine (M_1 and M_2 are energetically equivalent) and a double site in orthopyroxene (M_1 and M_2 are energetically distinct). Equation (13) therefore appears to express satisfactorily the partitioning of iron and magnesium between these minerals at 900°C. Medaris also found that partitioning was not significantly temperature dependant between 900 and 1300°C.

Despite the fact that temperatures of equilibration cannot be determined from the composition of coexisting olivine and orthopyroxene it is still useful to compare the distribution

of iron and magnesium with the experimentally determined curve in order to see if the minerals crystallised under equilibrium conditions. Fig. 27 is a plot of $(X_{Fe}/X_{Mg})_{ol}$ versus $(X_{Fe}/X_{Mg})_{opx}$ on a logarithmic scale. The curved line is the partitioning curve determined by Medaris (1969). All pairs plot close to, but slightly below the curve. This is in agreement with other olivine-orthopyroxene pairs from lherzolite nodules (Medaris 1969). The points for both the Jacques Lake and Castle Rock pairs lie parallel to the curve which suggests that all the pairs crystallised under equilibrium conditions.

The effects of pressure on the distribution coefficient has been given in equation (6). Using molar volume data on synthetic olivine and orthopyroxene Medaris (1969) found that $K_D(1)$ is not significantly dependant on pressure. However this conclusion is based on the assumption that ΔV^0 does not change with pressure or temperature. The change in volume for reaction (7) is given by:

$$\Delta V^0 = V_{MgSiO_3}^0 + V_{FeSi_{10.5}O_2}^0 - V_{FeSiO_3}^0 - V_{MgSi_{10.5}O_2}^0 \quad (14)$$

where V_j^0 is the molar volume of phase j.

However the orthopyroxenes contain a considerable amount of Al (substituting for Si and (Mg,Fe)). Therefore the volumes which are used in equation (14) should be partial molar volumes and not the volumes of the pure end-member components. Since the Al content of the orthopyroxenes is different for each suite (Table 3), it is to be expected that ΔV^0 will be different for each suite and hence the effect of pressure cannot be entirely disregarded. It is possible that the differ-

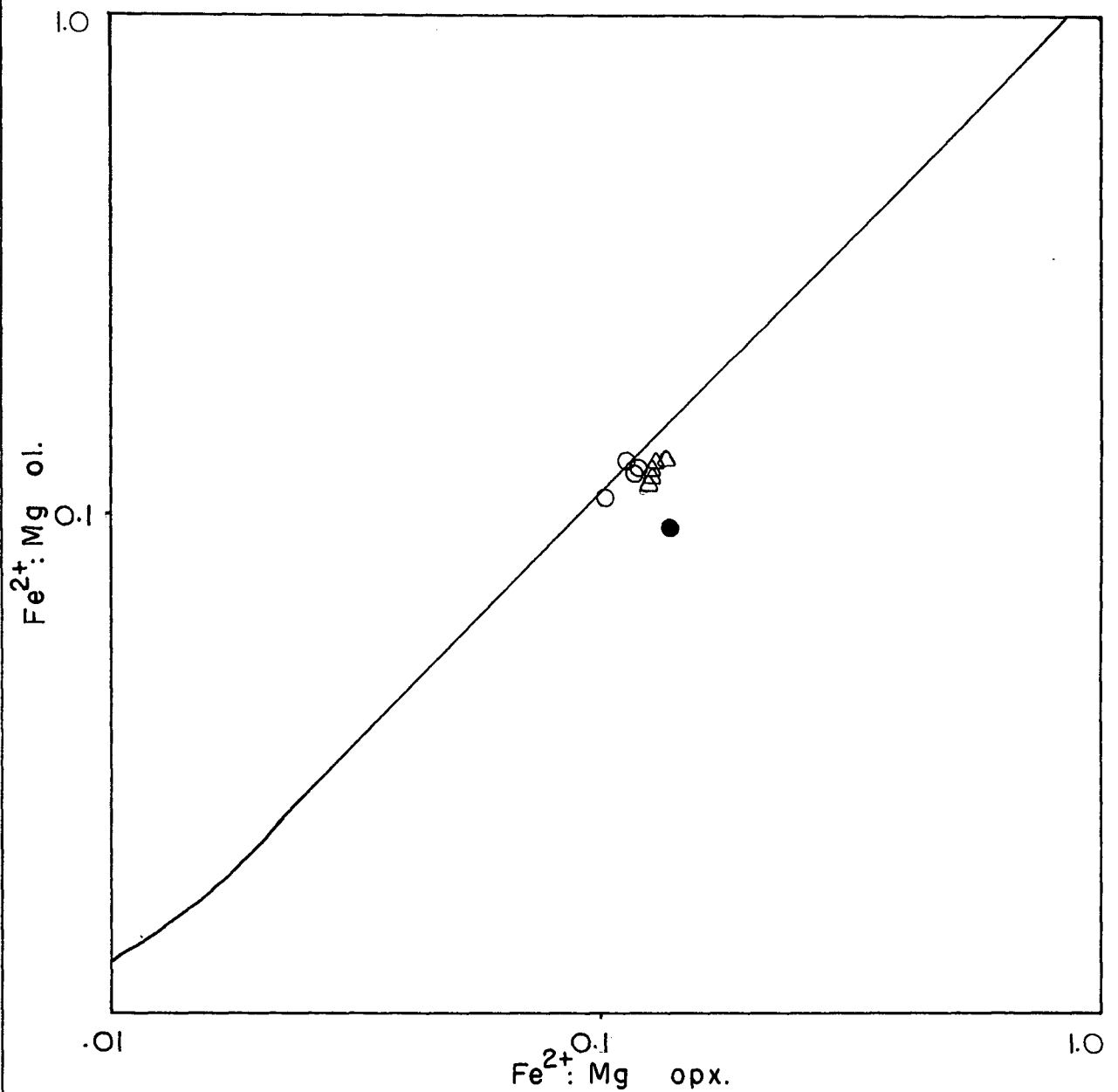


Fig. 27 : Distribution of Fe²⁺ and Mg between olivine and orthopyroxene. The curve is the equilibrium partitioning curve at 900°C determined by Medaris (1969).

Δ Jacques Lake : ○ Castle Rock: ● Nicola Lake.

ences in $K_D(1)$ between the suites may be due to differences in pressure. It is not possible to determine the direction of pressure change since the precision of the available data does not warrant the calculation.

Kretz (1963) has shown that the distribution of iron and magnesium between coexisting pyroxenes is a function of temperature and is constant with respect to pressure. Kretz (1963) also showed that $K_D(2)$ increases with temperature for igneous and metamorphic pyroxenes and that the values for pyroxenes from ultramafic nodules tend to approach unity. The data from this study agree with the latter observation. The data suggest that all the pyroxene pairs crystallised within the same range of temperatures since there is no difference in the range of values of $K_D(2)$ between the suites.

It will be shown in the next section that the Castle Rock nodules formed at a higher temperature than those of Jacques Lake and that the Nicola Lake nodule formed at a lower temperature than the others. It might be expected therefore that the $K_D(2)$ values might show this. This is not the case. Therefore it is likely that some other factor besides temperature is affecting the values of $K_D(2)$.

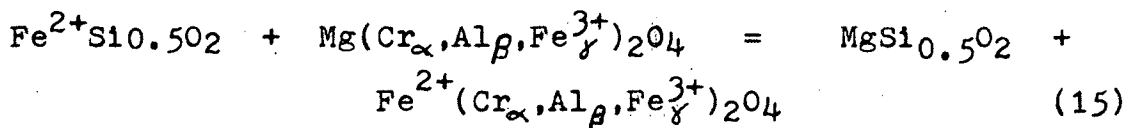
This factor is possibly the Al_2O_3 content of the pyroxenes, although no direct relationship between the Al_2O_3 content of the pyroxenes and $K_D(2)$ could be found. As with $K_D(1)$, the pressure effect on $K_D(2)$ is dependant on the quantity ΔV° . The effects of Al_2O_3 on this are unknown, so that $K_D(2)$ could change

significantly with pressure. Also, ΔH° may be affected by the Al_2O_3 content of the pyroxenes. Therefore it is not possible to determine the conditions of formation of these minerals from the distribution of iron and magnesium between them.

No experimental or empirical data on the effect of temperature and pressure on the distribution of iron and magnesium between coexisting olivine and clinopyroxene are available in the literature. It is evident from Table 6 that iron and magnesium are distributed differently between these minerals in each nodule suite. It is assumed that this is a result of different conditions of formation. It is not possible to evaluate variations in $K_D(3)$ with respect to pressure and temperature using data for the iron-magnesium end-members since Al_2O_3 in the clinopyroxenes probably affects the appropriate thermodynamic functions.

(d) The distribution of iron and magnesium between coexisting olivine and spinel.

The distribution of iron and magnesium between coexisting olivine and spinel has been discussed in detail by Irvine (1965). A reaction expressing the Mg-Fe^{2+} exchange between olivine and spinel can be written:



where α, β, γ are mole fractions of trivalent cations in the spinel and $\alpha + \beta + \gamma = 1$. The thermodynamic equilibrium distribution coefficient for equation (15) is:

$$K_D(4) = \frac{a_{\text{MgSi}_{0.5}\text{O}_2} \cdot a_{\text{FeCr}_2\text{O}_4}^{\alpha} \cdot a_{\text{FeAl}_2\text{O}_4}^{\beta} \cdot a_{\text{FeFe}_2\text{O}_4}^{\gamma}}{a_{\text{FeSi}_{0.5}\text{O}_2} \cdot a_{\text{MgCr}_2\text{O}_4}^{\alpha} \cdot a_{\text{MgAl}_2\text{O}_4}^{\beta} \cdot a_{\text{MgFe}_2\text{O}_4}^{\gamma}} \quad (16)$$

where a_j is the activity of end-member j . This can be expressed in compositional terms by replacing a_j with $(\gamma_j X_j)$ where γ_j is the activity coefficient and X_j is the mole fraction of the appropriate end-member. If ideal behavior is assumed, the activity coefficients are unity and equation (16) becomes:

$$K_D(4) = \frac{X_{\text{Mg}}^{\text{ol}} \cdot (X_{\text{FeCr}_2\text{O}_4}^{\text{sp}})^{\alpha} \cdot (X_{\text{FeAl}_2\text{O}_4}^{\text{sp}})^{\beta} \cdot (X_{\text{FeFe}_2\text{O}_4}^{\text{sp}})^{\gamma}}{X_{\text{Fe}}^{\text{ol}} \cdot (X_{\text{MgCr}_2\text{O}_4}^{\text{sp}})^{\alpha} \cdot (X_{\text{MgAl}_2\text{O}_4}^{\text{sp}})^{\beta} \cdot (X_{\text{MgFe}_2\text{O}_4}^{\text{sp}})^{\gamma}} \quad (17)$$

Since $X_{\text{FeCr}_2\text{O}_4}^{\text{sp}} = \left(\frac{\text{Fe}}{\text{Mg} + \text{Fe}^{2+}} \right) \left(\frac{\text{Cr}}{\text{Cr} + \text{Al} + \text{Fe}^{3+}} \right) = \alpha X_{\text{Fe}^{2+}}^{\text{sp}}$ etc.;

$\alpha + \beta + \gamma = 1$, equation (16) reduces to

$$K(4) = \frac{X_{\text{Mg}}^{\text{ol}} \cdot X_{\text{Fe}^{2+}}^{\text{sp}}}{X_{\text{Fe}}^{\text{ol}} \cdot X_{\text{Mg}}^{\text{sp}}} \quad (18)$$

This is a result similar to that for coexisting silicates but is derived in this way to show the effects of the trivalent cations of the spinel on $K_D(4)$.

Table 7 gives the values of $K_D(4)$ calculated from equation (18). The method of calculating the uncertainties in $K_D(4)$ is given in Appendix 2. The Table also gives the analysis of variance in $K_D(4)$ between the Jacques Lake and Castle Rock suites. The Nicola Lake pair is considered separately. As can be seen, the Nicola Lake sample has the highest $K_D(4)$. There is a

TABLE 7

Values of $K_D(4)$ for coexisting olivine and spinel, with analysis of variance.

Sample	Locality	$K_D(4)$	$\ln K_D(4)$
95	Castle Rock	$2.20 \pm .17$	$0.785 \pm .078$
S-3	"	$2.55 \pm .21$	$0.931 \pm .081$
CR-8	"	$1.93 \pm .16$	$0.651 \pm .080$
ERC-11	"	$0.93 \pm .10$	$-0.068 \pm .037$
JL-A	Jacques Lake	$2.77 \pm .20$	$1.014 \pm .071$
JL-39	"	$2.78 \pm .19$	$1.020 \pm .069$
JL-10	"	$2.81 \pm .20$	$1.031 \pm .071$
JL-B	"	$2.37 \pm .19$	$0.860 \pm .079$
JL-55	"	$2.74 \pm .19$	$1.004 \pm .069$
	Between suites	1.39	
Variance	Within suites	0.20	
	Between suites	1	
Variance	Within suites	7	
F		7.03	
Nicola Lake		$3.79 \pm .30$	$1.330 \pm .079$

TABLE 8

Temperatures of formation for coexisting olivine and spinel.

Sample	Locality	$T^{\circ}\text{C}$
95	Castle Rock	1632 ± 184
S-3	"	2214 ± 262
CR-8	"	1822 ± 231
ERC-11	"	10697
JL-A	Jacques Lake	1133 ± 99
JL-39	"	1037 ± 90
JL-10	"	1113 ± 98
JL-B	"	1142 ± 122
JL-55	"	1002 ± 88
NL-8	Nicola Lake	838 ± 71

significant difference in the $K_D(4)$ values between the Jacques Lake and Castle Rock suites since the value of F exceeds the 5% level of F (Snedecor and Cochran 1967). With one exception (S-3), all the Castle Rock $K_D(4)$'s are greater than those of Jacques Lake.

The distribution coefficient is related to the free energy of reaction (15) thus:

$$\ln K_D(4) = -\frac{\Delta G}{RT} \quad \text{and} \quad K_D(4) = \exp\left(\frac{-\Delta G}{RT}\right) \quad (19)$$

where $\Delta G = \sum G_j$ and G_j is the free energy of formation of the appropriate end-member in equation (15), R is the gas constant and T the temperature of formation of the coexisting mineral pair. Substituting the free energy values given by Jackson (1969, p.64) (these are temperature dependant), taking $R = 1.987$, and solving for T , we have:

$$T = \frac{5580\alpha + 1018\beta - 1720\gamma + 2400}{0.90\alpha + 2.56\beta - 3.08\gamma - 1.47 + 1.987\ln K_D(4)} \quad (20)$$

Temperatures derived from equation (20) are given in Table 8. The method of calculating the uncertainty in each temperature is given in Appendix 2.

The uncertainties listed in Table 8 represent the maximum possible errors in T which can be introduced as a result of analytical errors in the determination of Mg and Fe^{2+} in spinel and olivine and Cr , Al and Fe^{3+} in spinel. The error that may be introduced into the temperature values of Table 8 due to uncertainties in the free energy values are much larger than the

analytical errors. Possible maximum uncertainties in the free energies of the spinels alone could affect the temperature values by as much as $\pm 300^{\circ}\text{C}$ but these uncertainties are not large enough to reverse the direction of reaction (15) and will have little effect on the relative temperatures (Jackson 1969).

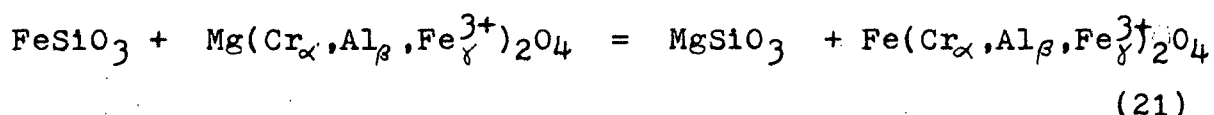
It is apparent from Table 8 that each nodule suite formed at a different temperature (within analytical error and assuming that all the minerals equilibrated at the same temperature). The nominal temperature of formation of the Nicola Lake suite is 838°C (assuming that sample NL-8 is representative of the suite). The nominal temperature of formation of the Jacques Lake suite is 1085°C (average of 5 temperatures).

The nominal temperature of formation of the Castle Rock nodules is more difficult to assess. There appears to be a range of temperatures but this may not be real as errors in $K_D(4)$, and hence in $\ln K_D(4)$, become increasingly important where $K_D(4)$ is small since this term appears in the denominator of equation (20). As the derived temperatures seem unrealistically high the nominal temperature of formation of the Castle Rock nodules is taken to be 1600°C . This is somewhat arbitrary but there can be little doubt that these nodules formed at temperatures much greater than those of Jacques Lake and Nicola Lake.

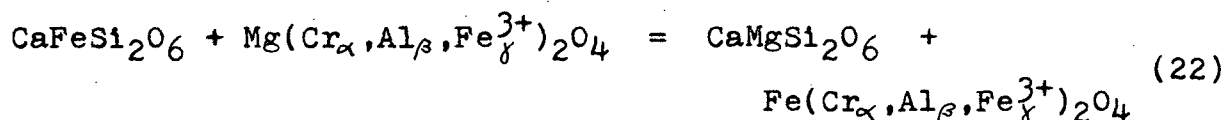
The effect of pressure on $K_D(4)$ is that given in equation (6). Irvine (1965) has shown that the pressure effect is negligible at moderate pressures. Data to evaluate $K_D(4)$ at high pressure is lacking, but any variation in $K_D(4)$ due to pressure is not likely to reverse the relative temperatures since any volume change will be small compared to the enthalpy change of equation (5).

(e) The distribution of iron and magnesium between coexisting spinel and pyroxenes.

Reactions equivalent to (15) can be written for orthopyroxene and clinopyroxene:



and



Analogous expressions for the distribution coefficients are:

$$K_D(5) = \frac{x_{\text{Mg}}^{\text{opx}} \cdot x_{\text{Fe}^{2+}}^{\text{sp}}}{x_{\text{Fe}^{2+}}^{\text{opx}} \cdot x_{\text{Mg}}^{\text{sp}}} \quad (23)$$

and

$$K_D(6) = \frac{x_{\text{Mg}}^{\text{cpx}} \cdot x_{\text{Fe}^{2+}}^{\text{sp}}}{x_{\text{Fe}^{2+}}^{\text{cpx}} \cdot x_{\text{Mg}}^{\text{sp}}} \quad (24)$$

Table 9 lists the values for $K_D(5)$ and $K_D(6)$ for the analysed pairs and also the variation in these for the Jacques Lake and Castle Rock suites.

There is no significant difference in these values between the suites. The values for ERC-11 are low in comparison to the others. This may indicate that the spinel in this nodule is not in equilibrium with the pyroxenes (and also with the olivine since $K_D(4)$ is low). Texturally, however, the spinel appears to be in equilibrium, so that the anomalous K_D 's may be the result

TABLE 9

Values of $K_D(5)$ and $K_D(6)$, with analysis of variance.

Sample	Locality	$K_D(5)$	$K_D(6)$
JL-A	Jacques Lake	2.74	3.14
JL-39	"	2.78	3.08
JL-10	"	2.84	3.32
JL-B	"	2.32	2.48
JL-55	"	2.71	2.99
95	Castle Rock	2.44	2.76
S-3	"	2.93	3.71
CR-8	"	2.24	2.85
ERC-11	"	1.00	1.13
Variance	Between suites	.631	.307
	Within suites	.313	.547
Degrees of freedom	Within suites	7	7
	Between suites	1	1
F		1.96	1.78
NL-8	Nicola Lake	2.89	3.12

of an imperfect analysis. As can be seen from Table 4, ERC-11 is the least close to the model formula.

Expressions analogous to (20) and (6) can be used to evaluate the temperature and pressure effects on $K_D(5)$ and $K_D(6)$. There is a considerable amount of Al_2O_3 in the pyroxenes. Therefore there will be an exchange of Al between the pyroxenes and the spinel which will undoubtedly influence the temperature and pressure effects. This effect is not known.

CHAPTER 7

The Distribution of Trace Elements
Between Coexisting Silicates.

(a) Theory.

The partitioning of trace elements between coexisting minerals has been discussed in detail by McIntyre (1963). An exchange reaction between two solid phases (Cr,Tr)A and (Cr,Tr)B can be written:



where Tr and Cr represent the trace element and the element for which it substitutes (the carrier element) respectively. A and B refer to that portion of the mineral which does not take part in the reaction. Cr and Tr have the same valence.

The equilibrium constant for reaction (25) is

$$K_{\text{Tr}} = \frac{a_{\text{TrA}} \cdot a_{\text{CrB}}}{a_{\text{CrA}} \cdot a_{\text{TrB}}} \quad (26)$$

where a_j is the activity of end-member j in equation (25). Equation (26) can be rewritten:

$$K_{\text{Tr}} = \frac{X_{\text{TrA}} \cdot X_{\text{CrB}} \cdot \gamma_{\text{TrA}}^{\text{Tr}} \cdot \gamma_{\text{CrB}}^{\text{Cr}}}{X_{\text{CrA}} \cdot X_{\text{TrB}} \cdot \gamma_{\text{CrA}}^{\text{Cr}} \cdot \gamma_{\text{TrB}}^{\text{Tr}}} \quad (27)$$

where X_j is the concentration of end-member j and γ_j^i is the activity coefficient of i in j . If ideal behavior is assumed, then equation (27) becomes:

$$K_{\text{Tr}} = \frac{(X_{\text{Tr}}/X_{\text{Cr}})_A}{(X_{\text{Tr}}/X_{\text{Cr}})_B} \quad (28)$$

The distribution coefficient (K_{Tr}) is a function of temperature and pressure. The temperature dependence, given in equation (5) is:

$$\left(\frac{\partial \ln K_{Tr}}{\partial T} \right)_P = \frac{\Delta H^\circ}{RT^2}$$

where ΔH° is the enthalpy of reaction (25), R the gas constant and T is the temperature in $^\circ K$. The pressure dependence, given in equation (6) is:

$$\left(\frac{\partial \ln K_{Tr}}{\partial P} \right)_T = \frac{-\Delta V^\circ}{RT}$$

where ΔV° is the molar change in volume of reaction (25), P the pressure and the other symbols are the same as before.

Unfortunately ΔH° and ΔV° for reactions involving trace elements are unknown so that trace element distributions cannot be used in geothermometry and geobarometry with any confidence. Nevertheless it is still useful to determine trace element distribution coefficients and anticipate that variations in these are due to variations in the conditions of formation of the mineral pair in question, if it can be shown that the distribution coefficient is not dependant on the concentration of any other element.

In olivine and pyroxenes the carrier element for divalent trace elements may be either Mg^{2+} or Fe^{2+} . It is assumed that the M2 site in clinopyroxene is completely filled with calcium and that no exchange between a divalent ion and calcium takes place. The choice of Mg^{2+} or Fe^{2+} is not entirely arbitrary as stated by Matsui and Banno (1970). Burns (1970) has shown that

transition metal ions have a preference for certain sites in silicate structures. He has listed, among others, the following site preferences:

olivine M1 ; $\text{Ni}^{2+}, \text{Co}^{2+}, \text{Mg}^{2+}$.

olivine M2 ; $\text{Mn}^{2+}, \text{Fe}^{2+}$.

orthopyroxene M1 ; $\text{Ni}^{2+}, \text{Mg}^{2+}$.

orthopyroxene M2 ; $\text{Mn}^{2+}, \text{Co}^{2+}, \text{Fe}^{2+}$.

clinopyroxene M1 ; $\text{Ni}^{2+}, \text{Co}^{2+}, \text{Mn}^{2+}, \text{Fe}^{2+}, \text{Mg}^{2+}$.

Thus Mg^{2+} will be the carrier for Ni^{2+} in olivine and orthopyroxene since both tend to occupy the same site in these minerals. Since both Mg^{2+} and Fe^{2+} occupy the M1 site in clinopyroxene the choice is not so clear. As there is a positive correlation between NiO and MgO in the analysed diopsides it is assumed that Mg^{2+} is the carrier for Ni^{2+} in the clinopyroxenes also. Similarly Fe^{2+} is the carrier for Mn^{2+} and Co^{2+} in all three silicates. It is assumed that all Co is in the divalent state in these minerals. Although Zn is not a transition element it appears to behave as one in these minerals since it is distributed regularly among the three silicates (Fig. 28). For this reason Zn is treated in the same way as Ni, Mn, and Co in this discussion. From size considerations it is likely that Zn^{2+} substitutes for Fe^{2+} in these minerals.

(b) The distribution of Ni, Mn, Co and Zn.

Since Ni, Mn, Co and Zn substitute for Mg or Fe in the olivine and pyroxene structure, the concentration of these elements is dependent on the concentration of the carrier element. In order to compare trace element concentrations, the ratio Tr/Cr

can be considered to be a measure of the trace element content of a mineral.

$(\text{Ni}/\text{Mg}) \times 1000$, $\frac{1}{2}(\text{Mn}/\text{Fe}) \times 100$, $(\text{Co}/\text{Fe}) \times 100$ and $(\text{Zn}/\text{Fe}) \times 100$ for olivine, orthopyroxene and clinopyroxene are listed in Table 10. The variation in these ratios between the Jacques Lake and Castle Rock suites is examined by means of Snedecor's F test and the results given in Table 12. The Nicola Lake sample is considered separately.

The Nicola Lake olivine contains more Ni and Co than the other olivines and the pyroxenes contain less Mn and Co. The Jacques Lake and Castle Rock olivines contain similar amounts of these elements. The Jacques Lake diopsides contain less Ni, Co and Zn than those of Castle Rock, and the enstatites less Mn and Co. These are all significant results since the value for F exceeds the 5% level of F in each case (Table 12). There is thus a fundamental difference in the concentration of some elements in the minerals of each suite of nodules. The minerals of each suite are characterised by a particular trace element "content".

The distribution of Ni, Mn, Co and Zn between olivine and the two pyroxenes is regular. Fig. 28 shows the relative concentrations of these elements in the three silicates. The relative enrichment of these elements in coexisting olivine and pyroxene

1. Ratios involving iron were calculated with the assumption that all the iron is in the ferrous state. Generally the minerals (especially clinopyroxenes) will contain some ferric iron. This will affect the magnitude of such ratios but the relative values will remain since there is a restricted compositional range which is assumed to apply to ferric iron also.

TABLE 10

(Tr/Cr) ratios of analysed minerals.

Sample	Locality	(Ni/Mg)x1000			(Mn/Fe)x100		
		ol.	opx.	cpx.	ol.	opx.	cpx.
JL-A	Jacques Lake	8.98	4.42	4.69	1.24	1.71	2.52
JL-39	"	9.46	4.34	4.52	1.24	1.77	2.69
JL-10	"	8.81	4.41	4.42	1.15	1.79	2.62
JL-B	"	8.04	3.99	4.20	1.21	1.80	2.67
JL-55	"	9.91	4.97	4.12	1.30	1.77	2.64
95	Castle Rock	8.20	4.32	5.20	1.25	1.86	2.57
S-3	"	8.03	4.23	5.00	1.14	1.81	2.70
CR-8	"	8.89	4.54	5.02	1.03	1.82	2.35
ERC-11	"	9.09	4.75	4.91	1.22	1.79	2.42
NL-8	Nicola Lake	5.95	5.25	6.40	1.08	1.77	2.28

Sample	Locality	(Co/Fe)x100			(Zn/Fe)x100		
		ol.	opx.	cpx.	ol.	opx.	cpx.
JL-A	Jacques Lake	.186	.132	.229	.076	.076	.089
JL-39	"	.168	.136	.230	.071	.072	.091
JL-10	"	.162	.136	.235	.080	.079	.094
JL-B	"	.172	.122	.261	.063	.095	.074
JL-55	"	.174	.125	.197	.061	.065	.075
95	Castle Rock	.161	.140	.263	.074	.089	.111
S-3	"	.202	.146	.284	.079	.080	.114
CR-8	"	.164	.141	.261	.066	.076	.102
ERC-11	"	.187	.152	.307	.083	.087	.098
NL-8	Nicola Lake	.203	.133	.272	.071	.079	.095

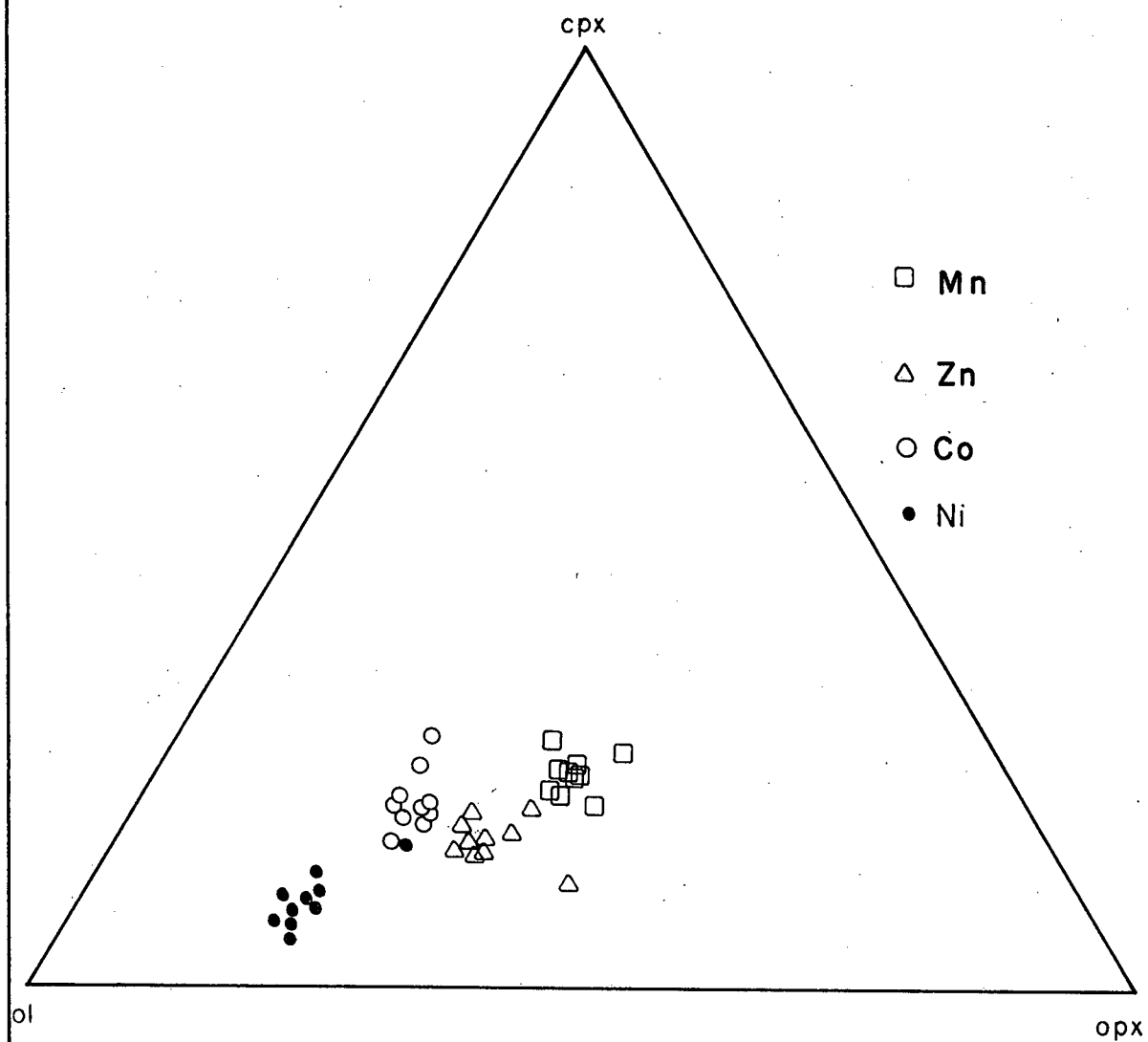


Fig. 28 : Relative proportions of Mn, Zn, Co and Ni between coexisting olivine, orthopyroxene and clinopyroxene.

is a function of size and site energy as predicted by Burns (1970). These enrichments are in agreement with the data from other ultramafic rocks (White 1966; Mercy and O'Hara 1967; Carter 1970).

The distribution of these elements between coexisting olivine, orthopyroxene and clinopyroxene is examined by means of the distribution function K_{Tr} (equation 28) where $Tr = Ni, Mn, Co$ or Zn , Cr is the appropriate carrier element (Mg or Fe) and A and B are coexisting olivine, orthopyroxene or clinopyroxene. The results are given in Table 11. The variation in each K_{Tr} is examined by means of Snedecor's F test (Table 12). This applies to the Castle Rock and Jacques Lake suites only; the Nicola Lake results are considered separately.

From Table 11 it can be seen that all the Nicola Lake K_{Ni} 's are less than the corresponding K_{Ni} 's for the other two suites and that $K_{Ni}(ol/opx)$ and $K_{Ni}(ol/cpx)$ for the Castle Rock pairs are less than the corresponding ratios of the Jacques Lake suite. $K_{Mn}(cpx/opx)$ for Nicola Lake is greater than the others; and for Jacques Lake ~~are~~ less than the Castle Rock coefficients. $K_{Co}(ol/opx)$ for Nicola Lake is greater than the Castle Rock and Jacques Lake coefficients. $K_{Zn}(ol/cpx)$ for the Jacques Lake samples are less than those of the Castle Rock minerals. These comparisons are significant since the value of F exceeds the 5% level of F in each case (Table 12).

The consistency of the distribution coefficients within each suite suggests that the minerals are in equilibrium with respect to the elements which have been discussed.

TABLE 11

Trace element distribution coefficients.

Sample	Locality	K_{Ni}			K_{Mn}		
		ol/opx	ol/cpx	opx/cpx	ol/opx	ol/cpx	opx/cpx
JL-A	Jacques Lake	2.03	1.19	0.94	0.73	0.49	0.68
JL-39	"	2.18	2.09	0.96	0.70	0.46	0.66
JL-10	"	2.00	1.99	1.00	0.64	0.44	0.68
JL-B	"	2.02	1.91	0.95	0.67	0.45	0.67
JL-55	"	1.97	2.38	1.12	0.73	0.49	0.67
95	Castle Rock	1.90	1.58	0.83	0.67	0.45	0.67
S-3	"	1.90	1.58	0.83	0.67	0.49	0.67
CR-8	"	1.96	1.71	0.91	0.57	0.44	0.77
ERC-11	"	1.91	1.85	0.94	0.68	0.50	0.74
NL-8	Nicola Lake	1.13	0.93	0.82	0.61	0.47	0.78

Sample	Locality	K_{Co}			K_{Zn}		
		ol/opx	ol/cpx	opx/cpx	ol/opx	ol/cpx	opx/cpx
JL-A	Jacques Lake	1.14	0.81	0.58	1.00	0.85	0.85
JL-39	"	1.24	0.73	0.59	0.99	0.78	0.79
JL-10	"	1.20	0.73	0.59	1.01	0.85	0.84
JL-B	"	1.41	0.66	0.47	0.66	0.85	1.28
JL-55	"	1.39	0.88	0.63	0.94	0.81	0.87
95	Castle Rock	1.19	0.63	0.53	0.83	0.67	0.80
S-3	"	1.38	0.71	0.51	0.99	0.69	0.70
CR-8	"	1.16	0.63	0.54	0.87	0.65	0.75
ERC-11	"	1.23	0.61	0.50	0.95	0.85	0.85
NL-8	Nicola Lake	1.53	0.75	0.49	0.90	0.75	0.83

TABLE 12

Analysis of trace element variance between Castle Rock and Jacques Lake suites.

Ratio	Variance*		F	Significance#
	Between suites	Within suites		
(Ni/Mg)ol	.031	.337	12.17	Not significant
(Ni/Mg)opx	.002	.093	46.93	"
(Ni/Mg)cpx	.918	.037	24.81	Significant at 0.5%
(Mn/Fe)ol	.010	.040	1.76	Not significant
(Mn/Fe)opx	.010	.0014	7.14	Significant at 5%
(Mn/Fe)cpx	.030	.010	3.00	Not significant
(Co/Fe)ol	.0001	.0002	2.00	"
(Co/Fe)opx	.0005	.00003	16.67	Significant at 1%
(Co/Fe)cpx	.0052	.0005	10.61	Significant at 2.5%
(Zn/Fe)ol	.00002	.00007	3.50	Not significant
(Zn/Fe)opx	.00007	.00009	1.28	"
(Zn/Fe)cpx	.0002	.00007	28.50	Significant at 0.5%
K _{Tr}				
Ni ol/opx	.033	.004	8.25	Significant at 2.5%
Ni ol/cpx	.278	.029	9.59	Significant at 2.5%
Ni opx/cpx	.033	.009	3.68	Not significant
Mn ol/opx	.007	.002	3.50	"
Mn ol/cpx	.00005	.001	20.00	"
Mn opx/cpx	.006	.001	6.00	Significant at 5%
Co ol/opx	.018	.010	1.80	Not significant
Co ol/cpx	.026	.006	4.80	"
Co opx/cpx	.005	.002	2.32	"
Zn ol/opx	.0002	.015	73.86	"
Zn ol/cpx	.029	.004	6.86	Significant at 5%
Zn opx/cpx	.044	.097	2.20	Not significant

*Degrees of freedom are 1 and 7 for between and within suites respectively

#The significant levels of F are 16.24, 12.25, 8.07 and 5.59 at the 0.5, 1.0, 2.5 and 5.0% levels respectively (Snedecor and Cochran 1967).

Although the distribution of trace elements among these minerals cannot be related quantitatively to the conditions of formation, it is clear that some elements are distributed differently among these minerals and that the observed distribution cannot be related to different concentrations of trace or carrier element in the minerals. For example, it has been shown that Ni is distributed differently between olivine and enstatite in the Jacques Lake and Castle Rock suites, although the Ni content of these minerals in each suite is similar. Ni therefore appears to be sensitive to changes in environment. On the other hand, the Co content of the Jacques Lake pyroxenes is less than those of Castle Rock but the Co is distributed between the minerals in a similar way. Co is therefore not sensitive to changing conditions (at least in these minerals). The Nicola Lake pyroxenes contain less Mn than the other pyroxenes and is also distributed differently between these minerals.

Each nodule suite is apparently characterised by different trace element behavior. The difference may be a difference in the content of some elements in the minerals or may be a difference in element distribution among the minerals which presumably reflects different physical and chemical conditions at the source of the nodules.

The above discussion illustrates the importance of considering more than one element and pair of minerals when making inferences on the conditions of formation of a series of rocks. While one set of distribution coefficients may not be significant with respect to changes of environment, the evidence of several sets

may reveal that suites of similar rocks have formed under different conditions.

(c) Other elements.

Other trace elements such as Cu, Pb, Cr and Ti are not amenable to a treatment such as given to Ni, Mn, Co and Zn as the position of these elements in the mineral structure is more uncertain and because incorporation of these elements in the structure involves a coupled substitution.

Cu and Pb are distributed irregularly among the three silicates (Fig. 29). Because of this, the distribution of these elements is considered no further.

Tables 3 and 4 show that the concentration of Ti and Cr is greater in the clinopyroxenes than in the orthopyroxenes. This is in agreement with the data of White (1966). There appears to be no systematic difference between the suites in the Cr content of the pyroxenes. The exception to this is the Nicola Lake enstatite which is comparatively low in Cr. On the other hand the the pyroxenes of the Jacques Lake nodules have a higher Ti content than those of Castle Rock. The Nicola Lake pyroxenes have a similar Ti content to those of Jacques Lake.

The distribution of Ti and Cr between the coexisting pyroxenes is examined by means of the Nernst Distribution Law:

$$\text{Tr}_A/\text{Tr}_B = k_{\text{Tr}} \quad (29)$$

where Tr_j is the concentration of a trace element in phase j and k_{Tr} is a constant at any pressure and temperature. In this case A and B are orthopyroxene and clinopyroxene respectively.

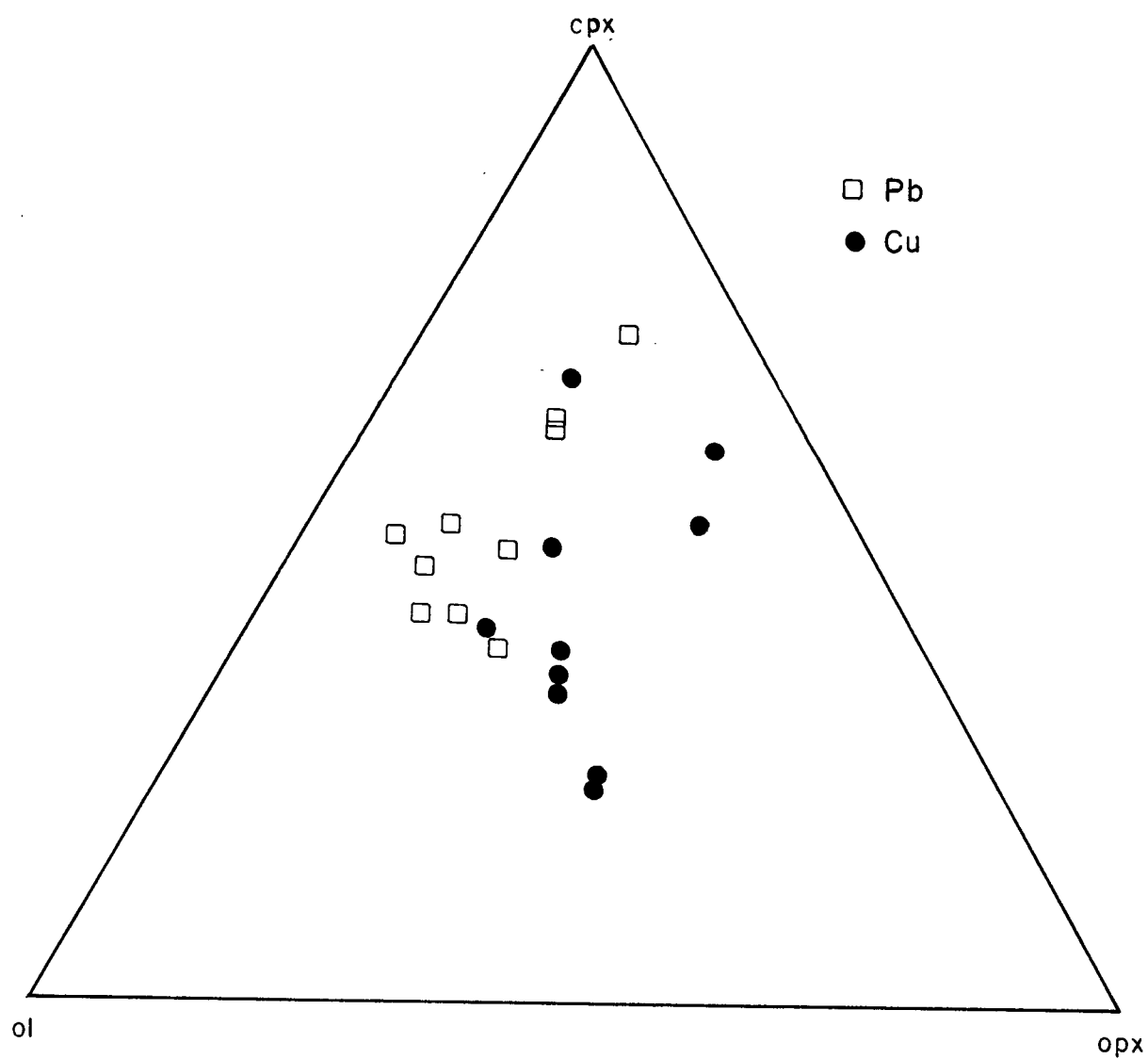


Fig. 29 : Relative proportions of Pb and Cu between coexisting olivine, orthopyroxene and clinopyroxene.

TABLE 13

Values of k_{T1} and k_{Cr} for coexisting pyroxenes with analysis of variance.

Sample	Locality	k_{T1}	k_{Cr}
JL-A	Jacques Lake	0.49	0.51
JL-39	"	0.41	0.56
JL-10	"	0.29	0.58
JL-B	"	0.27	0.41
JL-55	"	0.23	0.37
95	Castle Rock	0.28	0.42
S-3	"	1.20	0.38
CR-8	"	0.36	0.37
ERC-11	"	0.35	0.30
NL-8	Nicola Lake	0.25	0.10
Between suites		.097	.031
Variance	Within suites	.080	.006
Within suites		7	7
Degrees of freedom	Between suites	1	1
F		1.21	5.17

The values for k_{T1} and k_{Cr} are listed in Table 13. Also given is an analysis of the variance in k_{Tr} between the Jacques Lake and Castle Rock suites. The Nicola Lake pair are considered separately.

As can be seen both k_{T1} and k_{Cr} are variable and there is no difference between the suites. The exception is the low k_{Cr} of the Nicola Lake pair. The reason for this is not known. The foregoing suggests that the distribution of T1 and Cr between coexisting pyroxenes is not sensitive to different conditions of formation. The higher T1 content of the Jacques Lake pyroxenes is probably a result of a difference in the T1 content of the source rocks.

CHAPTER 8

The Origin of the Nodules.

(a) Temperature and Pressure.

On the basis of the distribution of iron and magnesium between coexisting mineral pairs it has been shown that each suite of nodules formed under different P/T conditions. Variations in K_D reflect different temperatures of formation. Nominal temperatures of formation are 838°C for the Nicola Lake suite, 1085°C for the Jacques Lake suite and 1600°C for the Castle Rock suite. While there is some doubt as to the absolute temperatures it is believed that each suite formed at different temperatures and that the relative temperatures are correct (Chapter 6).

The effects of pressure on K_D are unknown, but it is believed that different pressures are also responsible for variations in the distribution coefficients. This may be one reason for the comparatively high Castle Rock temperatures; the effects of pressure were not taken into account in the calculation of the temperatures. Al substitution in pyroxenes affects the values of K_D 's involving pyroxenes (Chapter 6), but unfortunately quantitative estimates of pressure cannot be made on the basis of variations in K_D .

Al occurs in both sixfold and fourfold co-ordination in the pyroxene structure. This is a result of the requirements of charge balance. The appropriate substitutions are $\text{Al}^{\text{IV}} + \text{Al}^{\text{VI}}$ for $\text{Mg}^{\text{VI}} + \text{Si}^{\text{IV}}$ and $\text{Al}^{\text{VI}} + \text{Na}^{\text{VIII}}$ for 2Mg^{VI} . If Al occurs in octahedral and tetrahedral co-ordination, then a Tschermak's component will appear in an end-member calculation. Since only partial chemical

analyses were done, the amount of Tschermak's component can only be estimated. This was done by assuming that the weight percent of $\text{SiO}_2 = 100 - \sum R_x\text{O}_y$ where $R_x\text{O}_y$ is the weight percent of any oxide. The calculation of the end-members was done by computer using the program PYREND (U.B.C. Dept. of Geology program; P.B. Read). The calculation of SiO_2 by difference and the fact that all iron was assumed to be in the ferrous state limits the accuracy of the results. The error in estimating SiO_2 will be the sum of all the errors in the determined oxides. Because of this only the results of the calculation of the Tschermak's components are given (Tables 3 and 4), since these are the most significant with respect to pressure (see below).

CaTs is a component of all the clinopyroxenes. There appears to be no difference between the suites in the amount of CaTs in these pyroxenes. Both CaTs and MgTs are components of the orthopyroxenes, except in the Nicola Lake enstatite. Fig. 30 shows the proportions of CaTs, MgTs, diopside and enstatite in the pyroxenes. Since CaTs and MgTs are present in solution (except for Nicola Lake) in diopside and enstatite respectively it is reasonable to suggest that these minerals formed at high pressure (Boyd 1963; Kushiro and Yoder 1966; Kushiro 1969a). The stabilities of Al-diopside and Al-enstatite coexisting with spinel and olivine are shown in Fig. 32.

Because the CaTs solubility in diopside is complexly related to temperature, pressure, the amount of jadeite in the diopside and the nature and composition of the coexisting phases, it is not possible to make precise estimates of the pressures at which

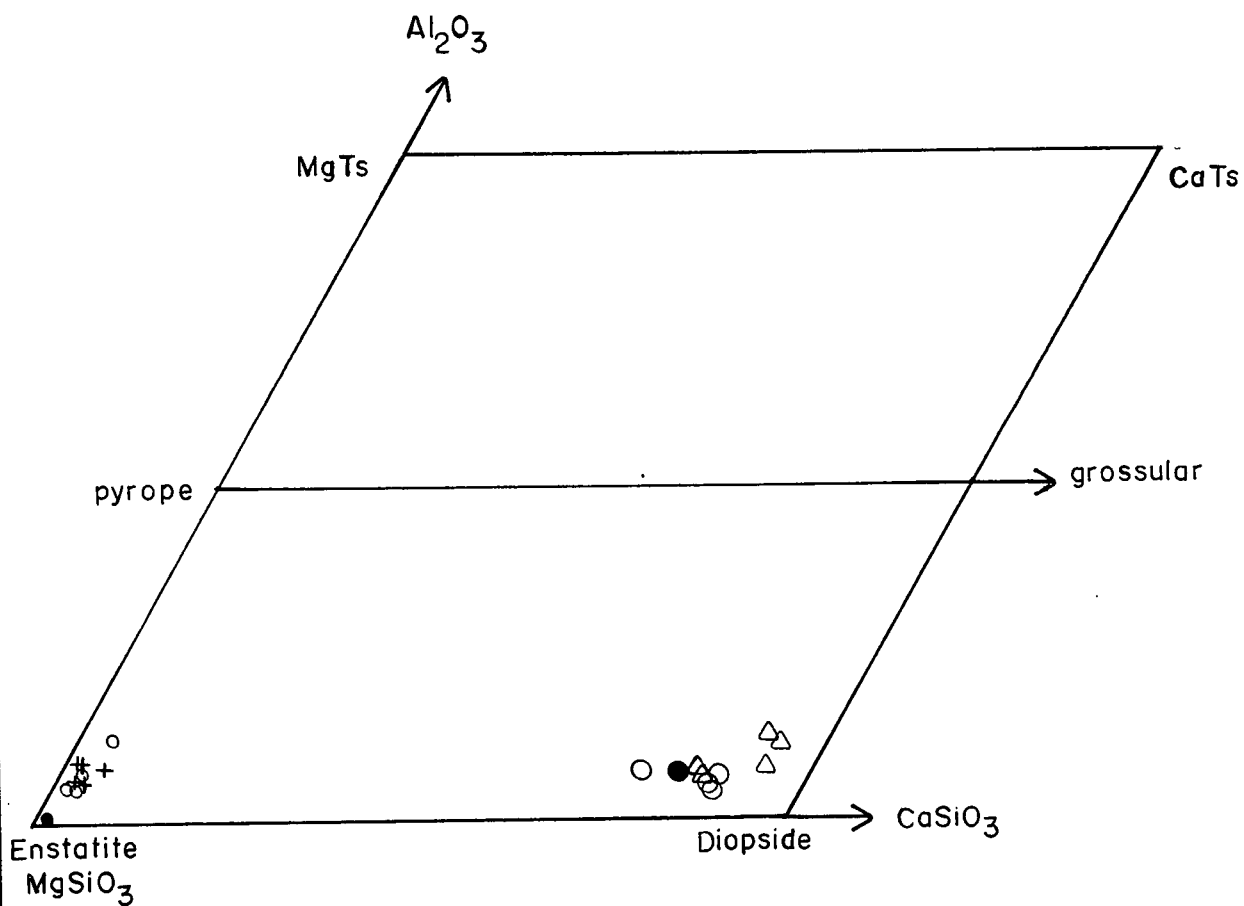


Fig. 30 : Composition of analysed pyroxenes in terms of MgSiO_3 - CaSiO_3 - Al_2O_3 .

<p>opx. {</p> <ul style="list-style-type: none"> + Jacques Lake. o Castle Rock. ● Nicola Lake. 	<p>cpx. {</p> <ul style="list-style-type: none"> Δ Jacques Lake. o Castle Rock. ● Nicola Lake.
---	---

the diopsides formed (Kushiro 1969a).

Boyd and England (1960) and Boyd (1963) have shown that the Al_2O_3 content of enstatite coexisting with olivine and garnet increases with increasing temperature and pressure due to the coupled substitution 2Al for $(\text{Mg} + \text{Si})$. Similar variations might be expected for enstatite coexisting with olivine and spinel. The Al_2O_3 content of the analysed enstatites varies with that of the spinels and also between spinel and diopside (Fig. 31). This suggests that the distribution of Al_2O_3 between spinel and pyroxene may be a function of pressure and temperature as is the case for co-existing pyroxene and garnet. Unfortunately there are no experimental data to confirm this.

The temperatures derived from the distribution of iron and magnesium between coexisting olivine and spinel, and the high pressures inferred from the Al_2O_3 content of the pyroxenes are consistent with the experimentally determined field of spinel lherzolite. The stability fields of various ultramafic mineral assemblages are shown in Fig. 32, taken from Green and Ringwood (1970). Spinel lherzolite has a fairly wide stability field which falls within upper mantle conditions. On the low pressure side of the lherzolite stability field plagioclase is stable and on the high pressure side garnet appears. The upper temperature limit of the stability of lherzolite is, of course, the lherzolite solidus.

Many experimental studies have been carried out to determine the position of these boundary curves. Reactions between olivine and plagioclase to yield aluminous pyroxenes and spinel have been investigated by Kushiro and Yoder (1966). Such a reaction is:

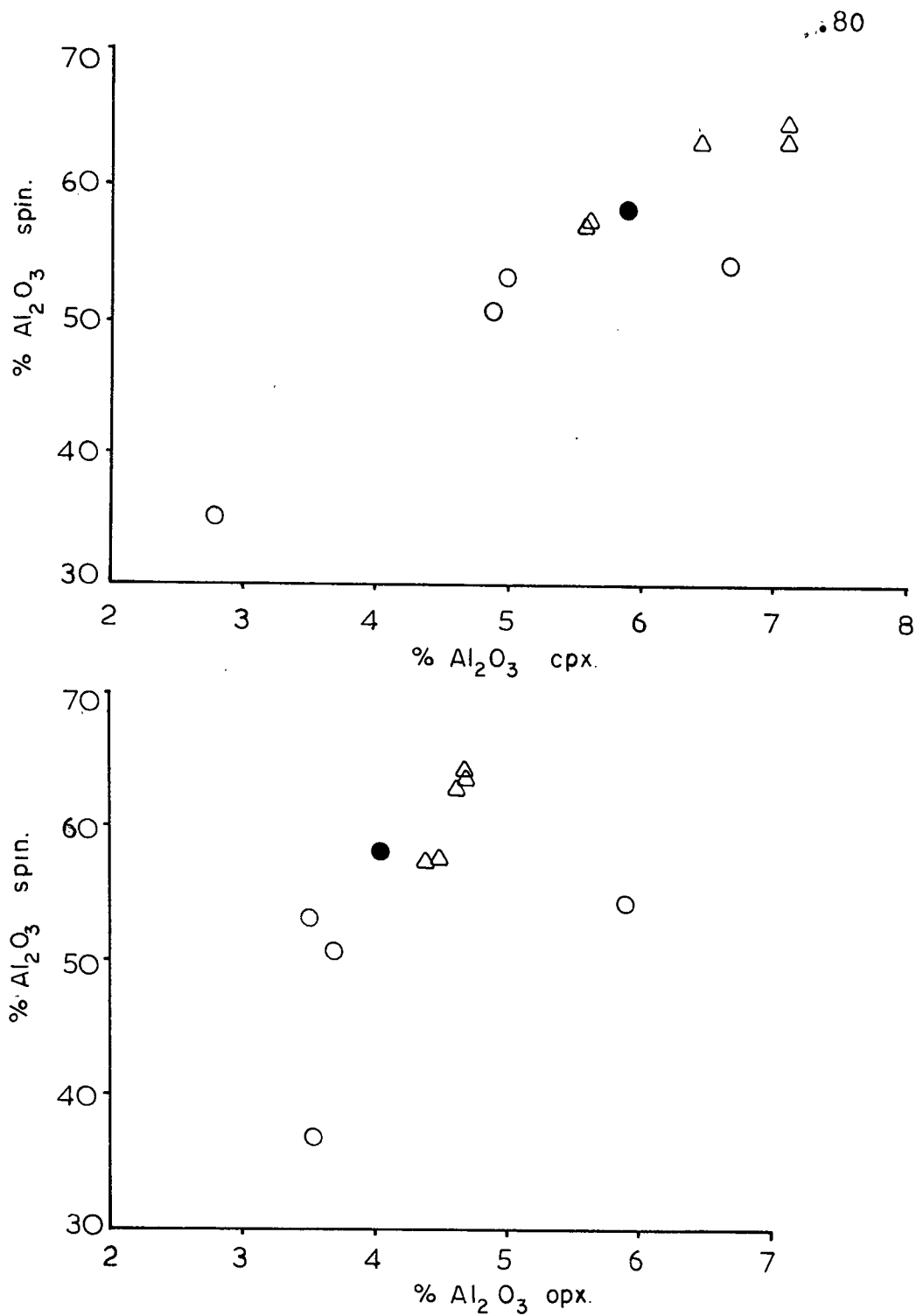


Fig. 31 : Variation of Al_2O_3 between spinel and pyroxenes.

Δ Jacques Lake : O Castle Rock : ● Nicola Lake.

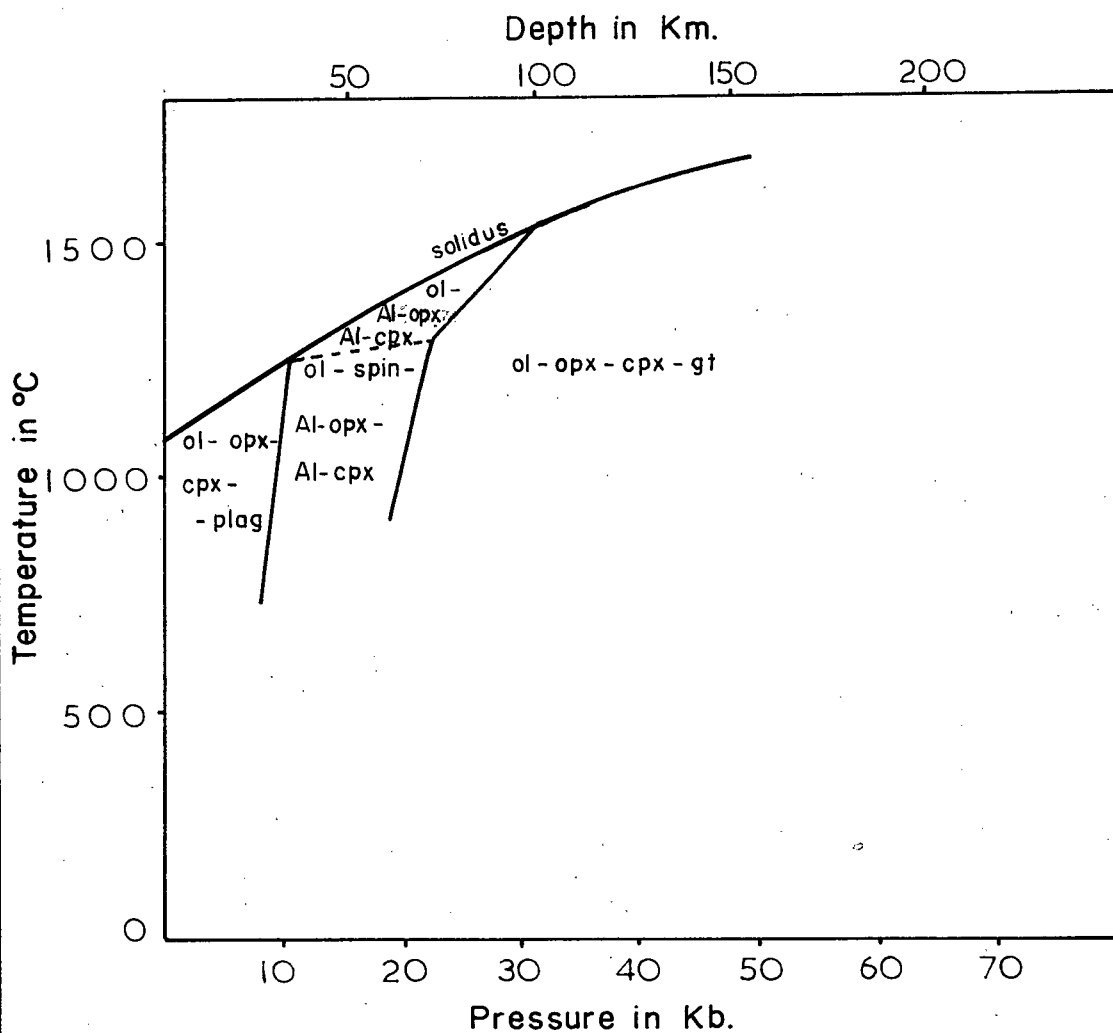


Fig. 32 : Relative stabilities of various ultramafic mineral assemblages. (after Green and Ringwood 1970)

forsterite + anorthite = Al-diopside + Al-enstatite + spinel

The exact position of the curve in natural systems is dependant on the compositions of the reacting phases which may vary. The relative stabilities of plagioclase and spinel bearing peridotites is, however, as shown in Fig. 32.

Reactions defining the breakdown of spinel and the incoming of garnet are:

enstatite + spinel = forsterite + pyrope

and

diopside + spinel = forsterite + grossular

(McGregor 1967). There is no general agreement on the exact position of the boundary curve (Green and Ringwood 1970). McGregor (1970) has shown that the stabilities of spinel and garnet bearing peridotites is strongly dependant on the $\text{Cr}_2\text{O}_3:\text{R}_2\text{O}_3$ ratio of the rock. Spinel peridotites with a high $\text{Cr}_2\text{O}_3:\text{R}_2\text{O}_3$ ratio are stable at higher pressures than those with a low $\text{Cr}_2\text{O}_3:\text{R}_2\text{O}_3$ ratio. It is to be expected that similar variations will also affect the lower limits of the stability of spinel lherzolite. At near solidus temperatures spinel lherzolites are stable to about 23Kb. depending on the ratio of trivalent oxides (McGregor 1968, 1970).

Despite the uncertainties in the experimental data, the mineral assemblages and partial mineral analyses suggest that the nodules formed in the upper mantle where at near solidus temperatures, the pressure would be between 11 and 23 Kb. (equivalent to a depth between 35 and 75 Km.) (Fig. 32). Each nodule suite apparently formed under different conditions within the mantle.

Of the three suites, the Nicola Lake nodules formed at the lowest temperature and probably pressure. The enstatite of the nodules from this suite contains no MgTs (Table 3) suggesting that most of the Al is in fourfold co-ordination and that this nodule formed at a lower pressure than those of the other suites. (Boyd 1963).

The Jacques Lake nodules formed at temperatures well below those of Castle Rock and slightly above the Nicola Lake nodules (Table 8). The relative pressures are not so certain. The Jacques Lake pyroxenes contain more Al_2O_3 than those of Castle Rock (Fig. 31) but whether this is due to temperature, pressure or bulk composition is not known. A higher temperature does not necessarily imply a higher pressure as the geothermal gradient in the Castle Rock region may be steeper than in the Jacques Lake region. However it is believed that the pressures at which the two suites of nodules formed were not the same. The basis of this inference is the different distributions of iron and magnesium between olivine and orthopyroxene for the two suites (Chapter 6). Supporting this is the different olivine fabrics in the suites (Chapter 4). The Castle Rock fabric may be due to relatively high pressure and temperature (Ave'Lallement and Carter 1970) but this requires experimental confirmation.

(b) The nature of the source.

The preceding discussion has shown that the lherzolite nodules probably originated in the upper mantle. It is now necessary to decide which aspect of the mantle they represent. Two hypotheses

are considered.

(a) They are crystal cumulates which precipitated from their present host rocks.

(b) They are fragments of the mantle which may have been depleted by partial melting.

If a cognate origin is proposed, it would be expected that there would be a wide range in the mineral proportions and compositions among a suite of lherzolite nodules. This is not the case for the Castle Rock or Jacques Lake suites. The range of compositions of the Nicola Lake suite is unknown. White (1966) and Kuno (1969) have shown that dunite, wehrlite and gabbro nodules have a wide compositional range and that the compositional trends of these nodules is distinct from those of lherzolite nodules. The variation in the wehrlite nodule series is thought to be due to crystal settling from a basaltic magma at depth. The narrow compositional range of lherzolite nodules is due to their being fragments of the mantle.

Binns (1969) has found both lherzolite nodules and megacrysts of undoubted cognate origin in the same lava flow. These megacrysts which may occur as clusters, include olivine, clinopyroxene, orthopyroxene and spinel and are quite distinct chemically (they are less magnesian) from the minerals of the lherzolites and appear to have originated at depth. It can be argued in this case that the lherzolites are not cognate but are residual mantle material and that the megacrysts represent the earliest crystal fraction of a basaltic magma produced in the upper mantle. Kutolin and Frolova (1970) and Aoki and Kushiro (1968) have examined

similar material and have come to the same conclusion.

The petrofabric study has shown that the Castle Rock and Jacques Lake nodules have been deformed in the solid state. If these nodules are cumulates, then the following sequence of events might have taken place. Partial melting in the mantle occurred. The liquid which was produced remained at depth while crystal fractionation took place. The cumulates which formed were then deformed before being brought to the surface. If this process did take place, it would require quiescent conditions in the upper mantle or lower crust to allow a crystal pile to accumulate. This is contrary to the conditions inferred from the olivine fabrics, and also contrary to conditions expected during partial fusion. On the other hand, a simple two-step process whereby fractional melting and ascent of the resultant liquid brought up fragments of the residual mantle rock would satisfy the requirement that the nodules have been deformed. The fabric is then due to processes which operated prior to or perhaps during partial melting.

It is possible that partial melting could result in the production of a basalt which remained at depth while precipitating crystals and forming a lherzolite. The magma could then have been removed and the lherzolite deformed. A second episode of melting could then have occurred and fragments of the lherzolite caught up in the resultant basalt which brought them to the surface.

Carter (1970) has examined lherzolites and other ultramafic nodules from a single locality. He found that those lherzolites ("typical 4-phase nodules") which have a mode close to the olivine apex of the olivine-orthopyroxene-clinopyroxene diagram (Fig. 3) generally have olivine with a composition more magnesian than F088.

Other lherzolites ("atypical 4-phase nodules") fall in the central part of the diagram and have olivines less magnesian than Fo₈₆. These lherzolites appear to be undeformed and have cumulate textures, as opposed to the typical lherzolites which appear to be deformed and recrystallised.

Carter (1970) proposes a model whereby atypical lherzolites (and also wehrlites and pyroxenites) are among the cumulates formed at depth from a basaltic magma. Typical lherzolites are probably residual products of partial melting, although in some cases an origin by accumulation cannot be discounted. This is similar to the model proposed by White (1966). Carter's (1970) model is based on experimental work by Kushiro (1969b) and on an analysis of possible crystal-liquid paths during partial fusion according to the methods of Presnall (1969). White's (1966) model is based on petrography and mineral chemistry.

Using the above model the lherzolites of this study fall into the category of "typical 4-phase nodules" (Table 2, Fig. 3). No wehrlites or pyroxenites were found with the Jacques Lake lherzolites. A comparison with the above model and with work by Aoki and Kushiro (1968), Kuno (1969), Binns (1969) and Kutolin and Frolova (1970) mentioned above suggests that the Jacques Lake nodules were not part of a cumulate series prior to their incorporation into the Jacques Lake tuff. The full range of nodule types at Castle Rock is not known but since all the nodules which were studied fall into the category of "typical 4-phase nodule" and appear to have been deformed, an origin by accumulation is discounted.

On the basis of the mode (Table 1) and the composition of the olivine ($\text{Fo}_{91.2}$) specimen NL-8 from Nicola Lake is a "typical" 4-phase nodule". The modes of the other nodules from this suite are variable (Fig. 3) although the full range is not known. The olivine fabric of this nodule and the textures of this and other nodules from this suite suggest that these nodules have formed by accumulation. The temperature at which the Nicola Lake nodules have inferred to have formed (nominal temperature is 838°C) is below any known lherzolite solidus, even under hydrous conditions (Fig. 33). The weight of the evidence therefore favours an origin by crystal settling and accumulation at depth for this suite. The nodules may be cognate with their enclosing basalt.

One essential characteristic of a parental mantle rock is that it is capable of producing a basalt on partial melting at high pressure. There are two ways to consider this proposition. Firstly, direct experiments on the melting behavior of possible mantle rocks (natural or synthetic) can be made. Secondly, mixtures of basalt plus refractory residuum can be examined to determine whether these pairs result in a proposed mantle composition.

Direct melting experiments on spinel lherzolite have been carried out by Kushiro et.al. (1968) and by Nishikawa et.al. (1970). The results of these studies and also of work by Kushiro (1969b) indicate that a silica undersaturated magma can be produced by partial melting of a spinel lherzolite. The type of magma which is produced depends on the degree of partial melting, on the presence or absence of water, and also the pressure at which melting took

place. The residue from such melting may be a more magnesian lherzolite, a harzburgite or a dunite. These may be produced under a wide pressure and temperature range and under both hydrous and anhydrous conditions.

In addition to the above experimental studies, work on the chemical relationships between basalt and ultramafic nodules has been done by Kuno (1969), Kuno and Aoki (1970) and Jackson and Wright (1970). They found that a basalt close to the composition of an olivine tholeiite could be produced from a pyroxene rich lherzolite, leaving a more magnesian lherzolite as residual material. Green and Ringwood (1969) argue that alkali olivine basalt can be produced by a low degree (<20%) of partial melting of lherzolite at depths of 35-70Km. With an increasing degree of partial melting, olivine tholeiite can be produced.

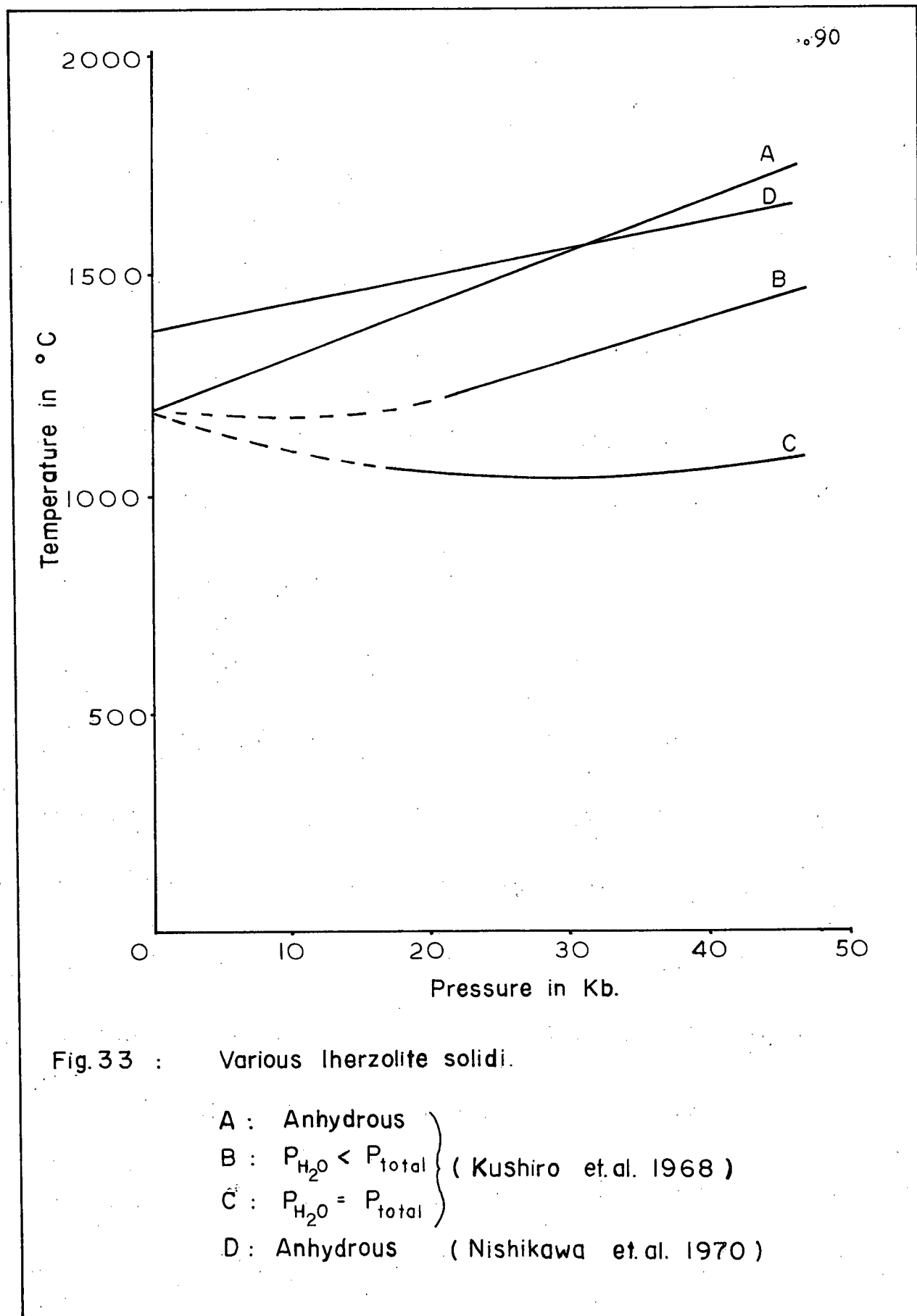
The above summary of recent work on basalt-lherzolite relationships shows that lherzolite may be a refractory residual material left after partial melting of primary mantle, which may itself be lherzolite (Kuno and Aoki 1970) or a mixture of lherzolite and garnet peridotite (Jackson and Wright 1970). Thus lherzolite nodules (including the nodules of this study) could be residual fragments of partially melted mantle. Lherzolite nodules are not generally considered to be parts of the primary mantle since they are too low in certain elements (K, Ti, P, Ba, Sr, Rb, Th, U and others) to produce basalt on partial melting (Harris et. al. 1967; Green and Ringwood 1969). The low K_2O content of the minerals of these nodules supports this (Tables 3 and 4).

No chemical data on the enclosing rocks of the nodules in this study are available. Nevertheless, in view of the close similarities in mineralogy, texture and mineral compositions of these nodules to nodules which have been studied in relation to their host rock chemistry, it is reasonable to suggest that these rocks are fragments of the mantle. A worldwide similarity of lherzolite nodules, regardless of the nature of the enclosing rocks, is an argument against lherzolite nodules in general being cumulates.

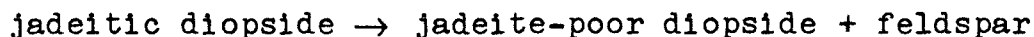
The temperatures at which the Castle Rock and Jacques Lake nodules are thought to have formed are consistent with the hypothesis that the Castle Rock and Jacques Lake lherzolites are residual fragments of the upper mantle. The Jacques Lake nodules appear to have formed at 1085°C . This temperature is close to the solidus temperature of lherzolite at high pressure where $P_{\text{H}_2\text{O}} < P_{\text{total}}$ and above the solidus temperature of lherzolite where $P_{\text{H}_2\text{O}} = P_{\text{total}}$ at high pressure (Kushiro et. al 1968) (Fig. 33).

While the above temperature could be applied to the argument that the Jacques Lake nodules formed at a basalt liquidus temperature, the same cannot be said for the Castle Rock suite. The calculated temperatures of formation of these nodules are greater than 1600°C . This is greater than any lherzolite solidus at pressures where spinel is stable, even under anhydrous conditions (Kushiro et. al. 1968; Nishikawa et. al. 1970). While there is some doubt as to the absolute temperatures at which the nodules formed, the relative temperatures are believed to be correct (p.60) so that these nodules appear to be refractory and may be residue from partial fusion of the mantle.

Textural evidence described in Chapter 3 suggests that the above



discussion is reasonable. It has been suggested that the marginal alteration of the diopsides of the Castle Rock and Jacques Lake nodules (Fig. 8) is due to the reaction:



If the reaction is of this form, then another phase must have participated (either as a reactant or a catalyst) since the reaction occurs only at the rims of the diopsides. Enclosing minerals such as olivine are unaffected (Fig. 10). A fluid phase could have been present, but if a fluid was present and participated in the reaction, then coexisting orthopyroxene should also have been affected since it has been shown that orthopyroxene is unstable at the margin of the nodules. Coexisting olivine and enstatite are unaffected by any reaction (Fig. 10). Therefore the breakdown of diopside is not due to reaction with a fluid phase and cannot be a polymorphic change due to variation in the pressure and temperature since reaction occurs only at the rims of the diopsides.

One explanation of this is that it is due to partial melting. It is possible that the liquid produced by partial melting of lherzolite was trapped and quenched when the nodules were brought to the surface. The glass then devitrified to form feldspar (in part at least).

Diopside is the first phase to melt in a lherzolite of likely mantle composition (Kushiro 1969b; Ito and Kennedy 1967). Dickey et. al. (1971) have found that Cr-bearing diopside melts incongruently to spinel and liquid above 5Kb. The effects of Al_2O_3 , Cr_2O_3 and other components on melting behavior at high pressure in the system Di-Fo-SiO_2 (a simplified peridotite system) which

was studied by Kushiro (1969b) are not known but in view of the behavior of Cr-bearing diopside (Dickey et. al. 1971) they are likely to be significant. It is not necessary for the minimum melting point of lherzolite to be a eutectic. In the simplified peridotite system it is not certain whether point P (Fig.34) is a eutectic or a reaction point. Point A on the Di-Fo join is a piercing point (Fig.34) (Kushiro 1969b). Thus melting of diopside in a natural system is a possible explanation of the described texture.

The weight of the evidence favours the hypothesis that the source of the Castle Rock and Jacques Lake nodules is the upper mantle and that these nodules could be fragments of the mantle which has been depleted by partial melting. There are two lines of evidence to suggest that the source of the Castle Rock nodules is layered. The majority of the samples available for study show some mineralogical layering. The olivine fabric of one of the layered specimens appears to be related to the layering (Fig.20). The massive specimens have a similar fabric which suggests that the mechanism which produced the layering was operative throughout the source rock, even though some of hand specimen sized nodules are apparently unlayered. Mesoscopic layering is therefore probably characteristic of the source of the Castle Rock nodules.

On the other hand, the source rock of the Jacques Lake nodules is unlikely to be layered, at least on a mesoscopic scale. Only a few of several hundred specimens observed in the field were layered. The olivine fabric of the nodules which were studied is different from the Castle Rock fabrics or other layered ultramafic rocks (Chapter 4).

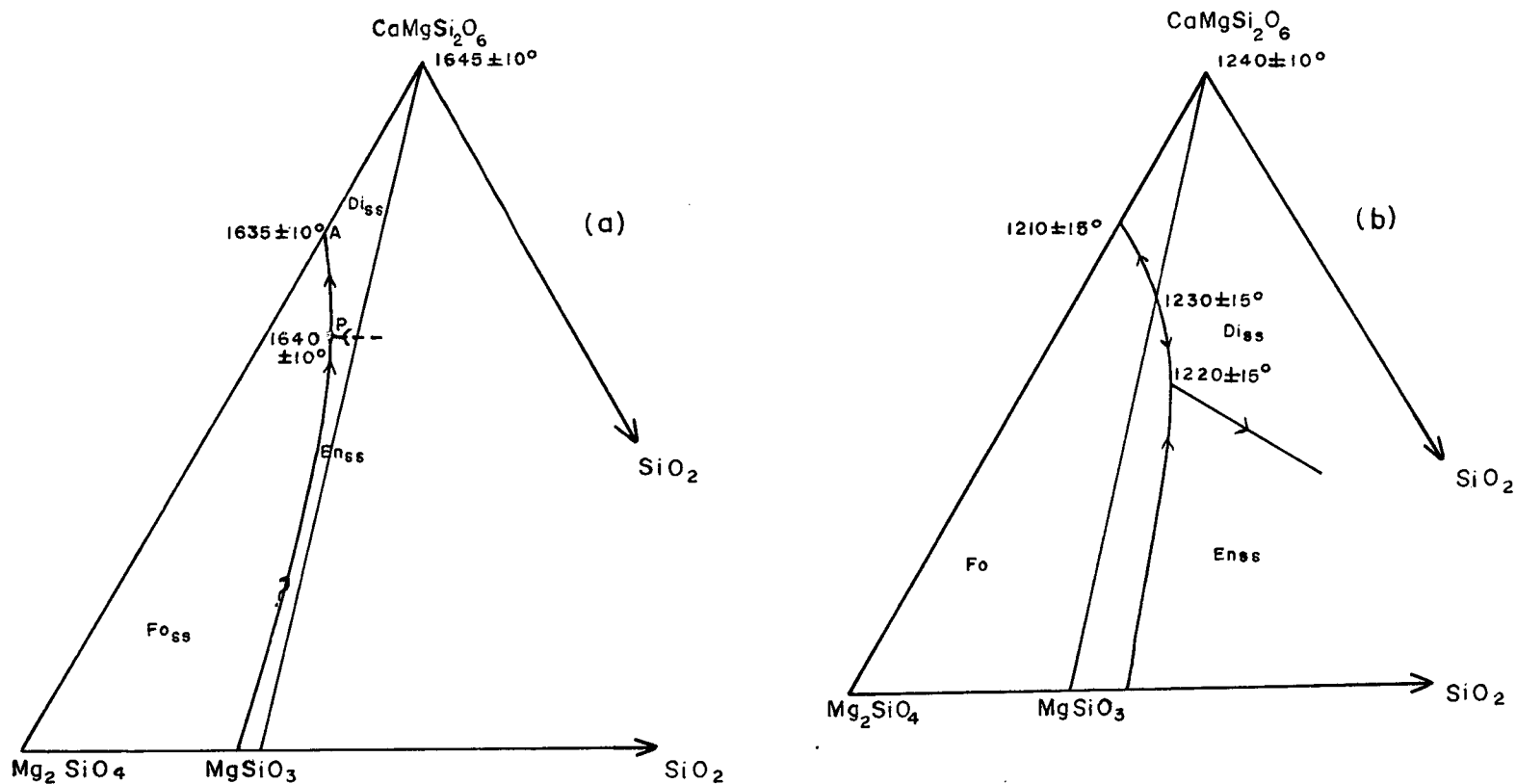


Fig. 34 : Part of the liquidus diagram of the system Fo-Di-SiO_2 at 20Kb. pressure ;
(a) hydrous , (b) anhydrous. (after Kushiro 1969b).

CHAPTER 9

The Upper Mantle in British Columbia.

It has been shown that the lherzolite nodules of Castle Rock and Jacques Lake are probably samples of the upper mantle. The differences and similarities between these suites of rocks are significant with respect to the constitution of the upper mantle in British Columbia. While much of the following discussion is speculative, it is nevertheless useful as a guide to what might be expected upon further study of the mantle in British Columbia.

The limited evidence from this study suggests that the upper mantle in British Columbia consists largely of spinel lherzolite. There is no evidence of regional differences in mineralogy nor of mineralogical zoning.

There is evidence of chemical variations. The Castle Rock pyroxenes are more magnesian and the spinels and pyroxenes are more aluminous than the corresponding minerals of the Jacques Lake nodules. This may be a result of a fundamental difference in the chemistry of the mantle in these areas or may be a result of different degrees of partial melting. The Castle Rock nodules are more refractory so if the upper mantle in British Columbia was originally homogeneous, different degrees of partial melting have resulted in the differences in mineral chemistry.

As well as major element variations there are variations in the trace element concentrations in the two areas. Both Castle Rock pyroxenes contain more Co, the diopsides contain more Ni and Zn, and the enstatites more Mn than the corresponding minerals of the Jacques Lake nodules. The upper mantle beneath Castle Rock

appears to be enriched in these elements relative to the mantle beneath Jacques Lake. This enrichment is probably a primary feature of the mantle in the Castle Rock region since the concentration of these elements is independent of major element variations.

Further sampling of nodules and also of the basaltic rocks of each area is required to support this suggestion. Analyses for more mobile elements such as Rb, Sr and the rare earths would be useful to test the hypothesis that geochemical provinces exist in the upper mantle in British Columbia. Data on these elements might allow one to evaluate the extent of partial melting and so distinguish primary variations in the chemistry of the mantle from variations due to different degrees of partial melting.

Physical as well as chemical variations exist in the upper mantle in British Columbia. It has been shown that the olivine fabrics of the Castle Rock and Jacques Lake nodules have resulted from deformation in the solid state, and that the suites have different characteristic fabrics. The fabrics are considered to have been imposed on the rocks prior to their inclusion in their enclosing rocks and are a result of stress within the mantle.

Hess (1964) showed that seismic anisotropy in the upper oceanic mantle is caused by the alignment of olivine in the direction of flow at major fracture zones. Keen and Barrett (1971) found that the mantle west of the Queen Charlotte Islands has an anisotropy related to the direction of sea floor spreading (Fig. 35). It is possible that this anisotropy extends into the mantle beneath British Columbia. Both the Castle Rock and Jacques Lake

olivines have a strong degree of preferred orientation suggesting that both regions are underlain by an anisotropic mantle. Each suite has a different fabric which suggests that the degree of anisotropy is not the same in each area. Also, the orientation of the olivine fabrics in the mantle and consequently the seismic velocity vectors in each area are likely to be different. Souther (1970) has suggested that the regional distribution of Quaternary volcanoes in British Columbia is controlled by major faults associated with mantle structures. (Fig. 34). If the orientation of olivine in the mantle is associated with fracture zones in the mantle, then different stress regimes associated with the two regions will produce different fabrics in the olivines and will result in varying degrees of anisotropy.

Castle Rock appears to lie in a zone of extension and Jacques Lake appears to lie in a zone of shear above the mantle. (Fig. 35). This might result in different fabrics being produced in the olivines in the mantle in these areas. Other factors such as strain rate, temperature, pressure and the presence or absence of water will also contribute to the type of fabric developed by a particular suite of rocks. Which of these is dominant is not known. Whatever the cause, it is likely that variations in the degree of anisotropy and consequently in the seismic behavior of the mantle in British Columbia are to be expected and that these may eventually be integrated into the regional tectonic framework.

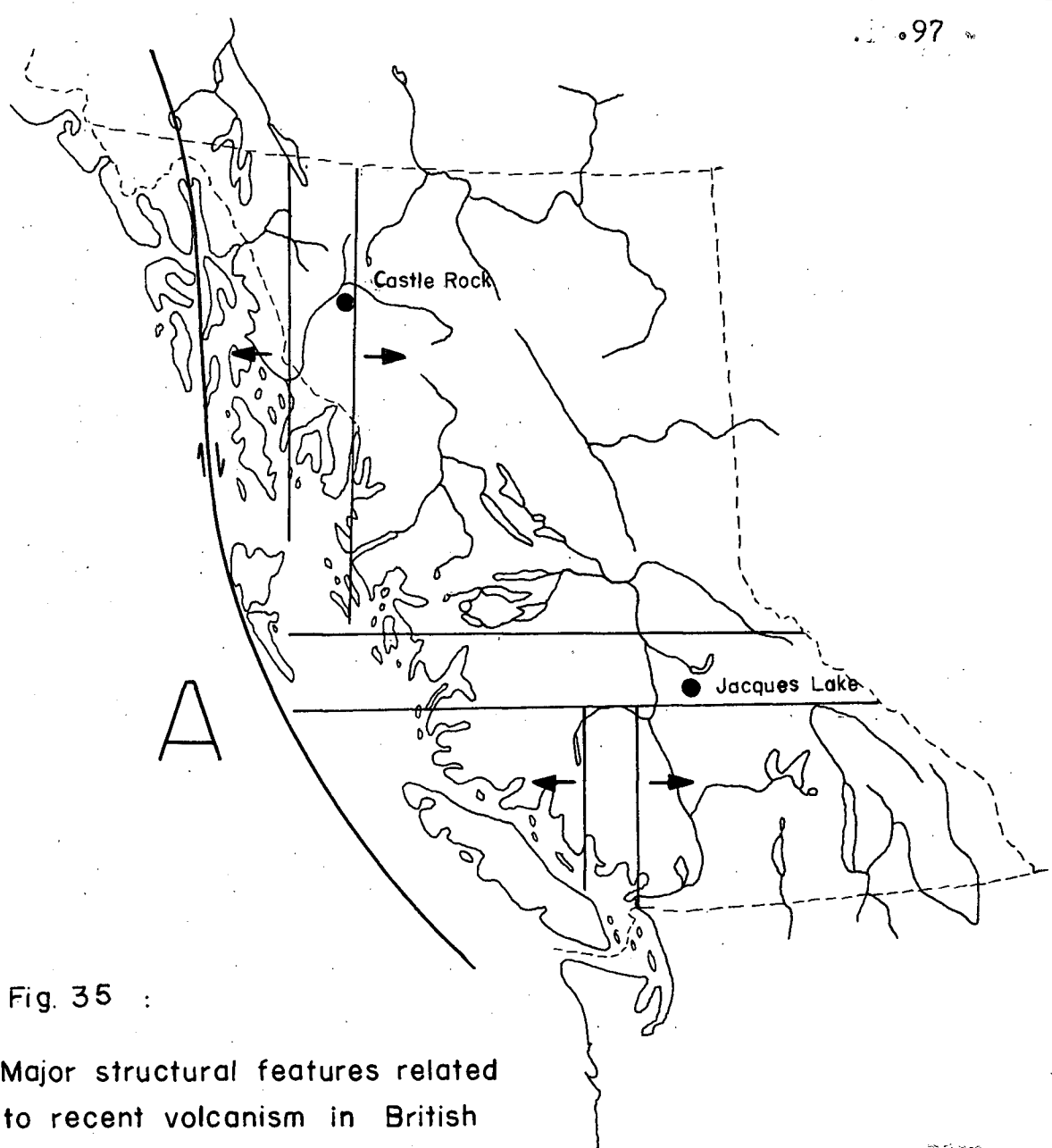


Fig. 35 :

Major structural features related to recent volcanism in British Columbia. (after Souther 1970)

- || Belts of Quaternary volcanoes.
- || Eastern limit of Tertiary and Recent transcurrent faulting (right lateral shear).
- ➔ Direction of inferred relative motion between adjacent segments of the Cordillera.
- A Area of mantle anisotropy. (Keen and Barret 1971)

CHAPTER 10

Conclusions.

The main finding of this study is that each suite of lherzolite nodules in basaltic rocks from British Columbia is characterised by its own range of mineral compositions and fabrics. The range of compositions for each suite is narrow and overlap to some extent. The distribution of some elements (eg. Fe, Ni, Mn, Co, Zn) between the minerals of each suite is different and is independent of mineral composition. The significance of this is that each suite probably formed under different P/T conditions.

Comparison with other studies and with relevant experimental work places the source of these nodules in the upper mantle. This agrees with the P/T conditions inferred from the mineral chemistry of these nodules.

Consideration of the textures and olivine fabrics of the Castle Rock nodules suggests that these rocks are fragments of the refractory upper mantle which is layered and has been deformed. The Jacques Lake nodules are also residual fragments of the mantle which has been deformed but in the Jacques Lake area is unlayered. The mineral chemistry of the nodules has shown that the Castle Rock lherzolites formed at higher temperatures and probably at greater depths than those of Jacques Lake. The Nicola Lake nodules are crystal accumulates, have not been deformed, and formed at lower pressures and temperatures than the other nodules. They could be cognate with their present host rocks.

The different chemical characteristics of the Castle Rock and

Jacques Lake nodules suggest that the mantle is chemically different in these regions. This may be a result of different degrees of partial melting of an originally homogeneous mantle but may also be a result of original heterogeneity

The strong preferred orientation of the olivine of the Castle Rock lherzolites and, to a lesser extent, those of Jacques Lake suggests that the mantle in these two regions is anisotropic. The different fabric types suggest that different deformational regimes are to be found from place to place in the mantle.

BIBLIOGRAPHY

- Aoki, K. (1968). Petrogenesis of ultrabasic and basic inclusions in alkali basalts, Iki Island, Japan. *Am. Miner.* 53, 241-256.
- Aoki, K. and Kushiro, I. (1968). Some clinopyroxenes from ultramafic inclusions in Dreiser Weiher, Eifel. *Contr. Miner. Petrol.* 18, 326-337.
- Ave'Lallement, H. and Carter, N.L. (1970). Syntectonic recrystallisation of olivine and modes of flow in the upper mantle. *Bull. geol. Soc. Am.* 81, 2203-2220.
- Bartholome, P. (1962). Iron-magnesium ratio in associated pyroxenes and olivines. In *Petrologic Studies*; Geol. Soc. Am. Buddington Volume, 1-20.
- Binns, R.A. (1969). High pressure megacrysts in basanitic lavas near Armidale, New South Wales. *Am. J. Sci. Schairer Volume* 267-A, 33-49.
- Black, P.M. and Brothers, R.N. (1965). Olivine nodules in olivine nephelinite from Tokatoka, Northland. *New Zealand J. Geol. Geophys.* 8, 62-80.
- Boyd, F.R. (1963). Some effects of pressure on phase relationships in the system $MgO-Al_2O_3-SiO_2$. *Yb. Carnegie Inst. Wash.* 62, 121-124.
- Boyd, F.R. and England, J.L. (1960). Aluminous enstatite. *Yb. Carnegie Inst. Wash.* 59, 49-52.
- Brothers, R.N. (1959). Flow orientation of olivine. *Am. J. Sci.* 257, 574-584.
- Brothers, R.N. (1960). Olivine nodules from New Zealand. *Proc. 21st. Int. geol. Congr.* 13, 68-81.
- Brothers, R.N. (1962). The relationship between preferred orientation of olivine in dunite and the tectonic environment: A discussion. *Am. J. Sci.* 260, 310-312.
- Brothers, R.N. (1964). Petrofabric analyses of Rhum and Skaergaard layered rocks. *J. Petrology* 5, 255-274.
- Brothers, R.N. and Rodgers, K.A. (1969). Petrofabric studies of ultramafic nodules from Auckland, New Zealand. *J. Geol.* 77, 452-465.
- Burns, R.G. (1970). Mineralogical applications of crystal field theory. London: Cambridge University Press.

- Cambell, R.B. (1961). Quesnel Lake, West Half, Cariboo District, British Columbia. Geol. Surv., Canada, Map 3-1961.
- Carter, J.L. (1970). Mineralogy and chemistry of the earth's upper mantle, based on the partial fusion - partial crystallisation model. Bull. geol. Soc. Am. 81, 2021-2034.
- Carter, N.L. and Ave'Lallement, H. (1970). High temperature flow of dunite and peridotite. Bull. geol. Soc. Am. 81, 2181-2202.
- Collee, A.I.G. (1963). A fabric study of lherzolites with special reference to nodular inclusions in the lavas of Auvergne, France. Leid. geol. Meded. 28, 1-102.
- Dickey, J.S., Yoder, H.S. and Schairer, J.F. (1971). Chromium in silicate-oxide systems. Yb. Carnegie Inst. Wash. 70, 118-125.
- Forbes, R.B. and Banno, S. (1966). Nickel-iron content of peridotite inclusions and cognate olivine from an alkali-olivine basalt. Am. Miner. 51, 130-140.
- Forbes, R.B. and Kuno, H. (1965). The regional petrology of peridotite inclusions and basaltic host rocks. Upper mantle symposium, New Delhi 1964. Copenhagen: Int. Un. geol. Sci., 161-179.
- Forbes, R.B. and Kuno, H. (1967). Peridotite inclusions and basaltic host rocks. In Ultramafic and Related Rocks, 328-337. Wyllie, P.J. (ed.). New York: Wiley.
- Fuster, J.M., Paez, A. and Sagredo, J. (1969). Significance of basic and ultramafic inclusions in the basalts of the Canary Islands. Bull. Volcan. 33, 665-693.
- Goles, G.C. (1967). Trace elements in ultramafic rocks. In Ultramafic and Related Rocks, 352-362. Wyllie, P.J. (ed.). New York: Wiley.
- Grover, G.E. and Orville, P.M. (1969). The partitioning of cations between coexisting single and multi-site phases with applications to the assemblages: orthopyroxene-clinopyroxene and orthopyroxene-olivine. Geochim. cosmochim. Acta 33, 205-226.
- Green, D.H. (1968). Origin of basalt magmas. In Basalts Vol. 2, 835-862. Hess, H. and Poldervaart, A. (eds.). New York: Interscience.

- Green, D.H. and Ringwood, A.E. (1969). The origin of basaltic magmas. *Monogr. Am. geophys. Un.* 13, 489-495.
- Green, D.H. and Ringwood, A.E. (1970). Mineralogy of peridotitic compositions under upper mantle conditions. *Phys. Earth planet. Interiors* 3, 359-371.
- Hamad, El.D. (1963). The chemistry and mineralogy of the olivine nodules of Colton Hill, Derbyshire. *Mineralog. Mag.* 33, 483-497.
- Harris, P.G., Reay, A. and White, I.G. (1967). Chemical composition of the upper mantle. *J. geophys. Res.* 72, 6359-6369.
- Hess, H.H. (1964). Seismic anisotropy of the uppermost mantle under oceans. *Nature* 203, 629-631.
- Irvine, T.N. (1965). Chromian spinel as a petrogenetic indicator. Part 1: Theory. *Can. J. Earth Sci.* 2, 648-672.
- Irvine, T.N. (1967). Chromian spinel as a petrogenetic indicator. Part 2: Petrologic applications. *Can. J. Earth Sci.* 4, 71-103.
- Ishibashi, K. (1970). Petrochemical study of basic and ultrabasic inclusions in basaltic rocks from Northern Kyushu, Japan. *Mem. Fac. Sci., Kyushu Univ., Ser.D, Vol. 20*, 85-146.
- Ito, K. and Kennedy, G.C. (1967). Melting of peridotite at 40Kb. *Am. J. Sci.* 265, 519-538.
- Jackson, E.D. (1961). Primary textures and mineral associations in the ultramafic zones of the Stillwater Complex, Montana. *Prof. Pap. U.S. geol. Surv.* 358.
- Jackson, E.D. (1968). The character of the lower crust and upper mantle beneath the Hawaiian Islands. *Proc. 23rd. Int. geol. Congr.* 1, 135-150.
- Jackson, E.D. (1969). Chemical variation in coexisting chromite and olivine in the chromite zones of the Stillwater Complex. *Symposium on Magmatic Ore Deposits, Econ. Geol. Monogr.* 4, 41-71.
- Jackson, E.D. and Wright, T.L. (1970). Xenoliths in the Honolulu Volcanic Series, Hawaii. *J. Petrology* 11, 405-430.
- Keen, C.E. and Barrett, D.L. (1971). A measurement of seismic anisotropy in the Northeast Pacific. *Can. J. Earth Sci.* 8, 1056-1064.
- Kretz, R. (1961). Some applications of thermodynamics to coexisting minerals of variable composition. Examples: orthopyroxene-clinopyroxene and orthopyroxene-garnet. *J. Geol.* 69, 361-387.

- Kretz, R. (1963). Distribution of magnesium and iron between orthopyroxene and calcic pyroxene in natural mineral assemblages. *J. Geol.* 71, 773-785.
- Kuno, H. (1967). Mafic and ultramafic nodules from Itonome-gata, Japan. In *Ultramafic and Related Rocks*, 337-342. Wyllie, P.J. (ed.). New York: Wiley.
- Kuno, H. (1969). Mafic and ultramafic nodules in basaltic rocks of Hawaii. *Mem. geol. Soc. Am.* 115, 189-234.
- Kuno, H. and Aoki, K. (1970). Chemistry of ultramafic nodules and their bearing on the origin of basaltic magmas. *Phys. Earth planet. Interiors* 3, 273-301.
- Kushiro, I. (1969a). Clinopyroxene solid solutions formed by reactions between diopside and plagioclase at high pressures. *Spec. Pap. mineralog. Soc. Am.* 2, 179-191.
- Kushiro, I. (1969b). The system forsterite-diopside-silica with and without water at high pressures. *Am. J. Sci. Schairer* Vol. 267-A, 269-294.
- Kushiro, I. and Yoder, H.S. (1966). Anorthite-forsterite and anorthite-enstatite reactions and their bearing on the basalt-eclogite transformation. *J. Petrology* 7, 337-362.
- Kushiro, I., Yasuhiko, S. and Akimoto, S. (1968). Melting of a peridotite at high pressures and high water pressures. *J. geophys. Res.* 73, 6023-6029.
- Kutolin, V.A. and Frolova, V.M. (1970). Petrology of ultramafic inclusions from basalts of Minusa and Transbaikalian Regions. *Contr. Miner. Petrol.* 29, 163-179.
- Langmyhr, F.J. and Paus, P.E. (1968). The analysis of inorganic siliceous materials by atomic absorption spectrophotometry and the hydrofluoric acid decomposition technique. Part 1: The analysis of silicate rocks. *Analytica chimica Acta* 43, 397-408.
- Loney, R.A., Himmelberg, G.R. and Coleman, R.G. (1971). Structure and petrology of the Alpine-type peridotite at Burro Mountain, California, U.S.A. *J. Petrology* 12, 245-309.
- Matsui, Y. and Banno, S. (1970). Partition of divalent transition metals between coexisting ferromagnesian minerals. *Chem. Geol.* 5, 259-265.
- McIntyre, W.I. (1963). Trace element partition coefficients. A review of theory and applications to geology. *Geochim. cosmochim. Acta* 27, 1209-1264.

- McGregor, I.D. (1967). Mineralogy of model mantle compositions. In *Ultramafic and Related Rocks*, 382-393. Wyllie, P.J. (ed.). New York: Wiley.
- McGregor, I.D. (1968). Mafic and ultramafic inclusions as indicators of the depth of origin of basaltic magmas. *J. geophys. Res.* 73, 3737-3745.
- McGregor, I.D. (1970). The effect of CaO , Cr_2O_3 , Fe_2O_3 and Al_2O_3 on the stability of spinel and garnet peridotites. *Phys. Earth planet. Interiors* 3, 372-377.
- Medaris, L.G. (1969). Partitioning of Fe^{2+} and Mg^{2+} between coexisting synthetic olivine and orthopyroxene. *Am. J. Sci.* 267, 945-968.
- Mercy, E. and O'Hara, M.J. (1967). Distribution of Mn, Cr, Ti and Ni in coexisting minerals of ultramafic rocks. *Geochim. cosmochim. Acta* 31, 2331-2341.
- Mueller, R.F. (1961). Analysis of relations among Mg, Fe and Mn in certain metamorphic minerals. *Geochim. cosmochim. Acta* 25, 267-296.
- Nafziger, R.H. and Muan, A. (1967). Equilibrium phase compositions and thermodynamic properties of olivines and pyroxenes in the system MgO - FeO - SiO_2 . *Am. Miner.* 52, 1364-1385.
- Nishikawa, M., Kono, S. and Aramaki, S. (1970). Melting of lherzolite from Itonome-gata at high pressures. *Phys. Earth planet. Interiors* 4, 138-144.
- O'Hara, M.J. (1963). Distribution of iron between olivines and calcium-poor pyroxenes in peridotites, gabbros and other magnesian environments. *Am. J. Sci.* 261, 32-46.
- O'Hara, M.J. (1967). Crystal-liquid equilibria and the origins of ultramafic nodules in basic igneous rocks. In *Ultramafic and Related Rocks*, 346-349. Wyllie, P.J. (ed.). New York: Wiley.
- O'Hara, M.J. (1968). The bearing of phase equilibria studies in synthetic and natural systems on the origins of basic and ultrabasic rocks. *Earth Sci. Rev.* 4, 69-133.
- Presnall, D.C. (1969). The geometrical analysis of partial fusion. *Am. J. Sci.* 267, 1178-1194.
- Ragan, D.M. (1969). Olivine recrystallisation textures. *Mineralog. Mag.* 37, 238-240.
- Raleigh, C.B. (1968). Mechanism of plastic deformation of olivine. *J. geophys. Res.* 73, 5391-5406.

- Ramberg, H. and DeVore, G.W. (1951). The distribution of Fe^{2+} and Mg^{2+} in coexisting olivines and pyroxenes. *J. Geol.* 59, 193-210.
- Ringwood, A.E. (1966). Mineralogy of the mantle. In *Advances in Earth Science*, 357-399. Hurley, P. (ed.). Cambridge: M.I.T. Press.
- Ringwood, A.E. (1969). Composition and evolution of the upper mantle. *Monogr. Am. geophys. Un.* 13, 1-17.
- Roedder, E. (1965). Liquid CO_2 inclusions in olivine-bearing nodules from basalts. *Am. Miner.* 50, 1746-1782.
- Ross, C.S., Foster, M.D. and Myers, A.T. (1954). Origin of dunites and of olivine-rich inclusions in basaltic rocks. *Am. Miner.* 39, 693-736.
- Rucklidge, J. and Gasparrini, E.L. (1969). Specifications of a computer program for processing electron microprobe analytical data. EMPADR V11. Dept. of Geol., University of Toronto, Toronto, Ontario.
- Sandell, E.B. (1959). *Colorimetric Determinations of Traces of Metals*. New York: Interscience.
- Snedecor, G.W. and Covhnan, W.G. (1967). *Statistical Methods*. Ames: Iowa State University Press.
- Simkin, T. and Smith, J.V. (1970). Minor element distribution in olivine. *J. Geol.* 78, 304-325.
- Soregaroli, A. (1968). *Geology of Boss Mountain Mine, British Columbia*. Ph.D. thesis. University of British Columbia, Vancouver.
- Souther, J.G. (1970). Volcanism and its relationship to recent crustal movements in the Canadian Cordillera. *Can. J. Earth Sci.* 7, 553-568.
- Talbot, J.L., Hobbs, B.E., Wilshire, H.G. and Sweatman, T.R. (1963). Xenoliths and xenocrysts from lavas of the Kerguelen Island Archipelago. *Am. Miner.* 48, 159-179.
- Thayer, T.P. (1960). Some critical differences between Alpine-type and stratiform peridotite-gabbro complexes. *Proc. 21st. Int. geol. Congr.* 13, 247-259.
- Tredger, P. (1970). *Petrology of nodules in olivine basalt from Quesnel Lake, British Columbia*. B.A.Sc. thesis. University of British Columbia, Vancouver.

- Turner, F.J. (1942). Preferred orientation of olivine crystals in peridotites with special reference to New Zealand examples. Trans. and Proc. Roy. Soc. New Zealand 72, 280-300.
- Wilshire, H.G. and Binns, R.A. (1961). Basic and ultrabasic xenoliths from volcanic rocks of New South Wales. J. ~~Geology~~ Petrology 2, 185-208.
- White, R.W. (1966). Ultramafic inclusions in basaltic rocks from Hawaii. Contr. Miner. Petrol. 12, 245-314.
- Yamaguchi, M. (1964). Petrogenetic significance of ultrabasic inclusions in basaltic rocks from Southwest Japan. Mem. Fac. Sci., Kyushu Univ., Ser.D, Vol.20, 163-219.

APPENDIX 1

Analytical Techniques.

(a) Mineral separation and sample preparation.

The constituent minerals of each nodule were separated by a combination of hand sorting and by use of a Franz magnetic separator. Purity was estimated by point-counting grains on a 1mm. transparent grid. The final purity of the mineral separates was greater than 99.5% in most cases and never less than 99.0%.

About 1g portions of olivine, orthopyroxene and clinopyroxene were ground to a fine powder (-100 to -200 mesh) by hand for 15 minutes in an agate mortar. A few grains of each spinel were mounted in Fibrolay epoxy and polished with tin oxide. Prior to the probe analyses each mount was coated with a thin layer of carbon.

(b) Electron microprobe analyses.

The spinel analyses were carried out with a JXA-3 electron microprobe X-ray analyser. The analyses were done by comparing intensities (measured as counts per second) of selected X-ray lines to those from standards of known composition. In all cases first order K_{α} lines were used. The voltage was 25Kv. for every element. A 10 second counting time was used in each case, 10 to 20 points on each grain being analysed. The average of each series of counts was taken as the true intensity. The standards were analysed before and after each run to determine instrumental drift. After each run the background was determined for both standards and samples.

Table 1 lists the elements which were determined, referred to the appropriate standard.

TABLE 1

Elements and standards used in electron microprobe analyses.

Element	Standard
Fe	Pure Fe metal
Cr	Pure Cr metal
Mg	Synthetic spinel*
Al	"

* Composition is : MgO 28.30; Al₂O₃ 71.55; FeO 0.02; CaO 0.02.

TABLE 2

Operating conditions for the hollow cathode lamps.

Element	Wavelength(Å)	Lamp current(ma.)	Slit()	Flame
Co	2407	5	25	acetylene-air
Cu	3247	3	50	"
Mn	2794	10	100	"
Ni	2320	8	50	"
Pb	2170	6	300	"
Zn	2138	6	100	"
Na*	5890	5	200	"
K*	7664	10	200	"
Ca#	4226	10	25	"
Mg#	2852	4	50	"
Fe	3719	5	50	"
Ti	3643	20	100	acetylene-nitrous oxide
Al	3091	11	100	"

*Cs added to samples and standards to suppress interferences.

#La added to samples and standards to suppress interferences.

The data were processed through the computer program EMPADR V11 which applies corrections for background, dead time if necessary, atomic number, absorption and fluorescence and converts the readings to weight percent of the appropriate oxide. (Rucklidge and Gasparrini 1969).

The precision of the analyses for each element calculated as

the standard error of the mean of each series of counts, is given below. For Al and Mg the error is close to 5% of the amount present and for Fe and Cr it is about 1%. The error is consistent from sample to sample except for Al which varies from 4 to 6%. Accuracy can be no better than precision so that the errors in counting alone can account for the deviations from 100% in the totals.

(c) Atomic-absorption analyses.

All elements expected to have a concentration of less than 2% were treated as trace elements in the analytical scheme. These were Co, Cu, Mn, Ni, Pb, Zn, Na, K, Ti, and Ca (in olivine). 0.3000g of the mineral powder was dissolved in 5ml of HF and 1ml of HClO_4 and the solution evaporated to dryness at 180°C on a hotplate. The residue was taken up in 3ml of HCl and the solution made up to 25ml with distilled water. Series of standards of appropriate concentration were made up in 1.5M HCl. The standards were aspirated into the flame of a Techtron AA-4 atomic-absorption spectrophotometer and a plot of concentration versus absorption prepared. The samples were then aspirated, after appropriate dilution if necessary, and the concentration read from the graph. The operating conditions of the hollow cathode lamps are summarised in Table 2.

For major elements (Mg, Fe, Al and Ca in pyroxenes) a method described by Langmyhr and Paus (1968) was used. 0.2000g of mineral powder was dissolved in 5ml of HF and evaporated to dryness at 180°C on a hotplate. A further 5ml of HF was then added and the solution warmed. 50ml of saturated boric acid solution was then added to dissolve the precipitated fluorides and to complex any

excess HF. The solution was made up to 100ml with distilled water. Standards of appropriate concentration were made up in the same way.

Each sample solution was aspirated four times into the flame of a Techtron AA-4 atomic-absorption spectrophotometer, bracketing it each time between standards of appropriate concentration. The order of aspiration was reversed after each set of readings. The concentration of the elements in each sample was calculated from the following equation:

$$C = A + K \frac{E_x - E_1}{E_2 - E_1}$$

where A is the concentration (wt.%) in the lower standard, K the difference in weight between the upper and lower standards, E_x , E_1 and E_2 are the absorbance of the sample solution, lower standard and upper standard respectively. The arithmetic mean of the four readings was taken as the concentration. Operating conditions for the hollow cathode lamps are summarised in Table 2.

Each batch of samples included a duplicate and a blank. No corrections for the blank were necessary. No corrections for background were required for any of the elements.

The precision of all the analyses was estimated as the standard deviation of the duplicate analyses. For all elements the precision was better than 5%, and generally about 3% of the amount present. The largest errors were in Mg due to the high dilution factor required and the sensitivity of the lamp, and in Al which is sensitive to the fuel flow.

(d) Determination of Cr_2O_3 .

Chromium was determined colorometrically using an adaption of

the methods described in Sandell (1967).

A 20ml aliquot of the solution used for the determination of Mg etc. by atomic-absorption was taken. 5ml of 6N H_2SO_4 was added and the solution warmed. A few drops of 0.1N KMnO_4 solution was added to this until the solution remained faintly pink on heating. The solution was boiled for ten minutes, allowed to cool and 0.1g of Na_2O and 10 - 20ml of 20% NaCO_3 solution added until a permanent precipitate appeared. The solution was then boiled for ten minutes, cooled and filtered. Enough 6N H_2SO_4 (10 -20ml) was added carefully with swirling to liberate CO_2 until the solution was approximately 0.2N in H_2SO_4 . 1ml of diphenylcarbazide solution was added and the solution made up to 50ml with distilled water. The purple colour so obtained was compared visually to a series of standard solutions containing 0.2 - 5ppm Cr made up with standard $\text{K}_2\text{Cr}_2\text{O}_7$ in the same way as the sample solutions.

Duplicate samples and a blank solution were run with each batch. Precision, determined as the standard deviation of the average of the duplicates, is 5% of the amount present. Due to the dilute solutions used, the limit of detectability is 200ppm. Consequently the chromium content of the olivines was not determined.

A slight error is introduced by using this method as some Cr is driven off as a fluoride during the initial decomposition. However this is not believed to be serious as the pyroxenes contain between 0.5 and 1.0% Cr_2O_3 and reproducibility is only 5%. Precision could be improved by making up fresh concentrated solutions, but for rapid convenient analyses, the above method is considered adequate in view of the errors in the other elements,

APPENDIX 2

Error propagation in temperature determination.

The precision in determining Mg and Fe in olivine (based on duplicate analyses) is less than 5% of the amount present. The precision in determining Mg and Al in the spinel is 5% of the amount present; for Fe and Cr precision is 1% of the amount present. These figures are based on counting statistics. Table 1 gives the uncertainties in ratios involving these elements, based on the above precisions.

Table 1

Uncertainties in element ratios.

Ratio	Uncertainty	Ratio	Uncertainty
$\frac{\text{Mg}}{\text{Mg} + \text{Fe}} \text{ ol}$	$\pm .004$	$\frac{\text{Cr}}{\text{Cr} + \text{Al} + \text{Fe}^{3+}}$	$\pm .003$
$\frac{\text{Fe}}{\text{Mg} + \text{Fe}} \text{ ol}$	$\pm .004$	$\frac{\text{Al}}{\text{Cr} + \text{Al} + \text{Fe}^{3+}}$	$\pm .003$
$\frac{\text{Mg}}{\text{Mg} + \text{Fe}^{2+}} \text{ sp}$	$\pm .006$	$\frac{\text{Fe}^{3+}}{\text{Cr} + \text{Al} + \text{Fe}^{3+}}$	$\pm .009 *$
$\frac{\text{Fe}^{2+}}{\text{Mg} + \text{Fe}^{2+}} \text{ sp}$	$\pm .005$		

* Uncertainty taken as 3x the uncertainty in $\frac{\text{Cr}}{\text{Cr} + \text{Al} + \text{Fe}^{3+}}$ as Fe_2O_3 calculated by assuming the model spinel formula.

The uncertainties in $K_D(4)$ were calculated from the expression:

$$|dy| \leq |fx_1(x_1 \dots x_n)|/|dx_1| + |fx_2(x_1 \dots x_n)|/|dx_2| + \\ |fx_n(x_1 \dots x_n)|/|dx_n|$$

where dy was set equal to $dK_D(4)$, x_1 to $x_{\text{Mg}}^{\text{ol}}$, x_2 to $x_{\text{Fe}}^{\text{sp}}$, x_3 to $x_{\text{Fe}}^{\text{ol}}$ and x_4 to $x_{\text{Mg}}^{\text{sp}}$. dx_1 , dx_2 , dx_3 and dx_4 were taken from Table 1.

(these were calculated using the above equation with the appropriate substitutions).

The uncertainties in the derived temperatures were calculated from the above equation where dy was set equal to dT , x_1 to x_7 to the variables on the right hand side of the equation for the calculation of the temperature:

$$T = \frac{5580\alpha + 1018\beta - 1720\gamma + 2400}{.90\alpha + 2.56\beta - 3.08\gamma - 1.47 + 1.987\ln K_D(4)}$$

and dx_1 to dx_7 were taken from Table 1 and Table 7 in the text.